CONFERENCE SERIES

Martin Beyer, Roland Wester, Paul Scheier, Irmgard Staud (Eds.)

XXIst Symposium on Atomic, Cluster and Surface Physics 2018 (SASP 2018)

February 11 – 16, 2018

Obergurgl, Austria

Contributions

innsbruck university press

CONFERENCE SERIES

innsbruck university press

universität
innsbruck

Universität Innsbruck
1st edition

www.uibk.ac.at/iup
ISBN 978-3-903187-15-3

Martin Beyer, Roland Wester, Paul Scheier, Irmgard Staud (Eds.)

XXIst Symposium on Atomic, Cluster and Surface Physics 2018 (SASP 2018)

February 11 – 16, 2018

Obergurgl, Austria

Contributions

XXIst Symposium on Atomic, Cluster and Surface Physics 2018 (SASP 2018)

February 11 – 16, 2018 Obergurgl, Austria

International Scientific Committee:

Daniela Ascenzi (Universitá degli Studi di Trento)
Martin Beyer (Universität Innsbruck)
Tilmann D. Märk (Universität Innsbruck)
Roberto Marquardt (Université de Strasbourg)
Nigel Mason (Open University, UK)
Stephen Price (University College London)
Martin Quack (Eidgenössische Technische Hochschule Zürich)
Tom Rizzo (EPFL Lausanne)
Paul Scheier (Universität Innsbruck)
Jürgen Stohner (Zürcher Hochschule für Angewandte Wissenschaften)
Roland Wester (Universität Innsbruck)

Organizing Committee:

Institut für Ionenphysik und Angewandte Physik, Universität Innsbruck

Martin Beyer, Paul Scheier, Roland Wester (chairpersons)
Arntraud Bacher, Chitra Perotti, Irmgard Staud, Claudia Wester

Preface

The international Symposium on Atomic, cluster and Surface Physics, SASP, is a continuing biennial series of conferences, founded in 1978 by members of the Institute of Atomphysik, now Institute of Ionphysics and Applied Physics of the University of Innsbruck, Austria. SASP symposia aim to promote the growth of scientific knowledge and effective exchange of information among scientists in the field of atomic, molecular, cluster and surface physics, stressing both fundamental concepts and applications across these areas of interdisciplinary science. A major focus of SASP 2014 is on ion-molecule reactions.

Since the beginning, the SASP format has been similar to that of a Gordon Conference, with invited lectures, hot topic oral presentations, posters and ample time for discussions. The attendance to the symposium has been kept to about 100 participants to favor interdisciplinary and multidisciplinary discussions.

SASP usually takes place in Austria, but every second time, it may be held in another alpine country. So far, the SASP conferences were held in the following locations:

1978 Zirog, Italy
1980 Maria Alm, Austria
1982 Maria Alm, Austria
1984 Maria Alm, Austria
1986 Obertraun, Austria
1988 La Plagne, France
1990 Obertraun, Austria
1992 Pampeago, Italy
1994 Maria Alm, Austria
1996 Engelberg, Switzerland
1998 Going, Austria
2000 Folgaria, Italy
2002 Going, Austria
2004 La Thuile, Italy
2006 Obergurgl, Austria
2008 Les Diablerets, Switzerland
2010 Obergurgl, Austria
2012 Alpe d´Huez, France
2014 Obergurgl, Austria
2016 Davos, Switzerland

SASP Erwin Schrödinger Gold Medal 2018

The „SASP Award for Outstanding Scientific Achievements" was initiated in 1992 by the SASP International Scientific Committee. This award is granted during the biennial SASP meeting to one or two scientists, chosen among those who have strong connections to the activities of SASP.

The recipient of the SASP award 2018 – in the form of the "Erwin Schrödinger Gold Medal" designed by Zdenek Herman – is

Thomas Rizzo, EPFL Lausanne, Switzerland

Thomas Rizzo, from the École polytechnique fédérale de Lausanne, Switzerland, has received this award for his outstanding contributions to experimental chemical physics, in particular to multiple-laser spectroscopy, spectroscopy of biological molecules in the gas phase as well as to inter- and intramolecular energy transfer.

At previous SASP meetings the Schrödinger Gold Medal was awarded to:

1992 David Smith, Birmingham, UK
1994 Zdenek Herman, Praha, Czech Republic
1996 Werner Lindinger and Tilmann Märk, Innsbruck, Austria
1998 Eldon Ferguson, Boulder, USA and Chava Lifshitz, Jerusalem, Israel
2000 Jean H. Futrell, Richland, USA
2002 Eugen Illenberger, Berlin, Germany
2004 Anna Giardini-Guidoni, Roma, Italy
2006 Davide Bassi, Trento, Italy and Martin Quack, Zürich, Switzerland
2008 Helmut Schwarz, Berlin, Germany
2010 Kurt Becker, New York, USA
2012 Dieter Gerlich, Chemnitz, Germany and John Maier, Basel, Switzerland
2014 Stephen D. Price, London, University College London, United Kingdom
2016 Roberto Marquardt, Strasbourg, Université des Strasbourg, France and Paul Scheier, Innsbruck, Universität Innsbruck, Austria

Program

	Sun, Feb 11	Mon, Feb 12	Tue, Feb 13	Wed, Feb 14	Thu, Feb 15	Fri, Feb 16
		Chair: Wester	Chair: Ernst	Chair: Quack	Chair: Beyer	Chair: Scheier
09:00		Ascenzi	Reid	Laskin	Kitsopoulos	Asvany
09:35		Bouwman	Signorell	Toker	Mackenzie	Dopfer
10:10		Romanzin	Ludwig	Farizon	Koch	Roithová
10:45		Coffee				
11:15		Matejcik	Xantheas	Slavicek	Balucani	SASP 2020
11:50		*Skouteris*	*Van der Linde*	*Ernst*	*Ren*	End
12:10		*Gianturco*	*Moravsky*	*Kocisek*	*Grygoryeva*	
12:30		Break				
16:00		Snack				
		Chair: GNS	Chair: Gianturco	Chair: Postler	Chair: Marquardt	
16:30		Sterrer	Farnik	Stohner	Narevicius	
17:05		Panosetti	*M. Mayer*	Douberly	Kresin	
17:40		*J. Meyer*	*Gatchell*	*Gordon*	*Goulart*	
18:00		*Harding*	*Oncak*	*Quack*	Rizzo	
18:20	Dinner				SASP Award	
19:00					Conf Dinner	
20:30	Dörner	Poster	*Kaiser*	Poster		
20:50			*Koehler*			
21:10	Martin		*Rakovský*			
21:30			*Price*			

Contents

Invited Papers

Hot Topic Papers

Contributed Papers

Invited Papers

The unusual stability of charged, endohedral and exohedral fullerenes

Yang Wang[1], Sergio Díaz-Tendero[1,2], Manuel Alcamí[1,3] and Fernando Martín[1,2,3*]

[1]Departmento de Química, Módulo 13, Universidad Autónoma de Madrid, 28049 Madrid, Spain.

[2]Condensed Matter Physics Center (IFIMAC), Universidad Autónoma de Madrid, 28049 Madrid, Spain.

[3]Instituto Madrileño de Estudios Avanzados, Campus de Cantoblanco, 28049 Madrid, Spain.

[*]fernando.martin@uam.es

Fullerene anions and cations, as well as endohedral and exohedral fullerenes, have unique structural, electronic, and chemical properties that make them substantially different from pristine neutral fullerenes. In fast collisions with ions, electrons and photons or in arc-discharge experiments where they are produced, the theoretical prediction of the most stable structures is a very challenging task due to the large number of isomeric forms accessible in such hot environments (e.g., more than 20 billion isomers for $C_{60}X_8$). In this talk, we present a simple model [1-3], exclusively based on topological arguments, that allows one to predict the relative stability of these fullerene species without the need for electronic structure calculations or geometry optimizations. We show that the subtle interplay between π delocalization, cage strain, and steric hindrance is responsible for, e.g., (i) the formation of non IPR (isolated pentagon rule) cage structures in contrast with their pristine fullerene counterparts, (ii) the appearance of more pentagon-pentagon adjacencies than predicted by the PAPR (pentagon-adjacency penalty rule), and (iii) the variations in fullerene cage stability with the progressive addition of chemical species. The most stable structures predicted by the model are in good agreement with those found in synthetic experiments performed in high-energy conditions.

Molecular Dynamics (MD) simulations have also been used to understand the interaction of charged fullerenes with He atoms in a He nanodroplet environment. Combination of these results with a simple model that describes the polarizability induced by the He atoms on the fullerene cage allows us to interpret the absorption line shifts as a function of the number of He atoms observed in recent experiments [4].

References

[1] Y. Wang, S. Díaz-Tendero, M. Alcamí, and F. Martín, *Nature Chemistry* **7** 927 (2015).
[2] Y. Wang, S. Díaz-Tendero, F. Martín, and M. Alcamí, *J. Am. Chem. Soc.* **138** 1551 (2016).
[3] Y. Wang, S. Díaz-Tendero, M. Alcamí, and F. Martín, *J. Am. Chem. Soc.* **139** 1609 (2017)
[4] M. Kuhn, M. Renzler, J. Postler, S. Ralser, S. Spieler, M. Simpson, H. Linnartz, A. G. G. M. Tielens, J. Cami, A. Mauracher, Y. Wang, M. Alcamí, F. Martín, M. K. Beyer, R. Wester, A. Lindinger, and P. Scheier, *Nature Comm.* **7** 13550 (2016)

Ion-molecule reactions of astrochemical relevance

Daniela Ascenzi
Department of Physics, University of Trento, Via Sommarive 14, I-38123, Povo, Trento, Italy

Reactions of charged species can play a relevant role in shaping the chemistry of the interstellar medium and planetary atmospheres. In the interstellar medium, the reactions of the most abundant atomic and molecular ions (He^+, H^+, H_3^+ and HCO^+) dominate the destruction of the vast majority of interstellar Complex Organic Molecules (iCOM), but little experimental information is available on rate constants and nature of products, and, in most cases, guesses based on “common sense” and chemical analogies are used for modelling the chemistry of such environments. In planetary atmospheres, such as Titan, a plethora of cations and anions has been discovered by the Cassini mission and the idea is put forward that ionic reactions play an active role in the formation pathways of complex molecules, but also in this case laboratory experiment on key reactions are sparse.

Our contribution is in the laboratory measurements of kinetic parameters (cross sections, branching ratios and their dependences on collision energy) for the reaction of charged molecules with neutrals, by using tandem mass spectrometric techniques and RF octupolar trapping of parent and product ions. As examples of destruction and formation processes driven by ionic species, results will be presented on the reactions of He^+ with two of the most abundant and ubiquitous iCOM (CH_3OCH_3 and $HCOOCH_3$) [1, 2] and on the isomer selected reactivity of $C_2H_2N^+$ cations with small hydrocarbons [3, 4, 5].

Acknowledgments
The work here presented is the result of an extensive collaboration between our group at Trento University and other research groups: Fernando Pirani & Nadia Balucani (Univ. Perugia IT), Cecilia Ceccarelli (IPAG Grenoble FR), Christian Alcaraz, Claire Romanzin, Roland Thissen, Allan Lopes (Univ. Paris Sud et Paris-Saclay, FR), Barbara Cunha de Miranda (SOLEIL synchrotron & Sorbonne Univ. FR), Glauco Tonachini & Andrea Maranzana (Univ. Turin, IT), Miroslav Polasek & Jan Zabka (Heyrovsky Institute of Physical Chemistry, Prague CZ)

References

[1] Cernuto A., Pirani F., Martini L.M., Tosi P., Ascenzi D. *ChemPhysChem* (2017) published on-line DOI: 10.1002/cphc.201701096.
[2] Cernuto A., Tosi P., Martini L.M., Pirani F., Ascenzi D*. Phys. Chem. Chem. Phys.* **217** (2017) 1463.
[3] P. Fathi, W.D. Geppert, F. Lindén, A. Cernuto, D. Ascenzi *Molecular Astrophysics* **5** (2016) 9-22.
[4] P. Fathi, W.D. Geppert, A. Kaiser, D. Ascenzi *Molecular Astrophysics* **2** (2016) 1-11.
[5] P. Fathi, W.D. Geppert, D. Ascenzi *Int. J. Mass Spectrom.* **411** (2016) 1-13.

Probing Molecular Dissociation using Large Scale Facilities; the Case of Astronomically Relevant Polyaromatics

Jordy Bouwman
Sackler Laboratory for Astrophysics, Leiden Observatory,
Leiden University, P.O. Box 9513, 2300 RA Leiden, The Netherlands
Email: bouwman@strw.leidenuniv.nl

The presence of interstellar polycyclic aromatic hydrocarbons (PAHs) is derived from the mid infrared (IR) emission bands that are observed at frequencies that correspond to the typical vibrational normal modes of polyaromatics.[1,2] The IR radiation is emitted as the molecules cascade down to the ground state after they have been excited by interstellar (vacuum) ultraviolet ((V)UV) radiation. [3] PAHs have been observed towards a large number of galactic and extragalactic sources and it has been derived that PAHs constitute up to 15% of the total cosmic carbon budget. [4]

Energetic processing of interstellar polyaromatics may also result in ionization and/or dissociation. It has been hypothesized that this chemical evolution is reflected in subtle changes in the observed mid-IR emission bands.[5] Observational and laboratory data suggest that dissociation of large interstellar polyaromatics eventually results in fullerene formation. [6,7] The underlying chemical processes involved in the dissociation of aromatics is not yet understood.

Our group characterizes the dissociation of polyaromatics by means of VUV synchrotron radiation and mid infrared free electron laser radiation. By combining these techniques with quantum chemical computations we obtain insight into the isomerization and dissociation at a molecular level of detail. [8-11] (See Figure 1) I will review our most recent results and will emphasize their importance in light of astronomical observations.

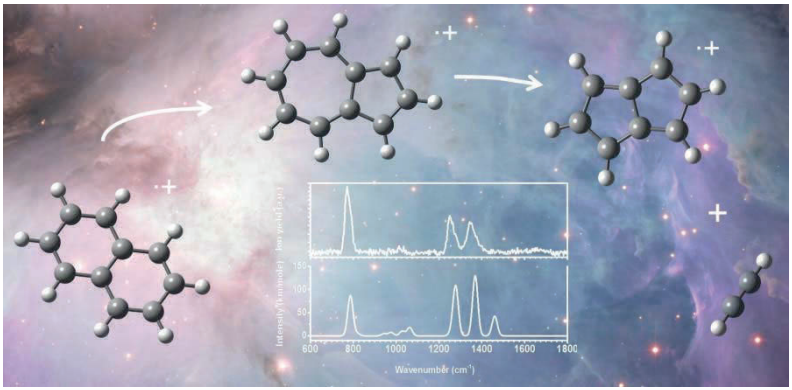

Figure 1: *Infrared spectroscopy at the free electron laser FELIX enabled the structural identification of the product formed from the dissociation of the smallest of polyaromatics, naphthalene.*

References

[1] Leger, A. & Puget, J. L. Identification of the Unidentified Ir Emission Features of Interstellar Dust. *Astron. Astrophys.* **137**, L5-L8 (1984).

[2] Allamandola, L. J., Tielens, A. & Barker, J. R. Polycyclic Aromatic-Hydrocarbons and the Unidentified Infrared-Emission Bands - Auto Exhaust Along the Milky-Way. *Astroph. J.* **290**, L25-L28, doi:10.1086/184435 (1985).

[3] Allamandola, L. J., Tielens, A. & Barker, J. R. Interstellar Polycyclic Aromatic-Hydrocarbons - the Infrared-Emission Bands, the Excitation Emission Mechanism, and the Astrophysical Implications. *Astrophys. J. Suppl. Ser,* **71**, 733-775, doi:10.1086/191396 (1989).

[4] Tielens, A. in *Annu. Rev. Astron. Astr.* Vol. 46 *Annual Review of Astronomy and Astrophysics* 289-337 (Annual Reviews, 2008).

[5] Peeters, E. *et al.* The Rich 6 to 9 mm Spectrum of Interstellar PAHs*. *A&A* **390**, 1089-1113 (2002).

[6] Berne, O. & Tielens, A. Formation of Buckminsterfullerene (C-60) in Interstellar Space. *Proc. Natl. Acad. Sci.* **109**, 401-406, doi:10.1073/pnas.1114207108 (2012).

[7] Zhen, J. *et al.* Laboratory Formation of Fullerenes from PAHs: Top-Down Interstellar Chemistry. *Astrophys. J. Lett.* **797**, doi:10.1088/2041-8205/797/2/l30 (2014).

[8] Bouwman, J. *et al.* Dissociative Photoionization of Quinoline and Isoquinoline. *J. Phys. Chem. A* **119**, 1127-1136, doi:10.1021/jp5121993 (2015).

[9] Bouwman, J., de Haas, A. J. & Oomens, J. Spectroscopic Evidence for the Formation of Pentalene^{+} in the Dissociative Ionization of Naphthalene. *Chem. Commun.* **52**, 2636-2638, doi:10.1039/C5CC10090A (2016).

[10] de Haas, A. J., Oomens, J. & Bouwman, J. Facile Pentagon Formation in the Dissociation of Polyaromatics. Phys. Chem. Chem. Phys. 19, 2974-2980, doi:10.1039/C6CP08349H (2017).

[11] Zhen, J. F. *et al.* Infrared Spectra of Hexa-Peri-Hexabenzocoronene Cations: HBC^+ and HBC_2^+. *Astroph. J.* **836**, doi:10.3847/1538-4357/836/1/28 (2017).

Gas phase ion-molecule chemistry: controlled reactions of methyl cations with O-bearing compounds and hydrocarbons

C. Romanzin, R. Thissen, A. Lopes, B. Cunha de Miranda, C. Alcaraz
LCP, UMR8000 CNRS-Univ. Paris-Sud & Paris-Saclay, Orsay, France

I. Zymak, J. Zabka, M. Polasek
J. Heyrovsky Institute of Physical Chemistry of the Czech Acad. of Sci., Prague, Czech Republic

M. Bertin
LERMA, Sorbonne Universités, UPMC Univ. Paris 06, Observatoire de Paris, PSL Research University CNRS, France

A. Cernuto, D. Ascenzi
University of Trento, Dept of Physics, Trento, Italy

The methyl carbocation is a reactive species whose presence has been detected in a lot of gaseous environments fed by high energy sources, such as the interstellar medium, planetary ionospheres and laboratory plasmas for methane conversion into higher hydrocarbons for instance. Its reactivity is generally well-known, yet the corresponding literature mainly concerns the cation in its ground state although excited species are likely to be present in the different environments of interest.

Here, new results on the reactivity of the methyl carbocation obtained with the CERISES setup (a guided ion-beam experiment) will be presented. The originality of these experiments is to investigate the effect of internal degrees of freedom (vibrational, electronic) on the reactivity of the CH_3^+ cation with different neutral species. This is made possible by producing the CH_3^+ ion *via* direct photoionization of a molecular beam of $CH_3\cdot$ radicals. This way, we are able to produce the ion within a controlled degree of internal excitation just by varying the photon energy. To do so, the $CH_3\cdot$ radicals are formed by pyrolysis of an appropriate precursor molecule (here nitromethane CH_3NO_2) in an additional chamber coupled to the standard CERISES set-up [1] and further ionized thanks to VUV photons delivered by the DESIRS beamline at the synchrotron SOLEIL [2,3].

This so-called reactive monitoring method enables to probe the internal energy dependence of the cation reactivity and to justify further state-selected studies using the TPEPICO (Threshold PhotoElectron-PhotoIon Coincidence) technique.
In this contribution, we will focus on the reactive monitoring part and present results obtained with O-bearing compounds – formic acid HC(O)OH and methanol CH_3OH – and hydrocarbons (C_1-C_4). Branching ratios and absolute reaction cross-sections for the different reactive systems will be given and the dependence on the vibrational and electronic excitation of the parent-ion will be discussed.

Acknowledgments: This work has received the support of the RTRA “Triangle de la Physique” (RADICAUX and NOSTADYNE projects), of the French Planetology Program (PNP) and of the region ‘Ile de France’ DIM ACAV+ program (SitCOMs project).

References

[1] B. Cunha de Miranda, C. Romanzin, S. Chefdeville, V. Vuitton, J. Žabka, M. Polášek, and C. Alcaraz, *J. Phys. Chem. A* **119**, 6082 (2015).
[2] L. Nahon et al., *J. Synchrotron Radiat.* **19**, 508 (2012).
[3] A. Cernuto, A. Lopes, C. Romanzin, B. Cunha de Miranda, D. Ascenzi, P. Tosi, G. Tonachini, A. Maranzana, M. Polasek, J. Zabka and C. Alcaraz, *J. Chem. Phys.* **147**, 154302 (2017).

Electron induced fluorescence to molecules

Štefan Matejčík, Michal Ďurian, Juraj Országh, Marián Danko
Department of Experimental Physics, Comenius University Bratislava, Slovakia
matejcik@fmph.uniba.sk

The fundamental data regarding the electron – molecule interactions are of vital interest in several fields of the science such as plasma physics, radiation chemistry, astrophysics, etc. The Electron Induced Fluorescence (EIF) technique is a suitable instrument which can be applied to explore such electron interactions like the electronic excitation and dissociative excitation of molecules as well as other electron interaction associated with emission of photons e.g., electron ionisation and dissociative ionisation associated with excitation of ionic states.

In this contribution we are going to present the recent results obtained with EIF technique at Comenius University in Bratislava [1,2,3]. We are going to present data obtained in electron molecule interactions with such molecules like H_2, D_2, H_2O, CH_4, C_2H_2. The excitation and emission spectra of molecules are recorded at well defined electron energies and depend strongly on the electron energy. Besides the spectra of molecules we are going to present excitation emission cross sections for selected electronic transitions between in atomic and molecular fragment states. The electronic excitation initiated by dissociative excitation process may result in electronic transition between bond electronic state and dissociative states which is responsible for appearance of continuum radiation from molecules. We are going to present such transitions for H_2, D_2 and C_2H_2 molecules.

This research was supported by the Slovak Research and Development Agency under contract No. APVV-15-0580. This project has received funding from the European Union's Horizon 2020 research and innovation programme under grant agreement number 692335.

[1] M. Danko et al., J. Phys. B: At. Mol. Opt. Phys. 46, (2013) 045203.
[2] M. Danko, A. Ribar, M. Ďurian, J. Országh and Š. Matejčík, Plasma Sources Sci. and Technol. 25, (2016) 065007.
[3] J. Országh, M. Danko, P. Čechvala and Š. Matejčík, Astrophys. J. 17, (2017) 841

Charging and Catalytic Activity of Metal Clusters and Molecules on Ultrathin MgO Films

Martin Sterrer
University of Graz, Institute of Physics

Oxides are ubiquitous on earth and play a prominent role in modern science and technology as they appear in a large variety of chemical composition and structure and, hence, physical and chemical properties. In the last decades, ultrathin oxide layers at the two-dimensional limit, i.e. with a thickness of only one or a few atomic layers that are usually supported by a metal substrate, have been actively investigated. While these layers were originally synthesized with the intention to electronically decouple adsorbates from a metal substrate, it was recently found that potentially interesting phenomena can arise from the reduced thickness and the variability of composition and structure in the ultrathin regime. In addition, the formation of the interface between the oxide layer and a metal substrate can lead to substantial variation of the metal workfunction and thus give rise to enhanced charge transfer to adsorbates. Ultrathin MgO(001)/Ag(001) thin films have emerged in the last decade as a most suitable model system for studying charge transfer phenomena into molecules and metal atoms. The growth of MgO(001) thin films on Ag(001) leads to a substantial workfunction reduction of the Ag(001) substrate by more than 1 eV. As a consequence, electron tunnelling through the MgO film into adsorbates exhibiting high electron affinity becomes possible. In this talk, I will present two examples where charging of adsorbates on MgO(001)/Ag(001) has been observed: Au atoms and clusters as an example for catalytically active noble metal species, and pentacene (5A) as an example of a model organic semiconductor used in organic electronics. Atomic and molecular scale characterization of these adsorbates has been achieved by a combination of electron spectroscopy and scanning tunnelling microscopy in combination with calculations using density functional theory. The consequences of the charging of the adsorbed species will be discussed, in particular in light of the catalytic activity of supported gold.

Better (random) walking through chemistry: how not to get lost in vast cofigurational spaces

Chiara Panosetti
Technische Universität München, 85748 Garching b. München, Deutschland

…Ab initio structure prediction can systematically aid the computational discovery and rational design of new materials, as well as providing interpretative insights when atomistic details are difficult to resolve experimentally. However, global geometry optimization –the method of choice for finding chemically relevant (meta-)stable structures– is rarely applied to large-scale systems. The main challenge lies in the necessity of efficient ways to traverse configurational spaces in which the number of minima explodes with system size.

We adapt the basin hopping [1] global geometry optimization scheme to employ automatically-generated collective curvilinear coordinates. Due to the physical correspondence of these coordinates with vibrations, this enhances the generation of chemically meaningful trial structures for covalently bound systems.[2] In the application to hydrogenated Si clusters we concomitantly observe a significantly increased efficiency in identifying low-energy structures and a reduction of unphysical geometries when compared to the same number of typical random Cartesian trial moves.

We further propose to combine this and the ab initio thermodynamics idea [2] in a grandcanonical global optimization framework, where the function to minimize is no longer the total energy, but rather the Gibbs free energy at several values of the chemical potential of the components, in order to target systems with unknown or variable stoichiometry, such as metal silicides synthesized directly at surfaces, or non-stoichiometric surface reconstructions.

Following the fil rouge of the exploitation of chemically motivated trial moves, we further extend this to the study of organic molecules on surfaces [4] – by suitably imposing partial constraints– and to complex interfaces with variable or unknown stoichiometry – by applying strategies to alleviate the strain of newly generated structures upon grand-canonical particle insertion. A selection of prototypical results, with particular focus on hydrogenated silicon clusters and silicon surface reconstructions, will be presented to illustrate how all relevant portions of chemical space can be accessed with this approach,

whereas "conventional" sampling often even struggles to produce sensible structures besides the starting geometry at all.

[1] D. J. Wales, J. P. K. Doye, *J. Phys. Chem. A* **101**, 12209-12011 (1997).
[2] C. Panosetti, K. Krautgasser, D. Palagin, K. Reuter, R. J. Maurer, *Nano Lett.* **15**, 8044-8048 (2015).
[3] J. Rogal, K. Reuter. Ab Initio Atomistic Thermodynamics for Surfaces: A Primer. In Experiment, Modeling and Simulation of Gas–Surface Interactions for Reactive Flows in Supersonic Flights, pages 1–18 (2007).
[4] K. Krautgasser, C. Panosetti, D. Palagin, K. Reuter, R. J. Maurer, *J. Chem. Phys.* **145**, 084117 (2016).

Mass Transfer Dynamics Across a Gas-Liquid Surface from Single Droplet Measurements

Jonathan P. Reid, Bryan R. Bzdek, Florence Gregson, Allen E. Haddrell, Stephen Ingram, Aleksandra Marsh, Rachael E.H. Miles and Young-Chul Song
School of Chemistry, University of Bristol, Bristol, BS8 1TS, UK

Mass and heat transfer between the condensed and gas phases regulates aerosol particle size, composition and phase. The condensation or evaporation of volatile components are driven by changes in the surrounding gas phase conditions and composition and processes can occur over timescales spanning from the millisecond to the day [1]. For low viscosity solution droplets, the transfer of mass can be limited by molecular processes at the gas-liquid surface and regulated by the composition of the surface with, for example, monomolecular surface films delaying droplet evaporation. Alternatively, the kinetics may be limited by the inefficiency of heat transport, regulating mass transport as occurs during volatile droplet evaporation. For high viscosity particles, slow diffusion within the particle bulk may impair evaporation or condensation of volatile components in aerosol. The nature of the limiting process varies from context to context, but is important to identify and understand for atmospheric aerosols and the formation of cloud droplets, the delivery of drugs to the lungs or the fabrication of microparticles through processes such as spray drying.

We will report on the development of a variety of single aerosol particle tools to study the evaporation or condensation kinetics of volatile components in aerosol, and determine the surface and bulk properties of single particles [2]. In particular, we will show that measurements of evolving particle size can be made with millisecond time-resolution using elastic light scattering for particles captured in an electrodynamic balance or falling in a train. We will also show how the surface composition (surface tension) and bulk viscosity of particles can be measured directly using aerosol optical tweezers.

Using these single particle tools we will explore three limiting regimes governing mass transport across the gas-liquid surface of aerosol droplets. Initially, the condensation kinetics of water on evaporating volatile droplets will be examined, a process that is inherently limited by how rapidly gas transport is able to move mass towards the droplet surface. In a second regime, we will

examine the impact of surface active organic films on the evaporation kinetics of water droplets. Finally, we will explore the condensation kinetics of water on particles of varying viscosity, contrasting the rapid dissolution of a viscous core with the slow release of water from a glassy particle during evaporation.

[1] Bzdek BR, Reid JP. Perspective: Aerosol microphysics: From molecules to the chemical physics of aerosols. *J. Chem. Phys.* **147**, 220901 (2017).
[2] Krieger UK, Marcolli C, Reid JP. Exploring the complexity of aerosol particle properties and processes using single particle techniques. *Chem. Soc. Rev.* **41**, 6631–6662 (2012).

Low-energy electron transport in water: Clusters, droplets, and liquid bulk

Ruth Signorell
ETH Zurich, Laboratory of Physical Chemistry, 8093 Zürich

Even though low-energy electron scattering in liquid water is of high relevance for the modelling of radiation damage processes, radiolysis, and the analysis of photoelectron spectra, detailed scattering data have so far neither been accessible by experiment nor by theory [1-4]. For lack of liquid water data, current descriptions thus use the amorphous ice data [5] and/or rescaled gas phase parameters to describe the scattering of low-energy electrons (LEEs) (< 50eV electron kinetic energy). The important parameters are the multiple differential cross sections (MDCs) with respect to electron kinetic energy, energy loss, and scattering angle, of all relevant scattering processes (elastic; inelastic (electron-phonon, electron-vibron, electron-electron)). Our recent derivation of MDCs for liquid water from photoelectron imaging of water droplets and water clusters provides a starting point for definite answers to fundamental questions regarding the electron dynamics in liquid water [6-8].

[1] N. Ottosson, M. Faubel, S. E. Bradforth, P. Jungwirth, B. Winter, *J. Electron Spectrosc. Relat. Phenom.* **177** (2010) 60.
[2] S. Thürmer, R. Seidel, M. Faubel, W. Eberhardt, J.C. Hemminger, S.E. Bradforth, B. Winter, *Phys. Rev. Lett.* **111** (2013) 173005.
[3] Y.-I. Suzuki, K. Nishizawa, N. Kurahashi, T. Suzuki, *Phys. Rev. E* **90** (2014) 010302.
[4] H. Shinotsuka, B. da, S. Tanuma, H. Yoshikawa, C. J. Powell, D. R. Penn, *Surf. Interf Anal*. **49** (2017) 238.
[5] M. Michaud, A. Wen, L. Sanche, *Radiat. Res.* **159** (2003) 3.
[6] R. Signorell, M. Goldmann, B. L. Yoder, A. Bodi, E. Chasovskikh, L. Lang, D. Luckhaus, *Chem. Phys. Lett.* **658** (2016), 1. arXiv:1603.04188
[7] S. Hartweg, B.L. Yoder, G.A. Garcia, L. Nahon, R. Signorell, *Phys. Rev. Lett.* **118**, (2017), 103402 arXiv: 1612.02338
[8] D. Luckhaus, Y.-I. Yamamoto, T. Suzuki, R. Signorell, *Sci. Adv.* **3** (2017) e1603224.

Cationic clusters in ionic liquids: When cooperative hydrogen-bonding overcomes Coulomb repulsion between ions of like charge

Anne Strate, Thomas Niemann, Jan Neumann, Dietmar Paschek, Ralf Ludwig
Physikalische und Theoretische Chemie, Universität Rostock, Dr.-Lorenz-Weg 2, 18059 Rostock, Germany

“Unlike charges attract, but like charges repel”. This conventional wisdom has been recently challenged for ionic liquids (ILs). It could be shown that like-charged ions attract each other despite the powerful opposing electrostatic forces. In principle, cooperative hydrogen bonding between ions of like-charge can overcome the repulsive Coulomb interaction while pushing the limits of chemical bonding [1-5]. The key challenge of this solvation phenomenon is to establish design principles for the efficient formation of clusters of like-charged ions in ionic liquids. For that purpose we combined weakly coordinating anions with polarizable cations which are all equipped with hydroxyl groups for possible H-bonding. The formation of H-bonded cationic clusters can be controlled by the interaction strength of the counterion and the delocalization of the positive charge on the cations. Strongly interacting anions and localized charge on the cations result in hydrogen bonded ions of opposite charge, whereas weakly coordinating anions and delocalized charge on the cations lead to the formation of H-bonded cationic clusters up to cyclic tetramers. If we increase the distance between the hydroxyl groups and the positive charge center within the cation we can almost suppress hydrogen bonding between cation and anion to the benefit of cationic cluster formation. These clusters can be observed by infrared spectroscopy and interpreted by DFT calculated frequencies on neutral and ionic clusters. The cationic cluster formation is also reflected in NMR proton chemical shifts and rotational correlation times of the OH group. Additional molecular dynamics simulations provide information about the life-times of the hydrogen bonds in the cationic clusters compared to those in the typical ion pairs [6].

Besides developing the design principles for cationic cluster formation we can show for the first time that these clusters of like-charged ions characteristically influence the properties of ILs [7]. ILs comprising these clusters can be supercooled and form glasses. Crystal structures will be only obtained, if the ILs are dominantly characterized by attraction between opposite-charged ions

resulting in conventional ion pairs. That opens a new path for controlling glass formation and crystallization. The glass temperatures and the phase transitions of the ILs are observed by differential scanning calorimetry (DSC) and infra red (IR) spectroscopy.

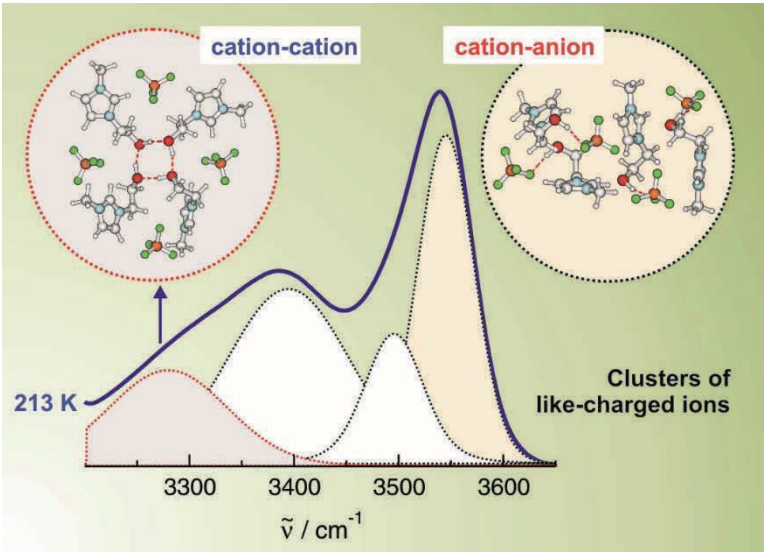

References

[1] A. Knorr, K. Fumino, A.-M. Bonsa, R. Ludwig, Phys. Chem. Chem. Phys. 2015, (17), 30978.
[2] A. Knorr, R. Ludwig, Sci. Rep. 2015, (5), 17505.
[3] A. Knorr, P. Stange, K. Fumino, F. Weinhold, R. Ludwig, ChemPhysChem 2016, (17), 458.
[4] A. Strate, T. Niemann, D. Michalik, R. Ludwig, Angew. Chem. Int. Ed. 2017, (56), 496.
[5] A. Strate, T. Niemann, R. Ludwig, Phys. Chem. Chem. Phys., 2017, (19), 18854.
[6] A. Strate, J. Neumann, V. Overbeck, A.-M. Bonsa, D. Michalik, D. Paschek, R. Ludwig, J. Chem. Phys., 2017, submitted.
[7] T. Niemann, D. Zaitsau, A. Strate, A. Villinger, R. Ludwig, Angew. Chem., 2018, submitted.

Analysis of bonding patterns in molecular systems exhibiting partial biradical character

Evangelos Miliordos[1] and Sotiris S. Xantheas[1,2]
[1] *Advanced Computing, Mathematics & Data Division, Pacific Northwest National Laboratory, PO Box 999, MS K1-83, Richland WA 99352*
[2] *Department of Chemistry, University of Washington, Seattle, WA 98195*

A quantitative scale of the biradical character ($0 \leq \beta \leq 1$) of a molecular system based on a Multi-Reference Configuration Interaction (MRCI) wavefunction is introduced and used to analyze its underlying electronic structure and bonding pattern. Triatomic ions in the FX_2^+ series, where X = O, S, Se, Te and Po are the terminal atoms, were found to exhibit unusually high biradical characters ($0.76 < \beta < 0.92$), the largest among the homologous, 18 valence electron molecules CX_2^{2-}, NX_2^-, X_3 and OX_2 (X = O, S, Se, Te and Po). The concept of biradical character was further used to investigate the bonding mechanism in ozone (O_3) and its sulfur-substituted analogues, SO_2, OS_2, and S_3. We demonstrate that the binding in these molecules can be described by a mixture of a closed shell structure with one and a half bond between the central and terminal atoms and an open-shell structure with a single bond and two lone electrons on each terminal atom. The analysis of the MRCI wavefunctions provides a simple measure of the relative mixture of the two bonding scenarios, yielding a biradical character of 3.5% for OSO, 4.4% for SSO, 11% for S_3, 18% for O_3, 26% for SOO, and 35% for SOS. Our analysis further offers an explanation for the different O-O, S-O and S-S bond lengths and singlet-triplet splittings of these species, the stabilization of OSO and SSO over the SOO and SOS isomers as well as the (X-YZ) relative binding energies (X=S, O), all based on their different biradical character.

Comprehensive cluster investigations in molecular beams: from atmospheric chemistry to biophysics

M. Fárník, J. Fedor, J. Lengyel, J. Kočišek, A. Pysanenko
J. Heyrovský Institute of Physical Chemistry of the Czech Academy of Sciences, Dolejškova 3, Prague 8, Czech Republic

1. Introduction

Molecular reaction dynamics investigates the elementary processes in molecular collisions and interaction of molecules with radiation, e.g., photons and electrons etc. In chemistry, these processes proceed in an environment, and the solvent plays often a decisive role in them. Clusters enable to investigate these processes and the role of the solvent at a detailed molecular level. That is the fundamental motivation of our research. Besides, clusters can mimic species and processes relevant to atmospheric chemistry and physics, astrophysics, biophysics, and various technologies. Several examples from these different areas will be reviewed.

2. Experiment

The experiments were performed on the CLUster Beam (CLUB) apparatus in Prague which enables different cluster experiments. The unique feature of the CLUB apparatus is that the data from different experiments can be directly compared, since they are obtained with a single molecular beam, i.e. with the same cluster species. Clusters produced by supersonic expansions can be doped with different molecules in pickup experiments. From the pickup experiments, the cluster cross sections can be evaluated [1,2] or dynamics and reactions of molecules on the clusters can be studied [3-5]. Photochemistry and photodissociation of molecules in clusters can be investigated using the velocity map imaging (VMI) [6-8]. Unique to our experiment is the TOF mass spectrometer where different ionization methods are implemented. Electrons of different energies from 0 to 90 eV can ionize the clusters positively (electron ionization –EI) or negatively (electron attachment –EA). Both ion polarities can be detected. The clusters can be also ionized by multiphoton (resonant or non-resonant) processes using UV lasers. Finally, a special method of Na-doping and subsequent photoionization (NaPI) has been implemented which is essentially fragmentation-free ionization technique for some cluster species. All these methods on CLUB have recently been reviewed in Ref. 9, and are shown schematically in **Fig. 1**.

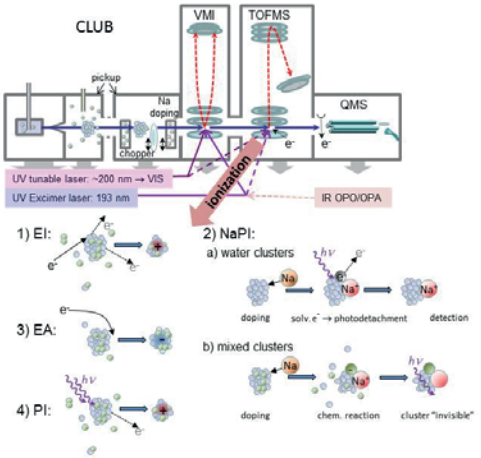

Fig. 1: *Schematic drawing of the CLUB apparatus and various implemented ionization methods for the cluster mass spectrometry: VMI –velocity map imaging; TOFMS –reflectron time-of-flight mass spectrometer; QMS –quadrupole mass spectrometer with electron ionization used, e.g., in cluster velocity measurement and pickup cross-section determination; EI – electron ionization (positive); NaPI – sodium doping and photodetachment of solvated electron; EA –electron attachment; PI –multiphoton ionization.*

3. Cluster ionization

Mass spectrometry is often used to analyse the sizes and compositions of clusters generated in supersonic expansions. However, one of the long-standing questions of the cluster research is the relationship between the measured mass spectrum of the ionized species and the original neutral clusters. Weak intermolecular bonds can break upon the ionization leading to substantial cluster fragmentation; on the other hand, the excess energy can be redistributed over the many degrees of freedom of the clusters lading to the cluster ion stabilization. Therefore we have implemented different ionization methods which yield different mass spectra for the same neutral clusters. Information about the neutral clusters can be learned from the complementary mass spectra, and insight can be gained into the processes ongoing in the clusters upon different interaction with electrons or photons.

This will be illustrated on a few examples of mixed clusters of nitrogen containing molecules (HNO_3, N_2O, NO) with water. These species are atmospherically relevant [10-13].

4. Electron attachment to clusters

The dissociative electron attachment [14] (DEA) to molecules is an important process playing important role in many areas. Here again we focus on the question: How the environment influences the DEA process?

We have studied the DEA to biomolecules (e.g. uracil, U) microhydrated with water. First, a new method was introduced to produce pure beams of biomolecules microhydrated with a few water molecules, e.g. $U{\cdot}(H_2O)_N$, free of clusters of biomolecules and water clusters (U_M, $U_M{\cdot}(H_2O)_N$, $M>1$, and $(H_2O)_N$).

Second, we have demonstrated a protective action of water environment on DEA to biomolecules: the water molecules inhibit the dissociative processes. While the electron attachment leads to hydrogen loss $(U\text{-}H)^-$ for the isolated U molecule, already the presence of a single water molecule in $U{\cdot}H_2O$ yields the stable molecular anion U^- [15].

The DEA is important also in technological processes, e.g. focussed electron beam induced deposition (FEBID). Precursor molecules, e.g. $Fe(CO)_5$ are deposited on a substrate and upon the action of a focussed electron beam the ligand CO molecules are evaporated and a 3D metal nanostructures are generated. To understand this process in detail, we deposit the $Fe(CO)_5$ molecules on large argon clusters and investigate the DEA to small $Fe(CO)_5$ clusters on Ar_N. An electron self-scavenging mechanism has been observed and described in these experiments.[16]

5. Pickup of Atmospheric molecules on acid clusters

To understand the generation and growth of atmospheric aerosols at the molecular level, we investigate the pickup of various atmospheric molecules on small acid clusters. The clusters are represented by the mixed clusters of nitric or sulfuric acid with water. Atmospheric molecules such as isoprene did not pick up on the acid clusters efficiently. Methanol was measured for comparison and adsorbed on the cluster very efficiently. Molecules similar to isoprene (2-methyl-3-buten-2-ol, 3-methyl-3-buten-1-ol) with free OH bonds were measured. These molecules picked up efficiently as well. Similarly, □-pinene was adsorbed on the acid clusters very inefficiently compared to analogical molecule with OH group, verbenol (**Fig. 2** shows the molecular structures).

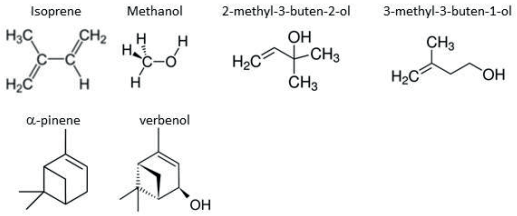

Fig. 2: *Structures of the molecules used for the pickup on nitric and sulphuric acid clusters.*

Acknowledgement: The Czech Science Foundation grant no.: 17-04068S and the Czech Academy of Sciences: “Praemium Academiae”.

References:

[1] J. Fedor, V. Poterya, A. Pysanenko, and M. Fárník, *J. Chem. Phys.* **135** (2011) 104305

[2] J. Lengyel, J. Kočišek, V. Poterya, A. Pysanenko, P. Svrčková, and M. Fárník, D. K. Zaouris, and J. Fedor: *J. Chem. Phys.* **137** (2012) 034304

[3] A. Pysanenko, A. Habartová, P. Svrčková, J. Lengyel, V. Poterya, M. Roeselová, J. Fedor and M. Fárník: *J. Phys. Chem. A* **119** (2015) 8991

[4] P. Rubovič, A. Pysanenko, J. Lengyel, D. Nachtigalová, and M. Fárník, *J. Phys. Chem. A* **120** (2016) 4720

[5] A. Pysanenko, J. Kočišek, D. Nachtigallová, V. Poterya and M. Fárník, *J. Phys. Chem. A* **121** (2017) 1069

[6] V. Poterya, J. Lengyel, A. Pysanenko, P. Svrčková, and M. Fárník, *J. Chem. Phys.* **141** (2014) 074309

[7] P. Svrčková, A. Pysanenko, J. Lengyel, P. Rubovič, J. Kočišek, V. Poterya, P. Slavíček and M. Fárník, *Phys. Chem. Chem. Phys.* **17** (2015) 25734

[8] V. Poterya, D. Nachtigalová, J. Lengyel, and M. Fárník, *Phys. Chem. Chem. Phys.* **17** (2015) 25004

[9] M. Fárník and J. Lengyel, *Mass Spec. Rev.* (2017)

[10] J. Lengyel, A. Pysanenko, J. Kočišek, V. Poterya, C. Pradzynski, T. Zeuch, Petr Slavíček and M. Fárník, *J. Phys. Chem. Lett.* **3** (2012) 3096

[11] D. Šmídová, J. Lengyel, A. Pysanenko, J. Med, P. Slavíček and M. Fárník, *J. Phys. Chem. Lett.* **6** (2015) 2865

[12] J. Lengyel, A. Pysanenko, P. Rubovič and M. Fárník, *Eur. Phys. J. D* **69** (2015) 269

[13] D. Šmídová, J. Lengyel, J. Kočišek, A. Pysanenko and M. Fárník, *Int. J. Mass Spectrom.* **421** (2017) 144

[14] I. I. Fabrikant, S. Eden, N. J. Mason, and J. Fedor in E. Arimondo, C. C. Lin and S. F. Yelin, editors, *Advances In Atomic, Molecular, and Optical Physics, Vol. 66, p. 546*

[15] J. Kočišek, A. Pysanenko, M. Fárník, and J. Fedor, *J. Phys. Chem. Lett.* **7** (2016) 3401

[16] J. Lengyel, J. Kočišek, M. Fárník, and J. Fedor, *J. Phys. Chem. C* **120** (2016) 7397

Rational Design of Solid Interfaces Using Soft-landing of Mass-Selected Ions

Julia Laskin, Grant E. Johnson, Venkateshkumar Prabhakaran, Jonas Warneke
Purdue University, Department of Chemistry

Deposition of complex molecules and clusters on supports plays an important role in a variety of disciplines including materials science, catalysis and biochemistry. In particular, deposition of clusters on surfaces has attracted considerable attention due to their nonscalable, highly size-dependent properties. The ability to precisely control the composition and morphology of clusters is crucial for the development of next generation materials with rationally tailored properties. Soft-landing of ions onto surfaces introduces unprecedented selectivity into surface modification by eliminating the effect of solvent and sample contamination on the quality of the film. The ability to select the mass-to-charge ratio of the precursor ion, its kinetic energy and charge state along with precise control of the size, shape and position of the ion beam on the deposition target makes soft-landing an attractive approach for surface modification. High-purity uniform thin films on surfaces generated using mass-selected ion deposition facilitate understanding of critical interfacial phenomena relevant to catalysis and materials science. Our studies focused on understanding charge retention by soft-landed cluster ions demonstrated that soft-landed stable anions efficiently retain charge in surfaces due to the high electron binding energy that prevents electron loss by the cluster. These findings provide the scientific foundation for the rational design of interfaces for advanced catalysts and energy storage devices. For example, we observed superior performance of redox supercapacitor electrodes prepared using soft-landing of mass-selected polyoxometalate cluster anions in comparison with conventional solution-phase deposition. We demonstrated that both the uniform deposition of polyoxometalate cluster anions onto carbon nanotubes and elimination of counter cations contribute to the improved device performance. High-coverage deposition of cluster anions provides access to unique layered materials with self-organization properties controlled by the electronic properties of the anion. These findings provide a path for the controlled design of layered architectures using cluster deposition.

Watching Molecules Change Their Shape

Yoni Toker
Bar-Ilan University, Israel

Gas phase fragmentation often involves complicated pathways involving isomerizations and cyclizations. Recently it has become possible to directly observe isomerizations and fragmentations using a two stage ion mobility spectroscopy (IMS-IMS) technique, as well as measure the barrier energies for isomerizations. Here we will demonstrate the power of the technique on the case of the retinal protonated schiff base chromphore, which is the photon detector used in vision. By comparing different derivatives of this chromophore we will show a correspondence between barrier energies for isomerization and fragmentation pathway.

References:

[1] L. Musbat, M. Nihamkin, Y. Toker, J. M. Dilger, D. R. Fuller, T. J. El-Baba, D. E. Clemmer, S. Sarkar, L. Kronik, A. Hirshfeld, N. Friedman, and M. Sheves, Measurement of the stabilities of isolated retinal chromophores. *Phys. Rev. E* **95** (2017), 012406.

[2] J. Dilger, L. Musbat, M. Sheves, A. B. Bochenkova, D. E. Clemmer, Y. Toker, Direct Measurement of the Isomerization Barrier of the Isolated Retinal Chromophore. *Ang. Chemie Int. Ed.* **127** (2015), 4830-4834. (Frontispiece)

Out of equilibrium dynamics of water nanodroplets

F. Berthias, P. Bertier, T. Salbaing, L. Feketeová, H. Abdoul-Carime, B. Farizon, M. Farizon
Université de Lyon; Université Claude Bernard Lyon1; Inst. de Physique Nucléaire de Lyon, CNRS/IN2P3 UMR 5822, 69622 Villeurbanne Cedex, France

F. Calvo
Univ Grenoble 1, CNRS, LIPhy UMR 5588, F-38041 Grenoble, France

T. D. Märk
Institut für Ionenphysik und Angewandte Physik, Leopold Franzens Universität, 6020 Innsbruck, Austria

The evaporation of a water molecule occurs through the breaking of one or several hydrogen bonds. These hydrogen bonds are responsible for many remarkable features of water. At the macroscopic scale, water is known for its exceptional ability to thermalize a system, while at the microscopic level, a high-speed transfer of vibrational energy via hydrogen bonds is observed. What happens when a small number of water molecule are involved?

In the experiment carried out with the device DIAM IPN Lyon, relaxation of protonated water nanodroplets is observed after electronic excitation of one of its molecules. The implementation of a velocity map-imaging (VMI) method associated with the COINTOF technique (Correlated Ion and Neutral Time-Of-Flight) allowed us the measurement of the velocity distribution of molecules evaporated from protonated water clusters, mass- and energy preselected. The behavior of the measured velocity distributions shows that even for extremely small water nanodroplets, the complete energy redistribution before the evaporation prevails and the velocity distributions of these events is closed to those expected for macroscopic droplets from around ten water molecules. However, these measurements of the velocity distributions also highlight a high speed distinct contribution corresponding to the evaporation of a molecule before complete redistribution of energy. The measured velocity distributions for heavy water nanodroplets show a proportion of these non-ergodic events more important that for normal water. The measurements carried out with different target atoms show that the proportion of non-ergodic events decreases with decreasing the energy deposited in the droplet.

References

Velocity of a Molecule Evaporated from a Water Nanodroplet: Maxwell–Boltzmann Statistics versus Non-Ergodic Events.
H. Abdoul-Carime, F. Berthias, L. Feketeová, M. Marciante, F. Calvo, V. Forquet, H. Chermette, B. Farizon, M. Farizon, and T. D. Märk, *Angewandte Chemie* **54** (2015) 14685-14689.

Collision-induced evaporation of water clusters and contribution of momentum transfer.
F. Calvo, F. Berthias, L. Feketeová, H. Abdoul-Carime, B. Farizon, and M. Farizon, *Eur. Phys. J. D* **71** (2017) 110.

Measurement of the velocity of neutral fragments by the "correlated ion and neutral time of flight" method combined with "velocity-map imaging.
F. Berthias, L. Feketeová, R. Della Negra, T. Dupasquier, R. Fillol, H. Abdoul-Carime, B. Farizon, M. Farizon, and T. D. Märk. *Rev. Sci. Instrum*. **88** (2017) 08301

Correlated Ion and Neutral Time of Flight Technique combined with Velocity Map Imaging: Quantitative Measurements for Dissociation Processes in Excited Molecular Nano-Systems.
F. Berthias, L. Feketeová, R. Della Negra, T. Dupasquier, R. Fillol, H. Abdoul-Carime, B. Farizon, M. Farizon, and T. D. Märk. *Rev. Sci. Instrum*., in press (2017).

Non-local Energy and Charge Transfer in Clusters and Liquids

Petr Slavíček[1,2)]
[1)]*Department of Physical Chemistry, University of Chemistry and Technology, Prague, Czech Republic Email: petr.slavicek@vscht.cz*
[2)]*J. Heyrovský Institute of Physical Chemistry v.v.i, Academy of Sciences of the Czech Republic, Prague, Czech Republic.*

Molecules upon X-ray irradiation appear in highly excited states, with vacancies in the core or inner valence orbitals. The relaxation is dominantly brought about by non-radiative processes such as Auger decay. Recently, non-local, intermolecular relaxation processes such as Intermolecular Coulomb Decay (ICD) or Electron Transfer Mediated Decay (ETMD) have been proposed theoretically and later confirmed experimentally.

In my talk, I will focus on modelling of the processes for hydrogen bonded clusters and liquids. The possible use of the above phenomena as novel liquid phase spectroscopies will be discussed as well.[1-2] I will emphasize the role of the entanglement between the electronic and nuclear motion.[3] At some instances, the nuclear motion closes the non-radiative deactivation.[4] On the contrary, the very same mechanism can greatly accelerate non-local transfer of energy and charge in other cases.[5] We revealed a new process, the so called Proton Transfer Mediated Charge Separation (PTM-CS) process, in which both the electronic and nuclear motions are combined.[6] Manifestation of this process will be discussed on several examples.[7-10] The implications of the PTM-CS process on the first few femtoseconds in radiation chemistry will be discussed. I will mostly focus on the results of theoretical simulations, showing results obtained with quantum dynamics, non-adiabatic semi-classical dynamics and real time density functional theory. In addition, I will discuss the respective experimental results.

Finally, I will discuss the results in a broader perspective of the emerging field of X-ray photochemistry. The area has become more attractive only recently as the number of various advanced light sources (synchrotrons, X-ray free electron lasers, high-harmonic generation or X-ray plasma sources) appeared and as numerous new experiments have been waiting for interpretation. At the same time, the field has an enormous application potential, e.g. in the context

of advanced radiation treatment or modern technologies such as EUV lithography.

References

[1] I. Unger, R. Seidel, S. Thürmer, M. N. Pohl, E. F. Aziz, L. S. Cederbaum, E. Muchová, P. Slavíček, B. Winter, N. V. Kryzhevoi, *Nature Chemistry* **9** (2017) 708.
[2] M. N. Pohl, C. Richter, E. Lugovoy, R. Seidel, P. Slavíček, E. F. Aziz, B. Abel, B. Winter, U. Hergenhahn, *J. Phys. Chem. B* **121** (2017) 7709.
[3] P. Slavíček, N. V. Kryzhevoi, E. F. Aziz, B. Winter, *J. Phys. Chem. Lett.* **7** (2016) 234.
[4] O. Svoboda, D. Hollas, M. Ončák, P. Slavíček, *Phys. Chem. Chem. Phys.* **15** (2013) 11531.
[5] P. Slavíček, B. Winter, L. S. Cederbaum, N. V. Kryzhevoi, *J. Am. Chem. Soc.* **136** (2014) 18170.
[6] S. Thürmer, M. Ončák, N. Ottosson, R. Seidel, U. Hergenhahn, S. E. Bradforth, P. Slavíček, B. Winter, *Nature Chemistry* **5** (2013) 590.
[7] S. Thürmer, I. Unger, P. Slavíček, B. Winter, *J. Phys. Chem. C* **117** (2013) 22268.
[8] I. Unger, D. Hollas, R. Seidel, S. Thürmer, E. Aziz, P. Slavíček, B. Winter, *J. Phys. Chem. B* **119** (2015) 10750
[9] D. Hollas, M. N. Pohl, R. Seidel, E. F. Aziz, P. Slavíček, B. Winter, *Sci. Rep.* **7** (2017) 756.
[10] I. Unger, S. Thürmer, D. Hollas, E. F. Aziz, B. Winter, P. Slavíček, *J. Phys. Chem. C* **118** (2014) 29142.

Acknowledgement

The support by Czech Science Foundation (projects no. 18-23756S).

Advances in synthesis of small chiral molecules

Jürgen Stohner
Zürich University of Applied Science (ZHAW), Institute of Chemistry and Biotechnology (ICBT), Campus Reidbach RT E309.3, Einsiedlerstrasse 31, CH 8820 Wädenswil, Switzerland
Email: sthj@zhaw.ch

Small chiral molecules (C_1- and C_2-compounds) are very useful target molecules at the border of chemistry and physics. Major efforts focus currently on the attempts to measure parity violating effects in molecular spectroscopy [1-3], the determination of anisotropy in chiral Photon Electron Detachment [4], very precise measurements of the specific rotatory power in gas-phase samples [5], as well as on the determination of the absolute configuration of gas-phase molecules [6,7].
Recent reviews summarize our current understanding of the role of molecular parity violation [2,3]. Understanding those effects require a detailed spectroscopic knowledge, often supported/accompanied by *ab initio* calculations. In relation to parity violating effects, we have shown recently, however, that the interpretation of line shifts require a deep understanding of the high-resolution spectroscopy, including for example the influence of nuclear spin on molecular rotation [8].

All chiroptical experiments mentioned in the preceding section require enantiopure target molecules. In the past, the resolution of a racemate into its enantiomers was almost exclusively achieved by fractional crystallization [9] by a method introduced at the beginning of what we now call “stereochemistry” starting when Louis Pasteur separated large crystals of sodium ammonium tartrate using tweezers and a magnifying glass in 1848 [10].

An alternative separation method is based on gas chromatography. The gas-chromatographic separation of enantiomers is very difficult when large quantities (a few gram) are involved. While a separation on an analytical scale (a few microgram) is possible by using chiral stationary phases, there is no guarantee that a separation can be achieved by up-scaling using the same chiral column material and larger columns. The search for column material, which facilitates such separation is of utmost importance but very difficult. We report our most recent achievements in this respect [11,12].

We devised a synthetic route to obtain halogenated chiral acetic acids, which serve as precursors to chiral methanes. We are able to obtain H- and D-isotopomers of the chiral halomethanes [13] and even explored a synthetic pathway to ^{35}Cl- and ^{37}Cl-chiral $CHCl_2F$ [14]. This isotopically chiral methane is especially interesting because enantio-separation is impractical by all current techniques. CHBrClF and $CH^{35}Cl^{37}ClF$ have been used to demonstrate the capability of gas-phase Coulomb explosion imaging (CEI) for the direct determination of the absolute configuration of molecules in the gas phase [6,7]. In case of $CH^{35}Cl^{37}ClF$, it is clear that COLTRIMS is the only method for the direct determination of the absolute configuration; other currently available techniques cannot cope with chirality caused by isotope substitution. We should mention that isotopically chiral target molecules have been used in the past to explore enzymatic processes by using H-, D-, and T-labeled chiral methanol, however, no isotopologues beyond hydrogen have been investigated in the past [15,16].

References

[1] M. Quack, *Angew. Chem. Int. Ed.* **41**, 4618 (2002).
[2] M. Quack and J. Stohner, *Chimia* **59**, 530 (2005).
[3] M. Quack, J. Stohner, and M. Willeke, *Annu. Rev. Phys. Chem*. **59**, 741 (2008).
[4] C. Lux, M. Wollenhaupt, C. Sarpe, T. Baumert, *ChemPhysChem* **16**, 115 (2015).
[5] P. Lahiri, K.B. Wiberg, P.H. Vaccaro, *J. Phys. Chem. A* **119**, 8311 (2015).
[6] M. Pitzer, M. Kunitski, A. S. Johnson, T. Jahnke, H. Sann, F. Sturm, L. Ph. H. Schmidt, H. Schmidt-Böcking, R. Dörner, J. Stohner, J. Kiedrowski, M. Reggelin, S. Marquardt, A. Schiesser, R. Berger and M. S. Schöffler, *Science* **341**, 1096 (2013).
[7] M. Pitzer, G. Kastirke, M. Kunitski, T. Jahnke, T. Bauer, C. Goihl, F. Trinter, C. Schober, K. Henrichs, J. Becht, S. Zeller, H. Gassert, M. Waitz, A. Kuhlins, H. Sann, F. Sturm, F. Wiegandt, R. Wallauer, L. Ph. H. Schmidt, A.S. Johnson, M. Mazenauer, B. Spenger, S. Marquardt, S. Marquardt, H. Schmidt-Böcking, J. Stohner, R. Dörner, M. Schöffler, R. Berger, *ChemPhysChem* **17**, 2465 (2017).
[8] F. Hobi, R. Berger and J. Stohner, *Mol. Phys.* **111**, 2345 (2013).
[9] B. Darquié, C. Stoeffler, A. Shelkovnikov, C. Daussy, A. Amy-Klein, C. Chardonnet, S. Zrig, L. Guy, J. Crassous, P. Soulard, P. Asselin, T. R. Huet, P. Schwerdtfeger, R. Bast and T. Saue, *Chirality* **22**, 870 (2010).
[10] L. Pasteur, *C. R. Acad. Sci. Paris* **26**, 535 (1848).
[11] S. Manov, V. Galati, M. Meister, M. Mazenauer, B. Spenger, J. Stohner, SASP 2016, Proceedings of the 20th Symposium on Atomic, Cluster and Surface Physics, J. Stohner and C. Yeretzian (Eds.), Innsbruck University Press, Innsbruck, Austria, p. 199 (2016).
[12] M. Meister, MSc Thesis, ZHAW Wädenswil (2017).

[13] M. R. Mazenauer, S. Manov, V. M. Galati, P. Kappeler, J. Stohner, *RSC Advances* (2017); accepted.
[14] V.M. Galati, MSc Thesis, ZHAW Wädenswil (2017).
[15] J. Lüthy, J. Rétey, D. Arigoni, *Nature* **221**, 1213 (1969).
[16] J. W. Cornforth, J.W. Redmond, H. Eggerer, W. Bückel, C. Gutschow, *Nature* **221**, 1212 (1969).

Bimolecular Oxygen Atom Reactions in Helium Nanodroplets

Joseph T. Brice and Gary E. Douberly
Department of Chemistry, University of Georgia, Athens, GA 30602

Catalytic thermal cracking of O_2 is employed to dope helium droplets with $O(^3P)$ atoms. Mass spectrometry of the doped droplet beam reveals an O2 dissociation efficiency larger than 60%; approximately 26% of the droplet ensemble is doped with single oxygen atoms. Sequential capture of $O(^3P)$ and HCN leads to the production of a hydrogen-bound O–HCN complex in a $^3\Sigma$ electronic state, as determined via comparisons of experimental and theoretical rovibrational Stark spectroscopy. Ab initio computations of the three lowest lying intermolecular potential energy surfaces reveal two isomers, the hydrogen-bound ($^3\Sigma$) O–HCN complex and a nitrogen-bound ($^3\Pi$) HCN–O complex, lying 323 cm^{-1} higher in energy. The HCN–O to O–HCN interconversion barrier is predicted to be 42 cm^{-1}. Consistent with this relatively small interconversion barrier, there is no experimental evidence for the production of the nitrogen-bound species upon sequential capture of $O(^3P)$ and HCN.

The HCN + $O(^3P)$ results presented here demonstrate the feasibility for analogous alkene + $O(^3P)$ spectroscopic studies, in which $O(^3P)$ and alkenes of varying substitution are combined in helium droplets via the sequential capture scheme. As the real reaction barrier (i.e., for the ethene and propene reactions) evolves to being submerged below the asymptotic limit (i.e., for the butene reactions), one might expect that strongly bound reaction intermediates, such as triplet biradicals, will be observed in helium droplets, rather than van der Waals complexes. Given the fact that a 10000 atom helium droplet can dissipate 140 kcal/mol, it should be possible to quench the internal energy of these reaction intermediates and probe them for the first time spectroscopically.

Studying Site Specific Dynamics and Kinetics on Surfaces using Velocity Selected Ion Imaging

Jannis Neugebohren[1], Dmitriy Borodin[1], Hinrich W. Hahn[1], Jan Altschäffel[1,2], Alexander Kandratsenka[2], Daniel J. Auerbach[2], Dirk Schwarzer[2], Alec M. Wodtke[1,2,3], Theofanis N. Kitsopoulos[2,5,6]

[1]Department of Dynamics at Surfaces, Max Planck Institute for Biophysical Chemistry, Am Faßberg 11, 37077 Göttingen, Germany [2]Department of Dynamics at Surfaces, Max Planck Institute for Biophysical Chemistry, Am Faßberg 11, 37077 Göttingen, Germany.

[3]International Center for Advanced Studies of Energy Conversion, Georg-August University of Goettingen, Tammannstraße 6, 37077 Göttingen, Germany.

[4] Department of Chemistry, University of Washington, Seattle, WA 98195-1700, USA

[5] Department of Chemistry, University of Crete, Heraklion, Greece

[6] Institute of Electronic Structure and Laser – FORTH, Heraklion, Greece

Charles T. Campbell

University of Washington, Seattle, WA 98195-1700, USA

Dan J. Harding

KTH - Royal Institute of Technology, Dept. of Chemical Engineering, SE-100 44 Stockholm, Sweden

Abstract

I will introduce how to apply slice ion imaging to study the dynamics and kinetics of reactions on surfaces. Our first application involves the study the site specific oxidation of CO on Pt(111) and Pt(332) crystals. This new method allows for measurements of the “kinetic traces” i.e., CO_2 product flux vs. reaction time. Because the symmetry and orientation of the active site strongly influences the speeds and desorption angles of newly formed products, we are able to identify the elementary reactions steps and extract the respective rate constants (activation energies and prefactors).

Infrared and velocity map imaging studies of decorated metal clusters and metal–ligand complexes

Alexander S Gentleman, Andreas Iskra, Ethan M Cunningham,
Alice S Green and Stuart R Mackenzie
University of Oxford, Physical and Theoretical Chemistry Laboratory

Small gas–phase metal clusters and metal–ligand complexes provide ideal model system in which to explore fundamental interactions which lie at the heart of many heterogeneous catalytic processes.

Here we present recent results from laboratory and free electron laser studies of important processes such as:

- Size–selective CO_2 activation on anionic platinum clusters, Pt_n^-
- N_2O binding motifs to individual metal / metal oxide ions
- CH activation at individual metal centres and
- Size– and charge–selective CO activation on mixed metal “nano–alloy” clusters.

All experimental data are interpreted with the help of quantum chemical calculations which shed light on details of the reactive free energy surface and the kinetic trapping of excited states far from the global minimum structure.

Photoelectron spectroscopy – from understanding photoelectron circular dichroism to strong field coherent control

Koch Christiane
Universität Kassel, 34132 Kassel

Photoelectron spectroscopy reveals important information on electron dynamics in atoms and molecules. A striking effect is photoelectron circular dichroism (PECD). It refers to the forward/backward asymmetry in the photoelectron angular distribution with respect to the light propagation axis. PECD has recently been demonstrated in femtosecond multi-photon photoionization experiments with randomly oriented chiral molecules [1,2]. We are able to explain the experimental observations, at least semi-quantitatively, by combining perturbation theory for the light-matter interaction with ab initio calculations for the bound spectrum and a single-center expansion of the photoelectron continuum [3]. In particular, we find the d-wave character of an intermediate state to be crucial for the observed PECD.

In the non-perturbative regime, tailoring the pulsed electric field in its amplitude, phase or polarization allows for the control of ultrafast dynamics. Optimal control theory can be used to enhance desired features in the photoelectron spectra and angular distributions or in the photoion. For example, XUV pulse shaping may result in directed electron emission [4] and improve hole coherence in the photoion. For the latter, we find interference between a one-photon and a three-photon pathway to be important but spectral chirps are required to counteract detrimental many-electron effects.

[1] C. Lux et al., *Angew. Chem. Int. Ed.* **51**, 5001 (2012).
[2] C. S. Lehmann et al., *J. Chem. Phys.* **139**, 234307 (2013).
[3] R. E. Goetz et al., *J. Chem. Phys.* **146**, 024306 (2017)
[4] R. E. Goetz et al., *Phys. Rev. A* **93**, 013413 (2016).

Reactions of oxygen and nitrogen atoms with aliphatic and aromatic hydrocarbons by crossed beam experiments

Nadia Balucani
DCBB Unitversità degli Studi di Perugia, Via Elce di Sotto, 06123 Perugia, Italy

In our laboratory, we have pursued a systematic investigation of bimolecular reactions involving atomic radicals and simple hydrocarbons (HCs) by means of the crossed molecular beam method with mass spectrometric detection (see, for instance, Ref. [1]). Advantage has been taken of an efficient, versatile radiofrequency discharge beam source for the production of atomic (C, N, O, S, CI) and diatomic (CN, OH, C_2) radicals [2]:
In this contribution, recent results on the reactions involving either atomic oxygen in its ground electronic state, O(^{3}P), or atomic nitrogen in its first electronically excited state, N(^{2}D), and unsaturated HCs, as well as benzene and toluene, will be presented. The investigated systems are of relevance in combustion chemistry (O+HCs, [3]) or in the chemistry of the upper atmosphere of Titan, the giant moon of Saturn (N(^{2}D)+HCs, [4]) with potential implications prebiotic chemistry [5].

Acknowledgments:
Support by Fondazione Cassa Risparmio Perugia (Project 2015.0331.021 Scientific and Technological Research), University of Perugia (Fondo Ricerca di Base 2014), and MIUR (PRIN 2015, STARS in the CAOS - Simulation Tools for Astrochemical Reactivity and Spectroscopy in the Cyberinfrastructure for Astrochemical Organic Species, 2015F59J3R) is greatfully acknowledged.

References

[1] P. Casavecchia et al., Int. Rev. Phys. Chem., 34, 161 (2015); and references therein.
[2] F. Leonori et al., Mol. Phys., 108, 1097 (2010).
[3] N. Balucani et al., Energy, 43, 47 (2012).
[4] V. Vuitton, O. Dutuit, M. A. Smith, N. Balucani, Chemistry of Titan's atmosphere, in: Titan: Surface, Atmosphere and Magnetosphere (ISBN-10: 0521199921), I. Mueller-Wodarg, C. Griffith, E. Lellouch & T. Cravens, Eds., Cambridge University Press, 2014.
[5] N. Balucani, Chem. Soc. Rev., 41, 5473 (2012); and refs. therein

Electric deflection of massive cold dipoles: Field-oriented polar molecules within helium nanodroplets

Daniel Merthe, John Niman, and Vitaly V. Kresin
Department of Physics and Astronomy
University of Southern California, Los Angeles, CA 90089-0484, USA

The use of electric fields to orient and deflect polar molecules dates back to electric deflection experiments on “molecular rays” in the late 1920’s [1]. This line of research has continued at full intensity for ninety years, and has been extended to nanocluster particles [2-4]. More recently, polar molecules have attracted a lot of interest in the pursuit of cooling add trapping applications [5,6]. However, ultracold trapping has been achieved only for a small number of diatomic molecules, while supersonic expansion cooling typically produces molecules at rotational and vibrational energies much greater than several Kelvin. In specialized cases, supersonic beams and buffer gas cooling [7] can reach temperatures just above 1 K, but this works for only a limited number of molecules and requires specialized optimization for each one.

On the other hand, by embedding polar molecules in a beam of superfluid helium nanodroplets one can reduce their temperatures to just 0.4 K, and the approach works for a very wide range of molecules and agglomerates [8]. Application of an external static electric field transforms their free rotational states into pendular ones [9], achieving nearly full orientation of the dipoles.

This presentation will describe how this extremely high degree of achievable orientation can be exploited in beam deflection experiments [10]. Despite having masses of up to several tens of thousands of Daltons (possibly the heavies species subjected to “deflectometry”), host helium droplets can be deflected by a very large distance: up to a few millimeters.

This approach has been demonstrated using helium droplets containing molecules of alkali halides, polar solvents (dimethyl sulfoxide and formamide), and amino acid molecules (histidine and tryptophan). As suggested by the breadth of this list, the attractiveness of the method is its wide applicability and its potential as a tool for determining, in a very direct manner, the dipole moments of molecules that are difficult to obtain by other means. The

measurements also provide evidence for the formation of highly polar systems by dipoles assembling into aligned structures within the droplets [11]:

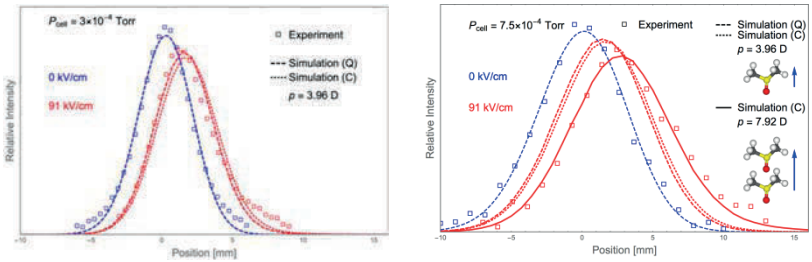

Deflection of droplets containing DMSO monomers and dimers. The left panel shows the deflection of droplet doped with single DMSO molecules, while the lower panel shows that higher density of dopants in the pick-up cell leads to the formation of highly polar DMSO dimers. In the legend, "(C)" indicates a classical treatment of rigid rotor orientation, and "(Q)" indicates a quantum rotational Stark effect treatment.

The deflection technique also provides a means to disperse droplets by size spatially. As an application of this capability, the presentation will describe a measurement of the droplet size dependence of the ionization charge transfer probability [11].

This work was supported by the U. S. National Science Foundation under grant CHE-1664601.

References

[1] R. G. J. Fraser, *Molecular Rays* (Cambridge University Press, London, 1931).

[2] M. Broyer, R. Antoine, I. Compagnon, D. Rayane, and P. Dugourd, "From clusters to biomolecules: Electric dipole, structure and dynamics," Phys. Scr. **76**, C135 (2007).

[3] W. A de Heer and V. V. Kresin, "Electric and magnetic dipole moments of free nanoclusters," in *Handbook of Nanophysics: Clusters and Fullerenes*, ed. by K. D. Sattler (CRC Press, Boca Raton, 2010).

[4] S. Heiles and R. Schäfer, *Dielectric Properties of Isolated Clusters: Beam Deflection Studies* (Springer, Dordrecht, 2014).

[5] S. A. Moses, J. P. Covey, M. T. Miecnikowski, D. S. Jin, and J. Ye, "New frontiers for quantum gases of polar molecules," Nat. Phys. **13**, 13 (2017).

[6] J. L Bohn, A. M. Rey, and J. Ye, “Cold molecules: Progress in quantum engineering of chemistry and quantum matter,” Science **357**, 1002 (2017).

[7] N. R. Hutzler, H.-I Lu, and J. M. Doyle, “The buffer gas beam: An intense, cold, and slow source for atoms and molecules,” Chem. Rev. **112**, 4803 (2012).

[8] J. P. Toennies and A. F. Vilesov, “Superfluid helium droplets: A uniquely cold nanomatrix for molecules and molecular complexes,” Angew. Chem. Int. Ed. **43**, 2622 (2004).

[9] M. Y. Choi, G. E. Douberly, T. M. Falconer, W. K. Lewis, C. M. Lindsay, J. M. Merritt, P. L. Stiles, and R. E. Miller, “Infrared spectroscopy of helium nanodroplets: Novel methods for physics and chemistry,” Int. Rev. Phys. Chem. **25**, 15 (2006).

[10] D. J. Merthe and V. V. Kresin, “Electrostatic deflection of a molecular beam of massive neutral particles: Fully field-oriented polar molecules within superfluid nanodroplets,” J. Phys. Chem. Lett. **7**, 4879 (2016).

[11] D. J. Merthe, J. Niman, and V. V. Kresin, to be published.

Cryogenic ion spectroscopy: A new tool for glycan analysis

Chiara Masellis and Thomas R. Rizzo
Ecole Polytechnique Fédérale de Lausanne, Laboratoire de chimie physique moléculaire, CH H1 621, Station 6, CH-1015 Lausanne, Switzerland

Neelam Khanal and David E. Clemmer
Department of Chemistry, Indiana University, 800 East Kirkwood Avenue, Bloomington, Indiana 47405

Glycans, or oligosaccharides, are ubiquitous in biological systems. Because they decorate the surface of cells, they play a key role in virtually all cellular recognition processes and are implicated in almost every major disease. Despite their importance, the characterization of glycan primary structure by mass spectrometry lags far behind that of proteins and DNA because of their intrinsic isomeric complexity. The isomeric nature of the monosaccharide building blocks, the stereochemistry of the glycosidic bond, the possibility of multiple attachment points, and the occurrence of isomeric branched structures all make glycans difficult to analyze.
We have recently demonstrated that cryogenic infrared spectroscopy provides unique vibrational fingerprints of glycans that distinguishes all the various types of isomerism [1, 2]. When combined with simultaneous measurements of mass and ion mobility, these fingerprints can be tabulated in a database and used to identify a given glycan from a mixture.

This talk will present our most recent results developing this technique and consider what will be needed to make it into a widespread analytical tool.

[1] Masellis, C., et al., *Cryogenic Vibrational Spectroscopy Provides Unique Fingerprints for Glycan Identification.* J. Am. Soc. Mass Spectrom., 2017. **28**: p. 2217-2222.

[2] Khanal, N., et al., *Glycosaminoglycan analysis by cryogenic messenger-tagging IR spectroscopy combined with IMS-MS.* Analytical Chemistry, 2017. **89**: p. 7601–7606.

Rotational spectroscopy in cryogenic ion traps

Oskar Asvany and Stephan Schlemmer
I. Physikalisches Institut, Universität zu Köln, Zülpicher Straße 77, 50937 Köln, Germany

1. Introduction

Rotational spectroscopy probes the transitions between the lowest quantum states of molecules and is therefore the main tool to detect these species in cold astronomical environments. For molecular structure investigations, in addition, rotational spectroscopy provides high resolution and is usually free of unwanted perturbations. This kind of spectroscopy is typically performed in standard absorption, FTMW or chirped pulse spectrometers. For the investigation of molecular ions, however, the usage of cryogenic ion traps emerged in recent years, as they offer the advantage of low-temperature operation, sensitivity, long interaction times, and mass selectivity.

The first demonstration of pure rotational spectroscopy in a cold ion trap was performed for H_2D^+ and D_2H^+ [1], leading to the detection of the corresponding THz transitions in space. This laboratory measurement was only feasible due to advantageous molecular parameters, namely large rotational spacings of the light ions, as well as the low reaction barrier which had to be surmounted in the detection process. Thus, such a scheme could not be transferred to other molecular ions in a direct manner. Therefore, several action spectroscopic schemes have been developed in the last decade to make rotational spectroscopy in traps a more general approach. One novel method is the state-selective attachment of He to cations, in which the rotational excitation of the naked molecular ion hinders the ternary attachment of helium atoms at a temperature close to 4 K [2,3,4]. Another family of approaches is a double-resonance scheme, in which the rotational excitation is followed by excitation into a vibrationally excited state [5,6,7] or by using photodetachment with a visible photon as the detection method [8]. This presentation will focus on recent developments in rotational double-resonance schemes.

2. Experimental methods

For the rotational double resonance spectroscopy in traps, the ions are irradiated with a (sub)mm-wave photon and a second photon (IR or visible) at the same time. One procedure of overlaying the two beams is shown in the Figure below (example is from the Cologne laboratories for the ion OH^-, figure taken from [6]). A hole in the elliptical mirror is a simple way to superpose the two beams, and the used diamond window has the advantage of being transparent over a large spectral range. For the action spectroscopy, several thousand mass-selected ions are kept and cooled in the ion trap (a 22-pole ion trap in this case [9]) and irradiated typically for one second. The excitation changes the mass composition of the ion trap content, which is detected in a mass-spectrometric detector (not shown in Figure). By keeping the second photon fixed on resonance and scanning the frequency of the rotational excitation (green and red arrows in inset of adjacent figure, respectively), a rotational line can be recorded. The adjacent example shows the measurement of the $2_{02} \leftarrow 1_{01}$ rotational transition of para-CH_2D^+ at a trap temperature of 10K [7]. In this case, the detection with the second photon involves excitation into a vibrational state with subsequent reaction. A Gaussian fit of the seen signal gives the center frequency of 534280.0217(24) MHz. Due to the cryogenic temperatures, a good signal-to-noise ratio, as well as atomic clock referenced (sub)mm-wave sources, the center frequencies can be generally determined with a relative precision approaching 10^{-9}.

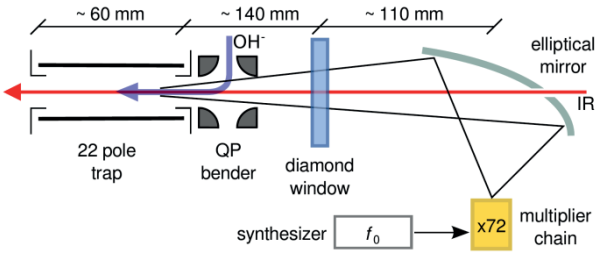

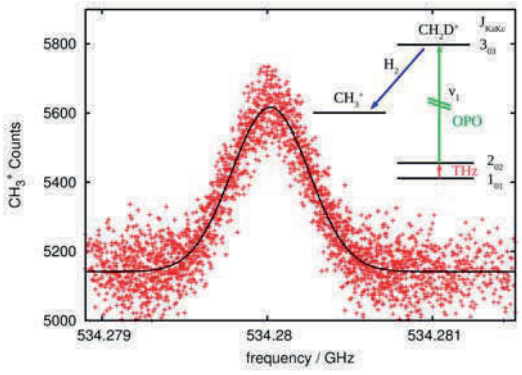

3. Double-resonance rotational spectroscopy of weakly bound ionic complexes

This talk reviews rotational action spectroscopic schemes in ion traps, in particular double-resonance schemes. The focus will be on a novel method developed in the Cologne laboratories, in which rotational excitation is followed by (IR) excitation into a dissociative resonance state. Its general applicability is demonstrated for the complex CH_3^+-He, which undergoes predissociation through its symmetric and antisymmetric C-H stretching motions v_1 and v_3 . This molecule has been chosen due to its simple spectrum (closed shell symmetric top molecule), its large dipole moment, and because its v_3 band is already known [10]. It is shown that while predissociation spectroscopy is hampered by lifetime broadening, this is not the case for rotational spectroscopy, enabling structural information with highest precision. Future challenging targets of this new method are molecular ions like H_3^+-He, HCO^+-He, or H_2^+-He. In particular H_2^+-He seems interesting, as no conclusive spectroscopic data exists for this fundamental three-electron-system. Also, this molecule may have played an important role in the early universe.

Acknowledgement

Our work is supported by the Deutsche Forschungsgemeinschaft via SFB956.

References

[1] O. Asvany et al., *Phys. Rev. Lett.* **100** (2008) 233004
[2] S. Brünken et al., *Astrophys. J. Lett.* **783** (2014) L4
[3] S. Brünken et al., *J. Mol. Spectr.* **332** (2017) 67
[4] J. L. Domenech, S. Schlemmer, and O. Asvany, *Astrophys. J.* **849** (2017) 60
[5] S. Gärtner et al., *J. Phys. Chem. A* **117** (2013) 9975
[6] P. Jusko et al., *Phys. Rev. Lett.* **112** (2014) 253005
[7] M. Töpfer et al., A&A **593** (2016) L11
[8] S. Lee et al., *Phys. Rev. A* **93** (2016) 032513
[9] O. Asvany et al., *Appl. Phys. B* **114** (2014) 203
[10] R. V. Olkhov, S. A. Nizkorodov, and O. Dopfer, *J. Chem. Phys.* **110** (1999) 9527

BerlinTrap: First applications of a new cryogenic 22-pole ion trap spectrometer

Otto Dopfer
Institut für Optik und Atomare Physik, TU Berlin (Germany)

The first applications of a new tandem mass spectrometer (BerlinTrap) combining an electrospray ion source, a quadrupole mass spectrometer, a cryogenic 22-pole ion trap (4-300 K), and an orthogonal reflectron time-of-flight mass spectrometer are described [1]. The trapped ions are cooled by helium buffer-gas cooling. The formation and solvation shell-structure of weakly-bound $He_nH_3O^+$ complexes and the electronic photodissociation spectrum of the protonated amino acid tyrosine are used to calibrate the setup for cooling, tagging, and spectroscopic capabilities. A vibrational temperature below 20 K is inferred for protonated tyrosine.

In a first application, the geometric and electronic structure of protonated and metalated flavins (lumichrome and lumiflavin) are elucidated by electronic photodissociation spectroscopy in the visible range at 20 K. These studies complement earlier IRMPD studies at room temperature [2-4] and provide insight into the effects of protonation and complexation with alkali ions on the electronic structure of the flavin.

In a second application, He_nX^{q+} clusters are grown in the cold ion trap by condensation of He atoms onto singly and doubly charged atomic and molecular cations (e.g., X=Na, Ba, Ca, Ne, Ar, OH, H_2O, H_3O, CH_3, CH_3OH_2), and the observed abundance ratios provide valuable insight into the He-ion binding energies and the structure of solvation shells.

References

[1] A. Günther, P. Nieto, D. Müller, A. Sheldrick, D. Gerlich, O. Dopfer, *J. Mol. Spectrosc.* **332**, 8-15 (2017).
[2] J. Langer, A. Günther, S. Seidenbecher, G. Berden, J. Oomens, O. Dopfer, *Chem. Phys. Chem.* **15**, 2550-2562 (2014).
[3] A. Günther, P. Nieto, G. Berden, J. Oomens, O. Dopfer, *Phys. Chem. Chem. Phys.* **16**, 14161-14171 (2014).
[4] P. Nieto, A. Günther, G. Berden, J. Oomens, O. Dopfer, *J. Phys. Chem. A* **120**, 8297-8308 (2016).

Spectroscopy in a low temperature trap

Jana Roithová
Charles University, Faculty of Science, Department of Organic Chemistry, Hlavova 2030/8, Prague 2, 128 43, Czech Republic
e-mail: roithova@natur.cuni.cz

Photodissociation spectroscopy serves to obtain optical spectra of mass-selected ions in the gas phase. Our approach relies on using helium-tagging of the ions in a low-temperature trap (3 K) [1]. Helium binds with extremely low energy and the helium tagged ions have very low internal energy. Therefore, our photodissociation spectra are single-photon and usually well resolved. We apply photodissociation in the infrared spectral range to study structure of ions and in the UV-vis range to study electronic structure of the ions. I will show application of our approach for investigation of hypervalent metal complexes.
Hypervalent metal complexes are usually studied as models for enzyme's active centers. They are often extremely reactive and can be generated in solution only at low temperature. We have shown that we can transfer these complexes to the gas phase by cryospray and characterize their structure by IR photodisocciation spectroscopy [2]. This approach is to a certain extent complementary to other methods (resonance Raman spectroscopy and nuclear resonance vibrational spectroscopy) but it has an advantage that the ions are isolated and their reactivity can be probed. Hence, we can directly correlate structure with reactivity [2,3]. Gas-phase chemistry allows us to go step further and by reduction of these complexes in the gas-phase prepare postulated intermediates that cannot be prepared in solution. I will show their spectral characterization and reactivity.
In the UV-vis range, helium tagging is not necessary because the energy of photons is sufficient for photofragmentation of bare ions [4]. I will show how this approach can be used to study photofragmentation reactions [5]. Finally, I will show our recent results for studying electronic structure of diatomic ions.

References:

[1] J. Roithová, A. Gray, E. Andris, J. Jašík, D. Gerlich, *Acc. Chem. Res.* **49** (2016) 223–230.
[2] E. **A**ndris, R. Navrátil, J. Jašík, T. Terencio, M. Srnec, M. Costas, J. Roithová, *J. Am. Chem. Soc.* **139** (2017) 2757–2765.
[3] E. Andris, J. Jašík, L. Gómez, M. Costas, J: Roithová, *Angew. Chem. Int. Ed.* **55** (2016) 3637–3641.

[4] Rafael Navrátil, Juraj Jašík, Jana Roithová, *J. Mol. Spec.* **332** (2017) 52–58.
[5] E. Andris, R. Navratil, J. Jasik, G. Sabenya, M. Costas, M. Srnec,J.Roithová, *Angew. Chem. Int. Ed.* **56** (2017) 14057-1406

Hot Topic Papers

Formation Mechanisms of Prebiotic Molecules in the Interstellar Medium

D. Skouteris, F. Vazart, V. Barone
Scuola Normale Superiore, Pisa

N. Balucani
Università degli Studi di Perugia

C. Puzzarini
University of Bologna

C. Ceccarelli
Institut de Planetologie et d'Astrophysique de Grenoble

The search for the origin of prebiotic species in space is an ongoing discipline of enormous interest in astrochemistry and in the study of the origin of life. It has been shown that essentially all biological macromolecules can be envisaged as forming from relatively simple precursors, such as formamide, which are relatively common in interstellar clouds (ISCs). Yet, the formation of formamide and other simple prebiotic molecules is difficult to explain in the harsh environments of ISCs, where very low temperatures and number densities prevail.

Dedicated experimental approaches have been developed to address prebiotic molecules formation mechanisms, in which either the low temperature or the low number density regimes are reproduced. Nevertheless, for some specific cases, the experimental techniques are difficult (if not impossible) to apply. For this reason, we have started a systematic investigation by using high-level electronic structure calculations coupled with kinetics calculations to elucidate the mechanisms of formation of complex organic molecules (COMs) of prebiotic interest which cannot be addressed experimentally. The mechanisms discussed take place exclusively in the gas phase, starting from reactants which are relatively abundant in ISCs. The species discussed include formamide (a possible precursor of both aminoacids and nucleobases), glycolaldehyde (a prototype for sugars), acetic acid (a possible precursor of glycine) and formic acid.

The most significant activities mentioned herein are performed in the framework of the ERC Advanced Grant Project DREAMS "Development of a Research Environment for Advanced Modelling of Soft Matter" , GA N. 320951.

Electrons from the Stars: dynamics of anion formations from C-rich and N-containing chains in the Interstellar Medium

F.A. Gianturco
Institut für Ionen Physik und Angewandte Physik , Innsbruck Universität, Technikerstr. 25, 6020 Innsbruck, Austria
Linacre College, University of Oxford, Oxford, UK

Quantum dynamics of the free electrons from starlight which can undergo attachment processes at low energies (< 10 eV) to carbon-rich gaseous molecules help us to understand the role of transient negative ions (TNIs) which can act as "doorway states" to molecular stabilization and/or fragmentation after resonant attachment of electrons produced in photon-dominated regions (PDR) and moving into dark molecular clouds in the ISM environments.

Several intermediates could be formed under conditions which justify and explainthe existence of stable carbonaceous anions in protoplanetary atmospheres, as found by observationaland laboratory data. It is in fact well established that microscopic processes give important information about the bulk properties of the interstellar medium (ISM), and further control several macroscopic features of it such as temperature and density [1]. We know already that every process of radiation-induced photoionization ofthe atoms and molecules which are present in the ISM yields electrons with a residual energy related to IP, the latter being the Ionization Potential of the species involved.

This excess amount of energy can in turn be shared between the surrounding gas and its constituents andtherefore provides an important heat source within the ISM. The above features therefore suggest quite convincingly that electrons can provide an interesting, and flexible, energy source for driving nanoscopic reactions within the ISM and thus participate in the possible formation of highly reactive anionic intermediates of both the atoms and molecules present in the stellar atmosphere.

The formation of polyatomic anions, therefore, has been predicted in astrophysical environments by earlier model studies [2, 3], where it was suggested that the initial step of the electron-molecule low-energy collisions could produce a metastable species, a transient negative ion (TNI), which then further stabilizes after radiative emission:

$M + e - = (M^-)^* = M^- + photon$

We also know that other possible paths could instead involve the loosing of the electron excess energy of the TNI complex by a dissociative electron attachment (DEA) process following Internal Vibrational Rearrangement (IVR) mechanisms: molecular ions like C_4H, C_6H, C_8H and C_3N (see [4] and references within) have triggered the search for the possible formation of metastable TNIs in even larger systems and, consequently, for the most likely paths to stable anions which could be proposed to occur in the interstellar environment. Our quantum modelling aims at uncovering the most likely pathways to anion-forming events and thus the characteristics of the negative ions that are likely to be formed and which could either fragment into smaller, albeit permanent, anionic species or directly into full molecular anions through dipole-driven scattering state. Further chemical paths can also be present involving reactions with negative ions of H, the most abundant atomic species present in the ISM.

. The work reported will deal with the identification of possible low-energy electron attachment events for the gas-phase Carbon-rich molecules. The search has been motivated by: (i) the experimental detection of anionic resonances for these systems and the presence of several fragmentation products related to DEA paths; (ii) the need to assess the possible molecular mechanisms which preside over the formation of anions in the planetary atmospheres and in the ISM, and (iii) the occurrence of exothermic reactions involving H^- and the related neutral chains, also observed in the ISM environments. All the above aspects will be addressed by the present talk, using quantum modellings of the dynamics for carbon polyynes and cyano-polyynes [6] anion formations.

References

[1] e.g. see: Dyson, J.C. and Williams, D.A.: The Physics of the Interstellar Medium, Taylor & Francis, 1997.
[2] Herbst, E.: *Nature* **289** (1981) 656-657
[3] Millar, T.J., Herbst, E. and Bettens, R.P.A.: MNRAS, Vol.316, pp. 195-203, 2000.
[4] Lucchese, R.R. and Gianturco, F.A.: *Int. Rev. Phys. Chem.* **15** (1996) 429-466
[5] Sebastianelli, F. and Gianturco, F.A.: *EPJD* **59** (2010) 389-398
[6] F.A.Gianturco et al., *ApJ* **774** (2013) 97

Towards imaging the dynamics of CH bond activation by transition metals

Jennifer Meyer, Franziska Krammer, Tim Michaelsen, Björn Bastian, Roland Wester
Institut für Ionenphysik und Angewandte Physik, Universität Innsbruck, Austria

We present first experiments towards imaging the dynamics of reactions of transition metal cations with small molecules like methane and hydrogen. Our aim is to get a deeper understanding of the factors governing the reactivity of transitions metal mediated catalytic cycles by understanding the dynamics of the elementary reaction steps of the catalytic cycle.

The activation of aliphatic CH bonds is a central topic in current catalysis research, e.g. methane activation and its controlled chemical transformation. Methane, however, is relatively inert in chemical reactions due to the high CH bond strength, its lack of a dipole moment, low polarizability and low electron affinity. To achieve an economical sensible conversion, a catalyst is needed. Catalytic cycles are commonly composed of several elementary steps which makes the fundamental understanding of the cycle a scientific challenge. Nowadays, most catalysts are based on highly dispersed transition metals. Transition metals exhibit a diverse and intricate reactivity. They do have a complex quantum nature which makes it hard to predict the reactivity as interactions with ligands or an environment can alter the quantum state of the transition metal.

Gas phase experiments can help to understand this complex system by using model systems and investigating individual elementary reactions one by one [1]. Using mass spectrometry based techniques allows the active control of reaction conditions by exactly defining reactant and product compositions, environment and energetics [2, 3]. Thereby, total cross sections, kinetic isotope effects and branching ratios can be measured. However, no direct information about the atomic level dynamics can be gained from these experiments. The use of crossed beams in combination with velocity map imaging allows the measurement of differential cross sections [4]. These give insight into the dynamics of the reaction and allow a deeper understanding how atoms rearrange during a reaction and how energy is partitioned within the available degrees of freedom [5]. Our group has investigated reaction

dynamics ranging from charge transfer reactions [6] to complex organic reactions [7].

We aim at understanding the dynamics of hydrogen bond activation in small molecules like methane and hydrogen. First experiments are planned on the activation of methane by tantalum Ta^+, iron Fe^+ and iron oxide FeO^+. We have built a laser vaporization source and interfaced it with a velocity map imaging spectrometer. Here, we present first experimental results along the way towards imaging the CH bond activation. We have characterized the ion beams of Fe^+ and Ta^+ produced by laser vaporization by velocity map imaging measuring the temporal profile and the kinetic energy spread of the ion beam. The first reaction to be investigated will be the reaction of $Ta^+ + CH_4$. The main product channel is the formation of the carbene $TaCH_2^+$ under hydrogen elimination [8,9]. The reaction takes place at room temperature and will allow us to optimize the overlap with the neutral beam. A supersonic beam of methane is produced by a home-built piezo electric valve.

The aim of the study is to learn more about the reactivity of transition metals towards methane and hydrogen. The close lying electronic states of the 3d transition metals have shown to exhibit a strong influence on the reactivity [10]. We hope to better understand the effects of the electronic structure on the reactivity by studying the dynamics. Our long term goal is to be able to deduce general concepts linking structure to reactivity.

[1] H. Schwarz, *Cat. Sci. & Techn.* 7, 4302
[2] J. Roithova and D. Schröder, *Chem. Rev.* **110**, 1170 (2010)
[3] H. Schwarz, *Angew. Chem. Int. Ed.* **50**, 10096 (2011)
[4] R. Wester, *Phys. Chem. Chem. Phys.*, **16**, 396 (2014)
[5] E. Carrascosa, J. Meyer, R. Wester, *Chem. Soc. Rev.* doi: 10.1039/c7cs00623c (2017)
[6] T. Michaelsen, B. Bastian, E. Carrascosa, J. Meyer, D. H. Parker, R. Wester, *J. Chem. Phys.* **147**, 013940 (2017)
[7] E. Carrascosa, J. Meyer, J. Zhang M. Stei, T. Michaelsen, W. L. Hase, L. Yang, R. Wester, *Nat. Comm.* 8, 25(2017)
[8] P. B. Armentrout, *Chem. Eur. J.* **23**, 10 (2017)
[9] K. K. Irikura and J. L. Beauchamp, *J. Am. Chem. Soc.* **117,** 4115 (2013)
[10] P. B. Armentrout *Science* 251, 175 (1991)

Velocity resolved kinetics of CO trapping-desorption on Ru(0001)

Dmitriy Borodin, Alec M. Wodtke, T. N. Kitsopoulos
Institute for Physical Chemistry, Universität Göttingen and
Max Planck Institute for Biophysical Chemistry, Göttingen, Germany

Dan J. Harding
Dept. of Chemical Engineering, KTH Royal Institute of Technology,
Stockholm, Sweden
djha@kth.se

The adsorption-desorption behaviour of CO on Ru(0001) has been reported to have a number of unusual features. Recently, combined experiments and theory have suggested that it is the presence of a weakly bound precursor state [1] that leads to the unusual behaviour while Loncaric et al have proposed that large rotational anisotropy of the CO-Ru(0001) potential energy surface [2] can explain the unusual feature in the CO sticking and scattering.
We use velocity resolved kinetics [3] to probe the trapping-desorption of CO on Ru(0001) over a broad range of surface temperatures, measuring desorption rates and speed distributions in an effort to provide further details of CO scattering which can help distinguish between the competing explanations. Our measured desorption rates and binding energy are consistent with previous experiments. Detailed analysis of the speed distributions will be used to try to determine whether a barrier to adsorption is present.

[1] Dell'Angela *et al*., *Science,* **339**, 1302 (2013)
[2] Loncaric *et al., Phys. Rev. Lett.*, **119**, 146101 (2017)
[3] Harding *et al., J. Chem. Phys.*, **147**, 013939 (2017)

Kinetics of the Reaction of $CO_3^-(H_2O)_n$, n = 0, 1, 2, with Nitric Acid, a Key Reaction in Tropospheric Negative Ion Chemistry

C. van der Linde, M. K. Beyer
Institut für Ionenphysik und Angewandte Physik,Universität Innsbruck, Technikerstraße 25, 6020 Innsbruck, Austria

Wai-Kit Tang, Chi-Kit Siu
Department of Chemistry, City University of Hong Kong, 83 Tat Chee Avenue, Kowloon Tong, Hong Kong SAR, China

The $CO_3^{\bullet-}$ carbonate radical anion and the mono- and dehydrated species $CO_3^{\bullet-}(H_2O)_{1,2}$ are among important tropospheric ions. While the $CO_3^{\bullet-}$ formation process in the atmosphere is well established, its reactivity towards various atmospheric compounds is mostly unknown despite its radical character. Reactions of $CO_3^{\bullet-}(H_2O)_n$ with different organic acids like formic acid and inorganic compounds like hydrogen chloride were studied recently. [1,2]

Especially the reaction of $CO_3^{\bullet-}(H_2O)_{0,1,2}$ with nitric acid HNO_3 are among the most important reactions of negative ions in the troposphere. An initial reaction mechanism was proposed by earlier flow reactor studies. [3,4] The mechanism is investigated here in more detail by quantum chemical calculations and experimental reactivity studies of mass selected ions under ultra-high vacuum conditions.

Bare $CO_3^{\bullet-}$ forms $NO_3^-(OH^{\bullet})$ as well as NO_3^-, with a total rate coefficient of 1.0×10^{10} cm^3/s. $CO_3^{\bullet-}(H_2O)$ in addition affords stabilization of the $NO_3^-(HCO_3^{\bullet})$ collision complex, and thermalized $CO_3^{\bullet-}(H_2O)$ reacts with a total rate coefficient of 5.5×10^{10} cm^3/s. A second solvent molecule quenches the reaction, and only black-body radiation induced dissociation is observed for $CO_3^{\bullet-}(H_2O)_2$, with an upper limit of 6.0×10^{11} cm^3/s for any potential bimolecular reaction channel. The rate coefficients obtained under ultra-high vacuum conditions are smaller than in the earlier flow reactor studies, due to the absence of stabilizing collisions, which also has a strong effect on the product branching ratio. Quantum chemical calculations corroborate the mechanism proposed by Möhler and Arnold. [4] The reaction proceeds through a proton-transferred $NO_3^-(HCO_3^{\bullet})$ collision complex, which can rearrange to NO_3^-

($OH^{\bullet}$)(CO_2). The weakly bound CO_2 easily evaporates, followed by evaporation of the more strongly attached $OH^{\bullet}$, if sufficient energy is available.

Literature:

[1] C. van der Linde, W. K. Tang, C.-K. Siu, M. K. Beyer. *Chem. Eur. J.* **22** (2016) 12684.
[2] W. K. Tang, C. van der Linde, C.-K. Siu, M. K. Beyer, *J. Phys. Chem. A* **121** (2007) 192.
[3] O. Möhler, F. Arnold, *J. Atmos. Chem.* **13** (1991) 33.
[4] C. Guimbaud, D. Labonnette, V. Catoire, R. Thomas, *Int. J. Mass Spectrom.* **178** (1998) 161.

Ion Mobility Spectrometry monitoring of degradation of organic compounds by plasma jet

L. Moravský, B. Michalczuk, M. Sabo and Š. Matejčík
Faculty of Mathematics, Physics and Informatics,
Comenius University in Bratislava,
Mlynská dolina F2, 842 48 Bratislava, Slovakia

Abstract: This contribution refers to the application of Corona Discharge Ion Mobility Spectrometry (CD-IMS) as a suitable analytical tool for monitoring decomposition of chemical substances by atmospheric pressure discharges. In this work we demonstrate application of CD-IMS for detection benzyl butyl phthalate (BBP) vapours and the degradation of liquid BBP using argon plasma jet treatment.

1. Proton transfer in positive mode of CD-IMS

Since early 1970s when Ion Mobility Spectrometry (IMS) was first time introduced as a trace gas analytical technique[1], it has been widely used all over the world. The reasons were: compact design, high sensitivity, variability in application, [2] quick response and either low investment or operation costs. Taking these advantages IMS has been applied in many fields including monitoring of environmental pollutants, drugs and explosives detection [3, 4], biomolecules [5].

The CD-IMS is working both in positive and negative polarities. In positive mode CD-IMS is using hydronium ions formed in CD for Atmospheric Chemical Ionisation (APCI) of sample molecules. This process can be described by reaction (1):

$$M + H_3O^+ \rightarrow [M+H]^+ + H_2O \qquad (1)$$

This reaction occurs only when proton affinity of M is higher than proton affinity of water which is equal to 697 kJ/mol [6].

The CD-IMS technique has been used to detect phthalates and to study the decomposition of the liquid phthalate sample by atmospheric pressure discharges. The high sensitivity, selectivity and fast response allows to monitor very efficiently decomposition of substances by analysis of the vapours of substances.

3. Experimental apparatus

We have applied kHz driven (9 kHz) DBD Argon Plasma Jet (Fig. 1) with gas flow 200 ml.min^{-1} and discharge voltage 7kV [8,9] for treatment of benzyl butyl phthalate (BBP - 98% Sigma Aldrich) in liquid phase (1 ml in PE vial).

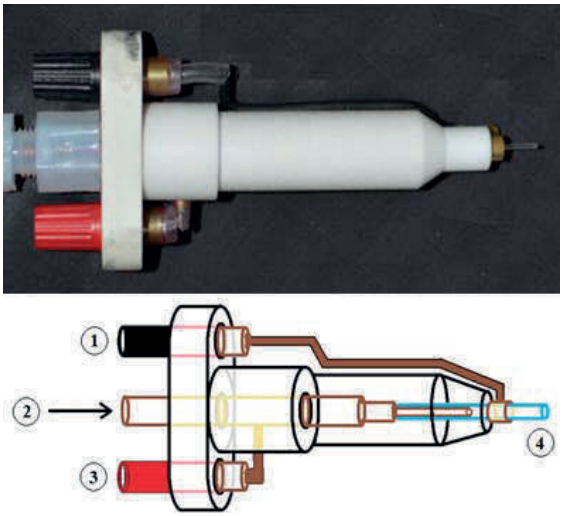

Fig. 1. *Schematic view of APPJ 1) grounded electrode, 2) gas inlet 3) high voltage electrode, 4) glass capillary*

The vapour pressure of BBP at standard conditions (20°C) is 6.47x10^{-6} mbar [10] what represents concentration of the BBP in ambient air ~10 ppb. The detection of the BBP by CD-IMS spectrometry was very fast and with strong response (Fig. 2a).

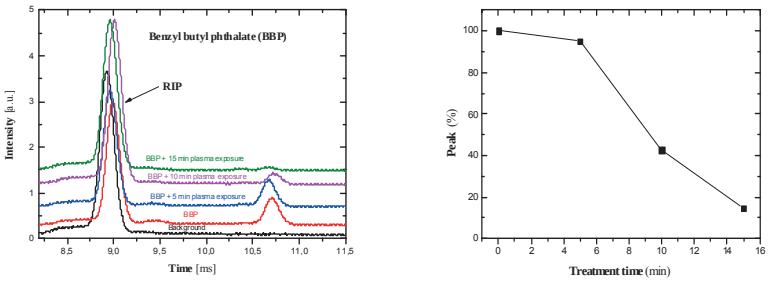

Fig. 2 *a): Positive IMS spectra of ambient air (black) and BBP sample before treatment (red) and after plasma treatment (blue, violet and green spectra). And b): Relative changes of the BBP peak with increasing treatment time.*

After that we have started treatment of the BBP liquid sample by Argon Plasma Jet. The plasma application time was from 5 to 15 minutes. After treatment we have measured the vapour pressure of the sample by the means of IMS spectrometry. With the increasing treatment time of the liquid sample, we have observed decrease of the BBP peak from the sample (Fig. 2b). The decrease of the vapour pressure BBP above the liquid surface we relate on the basis of the Raoult law to the decrease of the BBP concentration in the liquid due to decomposition of the BBP in the liquid sample.

This research has been supported by:

- European Union's Horizon 2020 research and innovation programme under the Marie Skłodowska-Curie grant agreement No 674911
- Slovak Research and Development Agency Project Nr. APVV-0259-12 and APVV-15-580
- European Union's Horizon 2020 research and innovation programm under grant agreement No 692335

4. References

[1] M.J. Cohen, F.W. Karasek, *J. Chromatogr. Sci.* (1970) 8 (6) 330-337.
[2] H. Borsdorf, T. Mayer, M. Zarejousheghani, G. A. Eiceman, Appl. Spectros. Rev., 41(2011) 323–375.
[3] S. Ehlert, A. Walte, R. Zimmermann, Anal. Chem., 85 (2013) 11047–11053.
[4] S. Armeta, S. Garriques, M. de la Guardia, J. Brassier, M. Alcala, M. Blanco, J. Chromatogr. A.,1384 (2015)1-8.
[5] D. E. Clemmer, M. F. Jarrold, J. Mass Spectrom. 32 (1997) 577.
[6] S. M. Collyer, T. B. McMahon, *J. Phys. Chem.,* 1983, 87 (6), 909–911.

[7] K. C. Hunter, A. L. L. East, *J. Phys Chem. A*, 2002, 106, 1346-1356
[8] G. Horvath, L. Moravský, F. Krčma, Š Matejčík, *IEEE Trans.Plasma Sci.* **41** (2013) 613.
[9] L. Moravský et al. *Open Chem*., 2015; **13**: 257–262.
[10] scorecard.goodguide.com/chemical profiles/html/butylbenzylphthalate.html

Bringing the Chemical Laboratory to the Reaction: Coupling of Microfluidics with IRPD Spectroscopy

Martin Mayer,[1] Maik Phal,[2] Detlev Belder,[2] and Knut R. Asmis[1]
[1] *Wilhelm-Ostwald-Institut für Physikalische und Theoretische Chemie, Universität Leipzig, Linnéstrasse 2, D-04103 Leipzig, Germany*
[2] *Institut für Analytische Chemie Fakultät für Chemie und Mineralogie, Universität Leipzig, Johannisallee 29, D-04103 Leipzig, Germany*

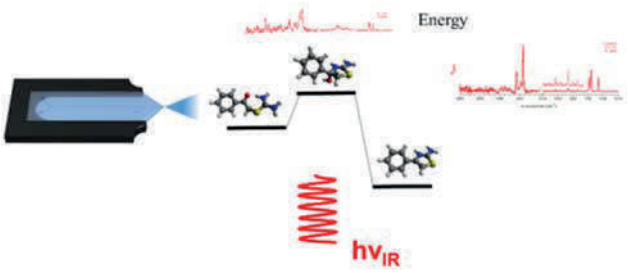

Chemical microreactors, such as microfluidic chips, have a great potential in reaction analysis and synthesis. Such systems are normally coupled to mass spectrometry, in order to determine reaction components and their structures. Nowadays, the mass spectrometer can be brought to almost any chemical reaction, due to the recent developments of ionization techniques.[1] Here, we demonstrate the coupling of a microfluidic chip with infrared photodissociation (IRPD) spectroscopy, bringing together the benefits of microfluidic reaction technology with the structure determining power of gas phase vibrational spectroscopy. A chemical reaction is carried out on the microfluidic chip and the outcome is electrosprayed into a ion trap tandem mass spectrometer, combined with an OPO/OPA laser system. The molecular structures are obtained by comparing experimental gas phase vibrational spectra with DFT calculations. The chemical reaction, studied by this novel technique is the Hantzsch thiazole synthesis of thiourea and 2-bromo-1-phenylethanone, giving aminophenylthiazole as reaction product. The Hantzsch reaction product is unambiguously identified by its IRPD spectrum in the range between 1000 and 3800 cm^{-1}. Two isobaric reaction intermediates are also identified and their individual IR fingerprints are measured isomer-selectively using the IR^2MS^2 technique from 2400-3800 cm^{-1}, allowing the identification of Hantzsch synthesis intermediates at different points of the reaction coordinate. The separation of isomeric reaction compounds is a unique feature of the demonstrated technique. To indicate the online analysis-potential, the concentrations of the reaction educts are inverted, shifting the

isomer ratio towards the intermediate occurring later on the reaction coordinate, which can be attributed to increased kinetics of the reaction.

[1] Andrew J. Ingram, Cornelia L. Boeser and Richard N. Zare, *Chem. Sci.*, 7, 39-55, (2016).

Knockout driven reactions in clusters of PAHs, fullerenes, and hydrocarbon chains

Michael Gatchell
Universität Innsbruck, Institüt für Ionenphysik und Angewandte Physik, Technikstraße 25, 6020 Innsbruck, Austria

Mark. H. Stockett, Michael Wolf, Linda Giacomozzi, Giovanna D'Angelo, Henning T.Schmidt, Henning Zettergren, Henrik Cederquist
Stockholm University, Department of Physics, 106 91 Stockholm, Sweden

Rudy Delaunay, Arkadiusz Mika, Alicja Domaracka, Patrick Rousseau, Bernd A. Huber
Normandie Univ., ENSICAEN, UNICAEN, CEA, CNRS, CIMAP, 14000 Caen, France

Energetic ions or atoms colliding with aggregates of matter, such as clusters of molecules, can lead to exotic bond-forming reactions on very fast (sub-picosecond) timescales [1]. An important mechanism in these events is the knockout of one or more atoms, where individual atoms are permanently displaced from molecules when momentum is deposited through elastic scattering in the collision [1], a process that dominates at collision energies typically found in many astronomical environments. Recently, we have performed a broad range of experimental and theoretical studies investigating knockout processes and subsequent reactions with isolated PAH, fullerene, and biomolecular targets [1,2,3,4], as well as in clusters of PAHs, fullerenes, and small hydrocarbon chains [1,5,6,7]. At the meeting I will be focusing on new results from measurements of the displacement energies for C atom removal from isolated C_{60} anions and impulse driven bond-forming reactions in fullerene clusters leading to a rich assortment of large products.

[1] M. Gatchell and H. Zettergren, *Journal of Physics B*, **49**, 162001 (2016)
[2] M. Gatchell et al., *International Journal of Mass Spectrometry*, **365-366**, 260 (2014)
[3] M. H. Stockett et al., *Physical Review A*, **89**, 032701 (2014)
[4] L. Giacomozzi et al., *Physical Chemistry Chemical Physics*, **19**, 19750 (2017)
[5] H. Zettergren et al., *Physical Review Letters*, **110**, 185501 (2013)
[6] R. Delaunay et al., *The Journal of Physical Chemistry Letters*, **6**, 1536 (2015)
[7] M. Gatchell et al., *Physical Chemistry Chemical Physics*, 19, 19665 (2017)

Theoretical Modeling of Photochemistry in Small Gas Phase Ions

Milan Ončák, Thomas Taxer, Tobias Pascher, Emanuel Oswald, Erik Barwa, Christian van der Linde, Martin K. Beyer
Institut für Ionenphysik und Angewandte Physik, University Innsbruck
Technikerstraße 25/3, 6020 Innsbruck, Austria
E-Mail: Milan.Oncak@uibk.ac.at

Microhydrated metal ions and other small ionic systems are popular model systems as they can be investigated in great detail both experimentally and theoretically due to their small size and well-defined composition. Despite the relative simplicity, analysis of their chemistry give us fundamental insight into various elementary processes, e.g. water splitting, charge separation or photocorrosion. At the same time, methods of theoretical chemistry can be benchmarked and further improved based on the experimental input.

Here, we discuss issues and challenges in modeling photochemistry of small ionic systems, with particular emphasis on microhydrated ions. The investigations are driven by experiments performed in our laboratory, in which an FT-ICR spectrometer is used, along with a tunable UV/VIS Optical Parametric Oscillator.

1. Modeling photochemistry and photodynamics of hydrated Mg^+.

Experiments show that small $Mg^+(H_2O)_n$ clusters, n = 1-5, have complicated photochemistry with combined one- and two-photon processes and several dissociation channels [1-3]. To understand the experiment, we used absorption spectra modeling and multireference *ab initio* calculations. We rationalize why the H_2O dissociation channel, which is preferred in the ground state, is suppressed in the excited state and why the H-dissociation channel is preferred (Figure 1). This trend changes only after the Mg^+ ion is fully hydrated (n > 20) when water dissociation becomes more favorable.

2. Photofragmentation of Cs_2I^+.

The Cs_2I^+ cluster is a model system for excitation in ionic systems, with charge transfer excitations from an anion to a cation [4]. Despite its simple linear structure, the Cs_2I^+ ion has a complicated photodissociation dynamics with three dissociation channels including non-intuitive formation of Cs_2^+. By

inclusion of spin-orbit effects and analysis of the excited state potential energy surfaces, we succeeded to reproduce and rationalize the experimental photodissociation spectrum (Figure 2).

3. Activation of carbon dioxide on hydrated Co^-.

Photoabsorption spectra can be also used to analyze molecular structure. Here, we trace activation of CO_2 on a hydrated cobalt anion by calculating absorption spectra as a function of the degree of hydration and their comparison to experimentally measured ones. We show that structure switches from $CoCO_2^-$ to $OCCoO^-.(H_2O)_n$ already when one water molecule is added. We argue that multireference photochemical calculations are of utmost importance to benchmark the widely used TDDFT method.

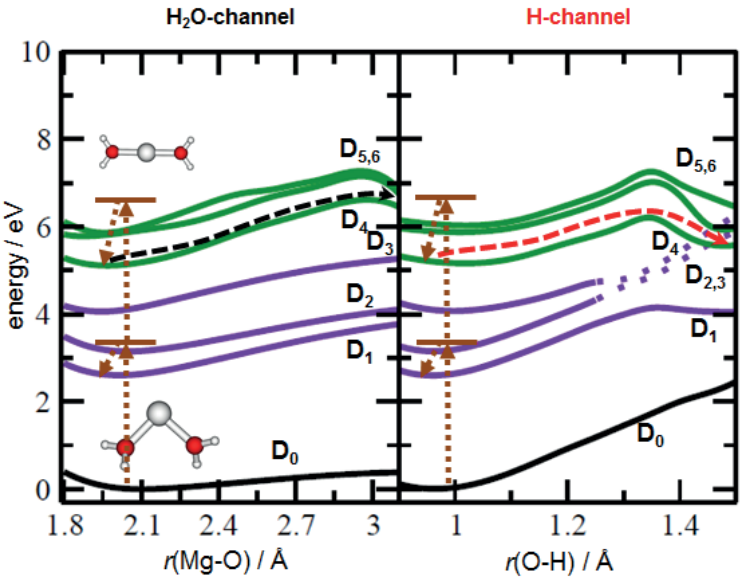

Figure 1 *– Photochemical pathways in $Mg^+.(H_2O)_2$ cluster along Mg-O and O-H dissociation coordinate. Calculated at the MRCI(3,5)//CASSCF(5,7) level of theory with the 6-31++g** basis set.*

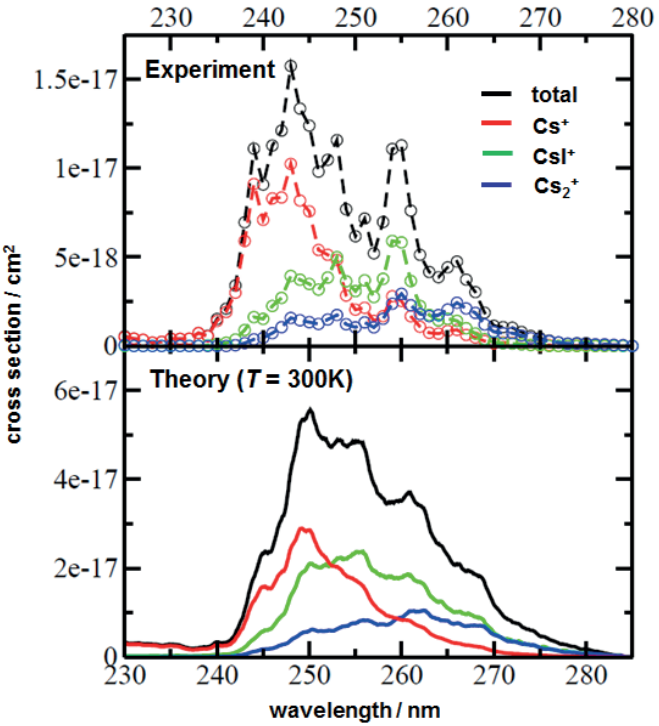

Figure 2 *– Experimental and theoretical photodissociation spectrum of* Cs_2I^+*, along with various dissociation channels. Calculations were performed at the MRCI(6/5)/Stuttgart level of theory, the ground state potential energy surface was sampled using molecular dynamics at 300K.*

Literature

[1] C. Berg, M. Beyer, U. Achatz, S. Joos, G. Niedner-Schattenburg, V. E. Bondybey *Chem. Phys.* **1998**, *239*, 379;
[2] Ch.-K. Siu, Z.-F. Liu *Phys Chem. Chem. Phys.* **2005**, *7*, 1005;
[3] F. Misaizu, M. Sanekata, K. Fuke, S. Iwata *J. Chem. Phys.* **1994**, *100*, 1161.
[4] X. Li, R. L. Whetten *J. Phys. Chem.* **1993**, *98*, 6170.

Isomeric broadening of the electronic excitation for $C_{60}He_n^+$ from a single He tag to full coverage

Alexander Kaiser, Martin Kuhn, Michael Renzler, Johannes Postler, Steffen Spieler, Malcolm Simpson, Milan Ončák, Martin Beyer, Roland Wester, Franco Gianturco, Paul Scheier
Institut für Ionenphysik und Angewandte Physik, University of Innsbruck, Technikerstraße 25, A-6020 Innsbruck, Austria

Ersin Yurtsever
Koç University, Chemistry Department, Rumeli Feneri Yolu, Sariyer 34450, Istanbul, Turkey

Florent Calvo
Univ. Grenoble Alpes, LIPHY, F-38000 Grenoble, France

1. Introduction

The experimentally measured line profiles of the ~958 nm and ~964 nm line of $C_{60}He_n^+$ show an interesting dependence on the number n of helium atoms adsorbed on the fullerene [1,2]. The helium atoms do not only induce a characteristic line-shift that is the result of a change in polarizability upon excitation, they also lead to a broadening in the excitation profiles that has a maximum at half-coverage, and points towards isomeric broadening. Assuming vertical excitation, a model with a spherically symmetric change in the polarizability cannot explain this isomeric broadening.

In an attempt to understand this broadening, we have carried out quantum chemical calculations on C_{60}^+ and $C_{60}He^+$ for the ground and excited state and Path Integral Molecular Dynamics (PIMD) calculations on $C_{60}He_n^+$ for n=1 to n=32 using a polarizable potential. The quantum chemical calculations indicate a charge transfer upon excitation as visualized in Figure 1.

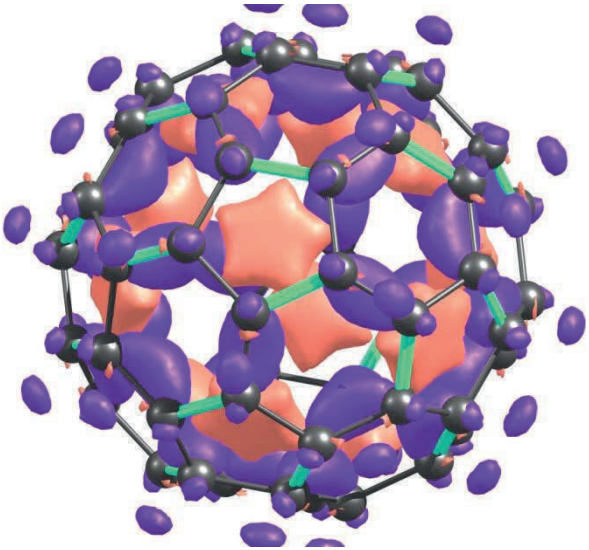

Figure 1. *Isosurfaces of the charge density difference of the ground and excited state of* C_{60}^+

This charge transfer affects 6-rings and 5-rings differently and may lead to a slight differences in the relative interaction strength of He-5ring / He-6ring interaction upon excitation and ultimately lead to the isomeric broadening. The ground state distributions of He_n for 5-rings and 6-rings were determined from PIMD simulations, and further processed by using experimental data for $C_{60}He_{31}^+$ to estimate the isomeric broadening for the full range n = 1 to n = 32. Additionally, PIMD results for the ground state energy distributions and temperature effects will be discussed.

[1] Kuhn, M., et al., Atomically Resolved Phase Transition of Fullerene Cations Solvated in Helium Droplets. *Nat. Comm.* **2016**, *7*, 13550.
[2] Campbell, E. K.; Holz, M.; Gerlich, D.; Maier, J. P., Laboratory Confirmation of C_{60}^+ as the Carrier of Two Diffuse Interstellar Bands. *Nature* **2015**, *523*, 322-323.

This work was supported by the Austrian Science Fund FWF (projects P26635, I978 and W1259) and the Swedish Research Council (Contract No. 2016-06625) and the European Commission (Grant Agreement number: 692335 — ELEvaTE).

Characterisation, Coverage, and Orientation of Functionalised Graphene using Sum-Frequency Generation Spectroscopy

Sven P. K. Koehler
School of Science and the Environment, Manchester Metropolitan University, Chester Street, Manchester, M1 5GD (United Kingdom)

Huda S. AlSalem, Chloe Holroyd
Photon Science Institute, The University of Manchester, Oxford Road, Manchester, M13 9PL (United Kingdom)

Graphene, a monolayer of sp^2-hybridised carbon atoms arranged in a two-dimensional hexagonal lattice, has received much attention due to its remarkable electronic, physical, and chemical properties. However, graphene does not possess a band gap, which limits its implementation in many proposed applications. Hence more attention has been recently paid to modified graphene and graphene derivatives which allow one to tune graphene's intrinsic properties such as its band gap and opto-electronic properties. Graphene is most commonly characterised by Raman spectroscopy, but this has a number of drawbacks when it comes to the investigation of functionalised graphene: 1) the D peak in a Raman spectrum only shows that the normally perfect 2D lattice of graphene now has defects, but it does not provide any information regarding the type of defect, i.e. one cannot distinguish between e.g. carbon atom vacancies in the 2D lattice as compared to sp^3 carbon atoms on functionalised graphene; 2) while it has been attempted to correlate the ratio of D/G peak intensities to the number density of defects, this calculation is ambiguous for certain coverage regimes, and furthermore requires a scaling factor in some cases. Alternatively, a number of groups have recently employed sum-frequency generation (SFG) spectroscopy as a means to characterise modified graphene. SFG is a powerful surface analysis technique owing to its surface sensitive and interface selective properties and has a major advantage over Raman spectroscopy for the characterisation of functionalised graphene: SFG allows one to identify the functional groups directly based on their vibrational signatures.

In the work reported here, we have chemically functionalised CVD graphene on a gold substrate using a benzene diazonium salt to chemisorb phenyl rings

to graphene, and by chemisorbing hydrogen atoms in a Birch reduction reaction.

Graphene samples were investigated by SFG spectroscopy to deliver vibrational spectra for the hydrogenated graphene samples, and those decorated with phenyl groups. The SFG spectra shown in the two Figures below show the aromatic C-H stretches of the phenyl rings on graphene (left), and the C-H stretches of hydrogenated graphene (right).

While comparison with a self-assembled monolayer of phenyl thiols allows us to extract surface coverages for the phenyl-decorated graphene (~2.0 × 10^{14} cm^{-2}, or ~5% of carbon atoms of graphene), the intensity of the C-H stretch of hydrogenated graphene can be correlated to the reaction times.

We have also established from polarisation-dependent SFG measurements that the functional groups are roughly aligned with

the graphene surface normal. Furthermore, the de-coherence times of the

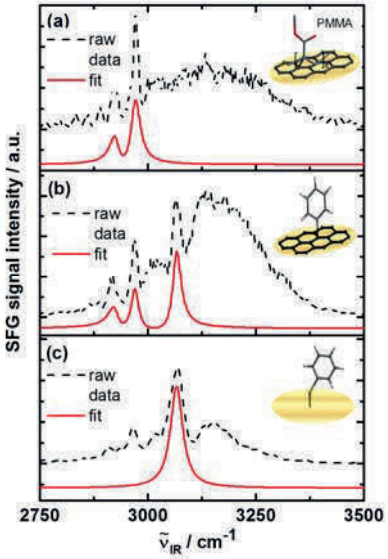

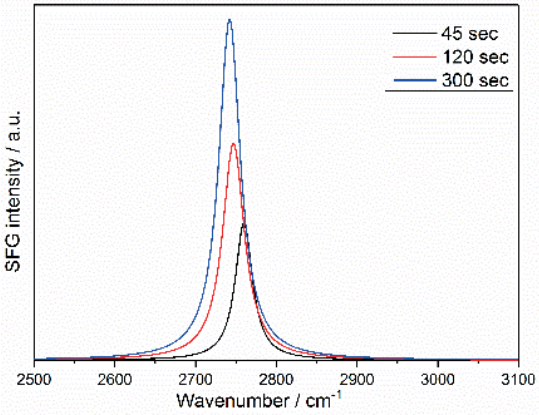

vibrationally excited aromatic C-H bond has been measured to be around 0.7 ps for both the functionalised graphene sample, as well as for the phenyl thiol, and hence seems independent of the presence of the graphene substrate.

Recognition of patterns produced by combination differences in high resolution overtone ro-vibration methanol spectra in region 7170-7220 cm^{-1}

J. Rakovský, O. Votava
J. Heyrovský Institute of Physical Chemistry of the Czech Academy of Sciences, Dolejškova 3, Prague 8, Czech Republic

1. Introduction

Methanol is the second most abundant organic molecule in the atmosphere[1]. It is present in the space[2] and can be detected in human breath as the product of metabolic processes[3]. From the point of view of high resolution spectroscopy its structure is interesting. Since it is near-prolate asymmetric-top molecule and one of the simplest molecules possessing hindered internal rotation[4] a structure of its ro-vibrational states is complicate.

The structure is even richer and more complicated for high vibrational states which can be probed by high resolution ro-vibrational overtone spectroscopy of jet-cooled molecular beams. However even at low temperature the overtone spectra are difficult to analyse[5] since they are congested and possess many irregularities. For the methanol, however, the most of the lines are still well separated with properly defined transition energies.

In this contribution, we point out a method to analyse the spectra. It is based on a searching or recognition of certain patterns in the experimental spectra. To the best of our knowledge, the method is not well documented within the literature and there is only one relevant paper using and briefly outlining the method[6].

2. Experiment

Experimental spectra are obtained by a tunable diode laser direct absorption spectrometer measuring a cold molecular beam produced by pulsed slit-jet supersonic nozzle. The extended cavity diode laser tunable in range of 7070–7300 cm^{-1} with output power 3 mW and bandwidth 1 MHz is used to record the spectra. Laser wavelength is measured by Michelson wavemeter in cooperation with a thermally stabilised Fabry-Pérot interferometer and a known position of a reference water line. The absolute positions are better than 10^{-3} cm^{-1}. The laser beam passes through the molecular beam produced by 0.1 x 40 mm slit and the pulsed valve with frequency of 3 Hz and duration

>1 ms. The expansion of small amount of methanol diluted in neon buffer gas produces rotation and translation temperatures approximately 20 K.
A more detailed description of the setup can be found in the references[5, 7-9].

3. Method

More than one transition can usually take place to the same upper state from different lower states in accordance with selection rules. When the lower states are connected by transitions with the common upper state such a structure will be referenced as a combination difference multiplet or simply a multiplet. The transitions of the multiplet create certain pattern in the spectra (see Fig.1) in which the spaces between the lines are defined by differences in the lower state energies and which position in the spectra is determined by the upper state energy.

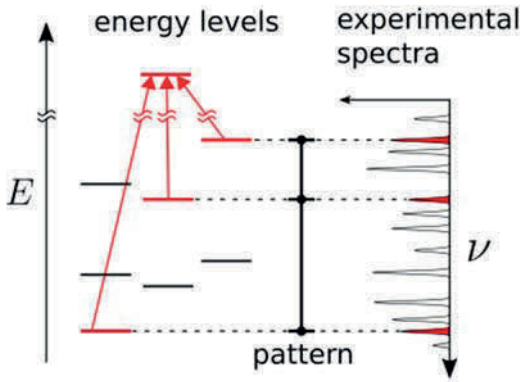

Fig. 1: *An illustration of the multiplet and the projection into the specific pattern of lines in the spectra. The multiplet is compose of the three lower states and the common upper state and produce the pattern of three lines in the spectra indicated by the filled peaks.*

For methanol, selection rules can be deduced, and thus the multiplets can be constructed. Also, the lower state energies are known and they define the spacing in the patterns[10]. What is not known and is the object of this method, are the values of the upper state energies which can be determined by the finding and recognition of the patterns' positions in the spectra. Although the core of the method is simple – to generate and find patterns – some complications have to be taken into account in terms of interpreting the output data of the search process.

Methanol's full multiplets – including maximum of the possible lower states – create from 2 to 9 lines in the patterns. Indeed, identifying patterns with a higher number of lines is more reliable, but it is not always possible to find all of them in the experimental spectra. This is even not needed and the multiplets can be reliably identified by incomplete patterns. However, one has to consider the fact that two different multiplets can share some of the lower states; and thus, they are unrecognisable by the pattern composed exclusively by the lines that share these lower states. For the methanol, with our experimental precision, 2 and 3 lines are not sufficient to identify any multiplet; at least 4 of 4 lines are needed. For the biggest possible multiplet with 9 lines 6 lines are minimum to identify it reliably.

The assessment of criteria for the minimal number of lines provides a secure assignment for the majority of the patterns but, a small amount of accidental coincidences. The reduced energy plot for the upper states is used to recognise the accidental coincidences. The states have a tendency to form progressions in J for different K quantum numbers. Outliers from the progressions can be considered individually and can be excluded.

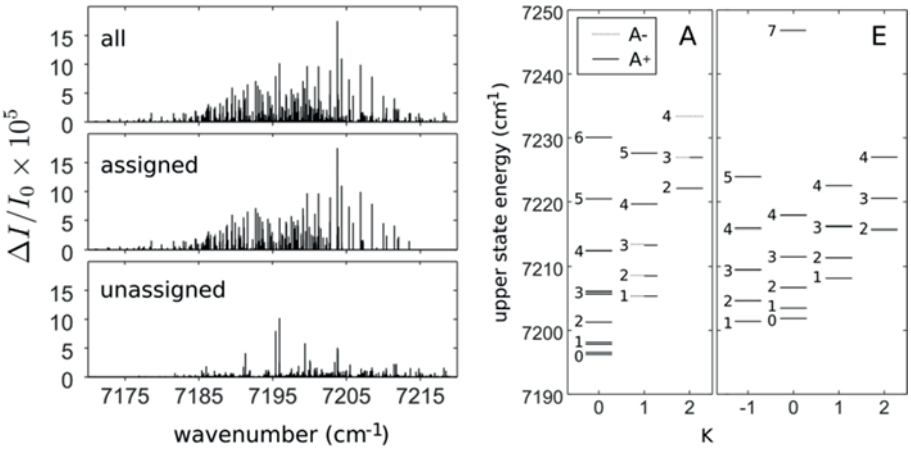

Fig. 2: Left: *The overview of the high resolution overtone spectra of the methanol. The measured spectra contains 1002 lines. The overall intensity of the assigned lines represents 63% of the total intensity of the all lines.* ***Right:*** *The upper state energy map of the overtone of the methanol for A and E components resulted from the assigned transitions. The K quantum number is indicated on the vertical axis and J is indicated by the number on the left side of the related state. For the A component there are two different symmetries indicated by full and dashed lines.*

4. Results

The spectra of methanol with 1002 lines (see **Fig.2**) have been analysed by the presented method. The 63 % of the total intensity produced by 295 lines was assigned to transitions and to 52 upper states.

Acknowledgement: The Czech Science Foundation grant no.: 17-04068S

References:

[1] L. J. Carpenter and P. D. Nightingale, *Chem. Rev.* **115** (2015) 4015
[2] S. Brünken and S. Schlemmer, *EAS Publ. Ser.* **75/76** (2016) 295
[3] B. Yuan, A. R. Koss, C. Warneke, M. Coggon, K. Sekimoto, and J. A. de Gouw, *Chem. Rev.* (2017)
[4] L. Xu, X. Wang, T. J. Cronin, D. S. Perry, G. T. Fraser, and A. S. Pine, *J. Mol. Spectr.* **185** (1997) 158
[5] V. Svoboda, V. Horká-Zelenková, J. Rakovský, P. Pracna, and O. Votava, *Phys. Chem. Chem. Phys.*, **17** (2015) 15710
[6] M. B. Dawadi, S. Twagirayezu, D. S. Perry, and B. E. Billinghurst, *J. Mol. Spectrosc.* **315** (2015) 10
[7] A. Campargue, L. Wang, S. Kassi, M. Mašát and O. Votava, *J. Quant. Spectrosc. Radiat. Transfer,* **111** (2010) 1141
[8] O. Votava, M. Mašát, P. Pracna, S. Kassi and A. Campargue, *Phys. Chem. Chem. Phys.* **12** (2010**)** 3145
[9] M. Mašát, P. Pracna, D. Mondelain, S. Kassi, A. Campargue and O. Votava, *J. Mol. Spectrosc.* **291** (2013), 9
[10] Xu, L. H., Hougen, J. T., *J. Mol. Spectrosc.* **169** (1995) 396

Multiple ionisation of PH_3 and reactions of PH_n^{2+} ions.

Jess Lee, Helena Pradip and Stephen D Price
Chemistry Department, University College London, 20 Gordon Street, London WC1H 0AJ, UK.

This poster reports the results from coincidence investigations of the electron ionisation of PH_3. These experiments involve the measurement of relative precursor-specific partial ionisation cross sections for this molecule, for the first time. These cross sections quantify the intensities and origins (single, double, triple ionization) of the ions formed following electron collisions with phosphine molecules over the electron energy range 30 - 200eV.[1,2] Significant numbers of ions are shown to be formed by multiple-ionisation in these electron-molecule encounters, including a number of different dications. In subsequent experiments the reactivity of some of these dications are investigated in a crossed beam experiment.[3-5] In these experiments the PH_3^{2+} ion is shown to behave as a super-acid; for example it readily donates a proton to argon. Our experiments allow us to bracket the proton affinity for PH_2^+ ($PH_2^+ + H^+ \rightarrow PH_3^{2+}$) as lying between that of argon and neon. A variety of interesting self-protonation reactions are observed following interactions of PH_3^{2+} with PH_3, including the formation of PH_4^{2+}.

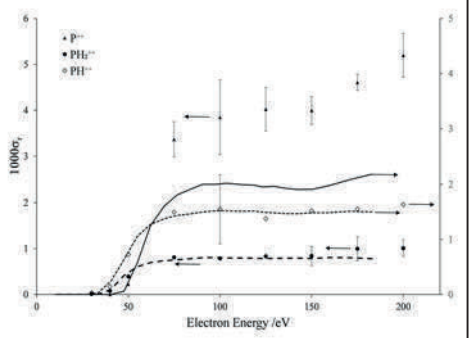

Relative precursor-specific partial ionization cross sections for forming fragment dications following electron

References:

[1] J.D. Fletcher, M.A. Parkes and S.D. Price *J.Chem.Phys.* **138** (2013) 184309
[2] S.J. King and S.D. Price *J. Chem. Phys.* **134** (2011) 074311
[3] J.D. Fletcher, M.A. Parkes and S.D. Price *Int.J.Mass Spectrom* **377** (2015) 101
[4] J.D. Fletcher, M.A. Parkes and S.D. Price *Mol. Phys.* **113** (2015) 2125
[5] M.A. Parkes, J.F. Lockyear and S.D. Price *Int. J. Mass Spectrom.* **365** (2014) 68

Driving molecular machines with electrons on surfaces: walkers and nanocars

Gitika Srivastava, Manfred Parschau, Laura Zoppi, Karl-Heinz Ernst
Empa, Swiss Federal Laboratories for Materials Science and Technology, Dübendorf, Switzerland

Peter Stacko, Ben Feringa
Zernike Institute, University of Groningen, 9700 AB Groningen, The Netherlands

1. Introduction

Artificial robots and machines at the nanoscale are one of the great challenges and goals of Nanotechnology. Nature has mastered to use of molecular machines for directed transport of cargo or performing mechanical work needed in cellular processes. Motor proteins, for example, undergo conformational changes by using chemical fuel and perform work in the biological cell [1]. Chemists spend tremendous efforts to create artificial machines, but not many have been successful towards unidirectional movement [2].

Scanning tunneling microscopy (STM), the founding method of Nanotechnology, has been successfully used to move atoms [3] and molecules [4] as well as inducing various molecular dynamical processes at surfaces, such as molecular desorption [5], dissociation [6], formation of chemical bonds [7], changes in conformation [8], and rotation or hopping of molecules [9]. However, all these manipulations did not involve any preferential movement of the species, unless dragged or pushed by the STM tip.

Rotatory directional switching with electrons emanating from an STM tip has successfully been performed recently [10]. Here we briefly review our work of unidirectional translational motion of a 'four-wheeled' molecule, induced by electronic and vibronic excitation of four rotor units [11], and present a new molecular design for further studies.

2. Materials and Methods

Experiments were performed in ultrahigh vacuum (UHV, $p \approx 10^{-8}$ Pa). The Cu(111) crystal surface was exposed to the motor molecules, evaporated from effusion cells after being cleaned *in vacuo* via standard sputtering and annealing. Cleanliness and quality of the surfaces and the surface coverage of the adsorbate systems have been determined with STM. Molecules were

usually adsorbed with the metal surface held at room temperature. STM images were acquired at cryogenic temperatures (7 K) in constant current mode with the bias applied to the tip. We induced molecular motion by applying a voltage pulse to the sample while the tunnelling current was recorded. The STM tip was positioned over the centre of a molecule, the feedback was turned off, and the tip was moved vertically to give the desired initial current during the pulse. For details of the chemical synthesis of the 'four-wheeler', reference [11] and its Supplementary Information.

3. Results and Discussions

In order to have an unidirectional motion an asymmetric 'ratchet-like' potential landscape is required (Fig. 1) [12]. Here, a system excited out of a potential well has a higher probability of overcoming the barrier on one side of the well than the other.

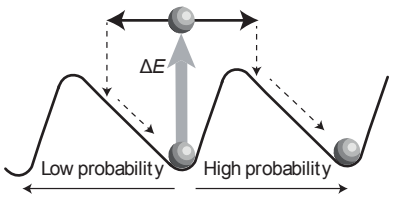

Fig. 1. *Principle of unidirectionality due to a saw-tooth potential landscape. After electronic excitation (ΔE), the molecule becomes ro-vibrationally excited and shakes with a larger amplitude (solid arrows). Owing to the asymmetric potential, there is a significantly higher probability of crossing the barrier on one side than the other before the system gets de-excited and returns to the minimum energy configuration (dashed arrows).*

Creating a molecular machine that performs the task of unidirectional movement is very difficult, but was mastered by the Feringa group at the end of the last millennium [13]. A unidirectional rotor of a helically overcrowded system was synthesized and brought into action by light excitation. Over time, Feringa's group improved the

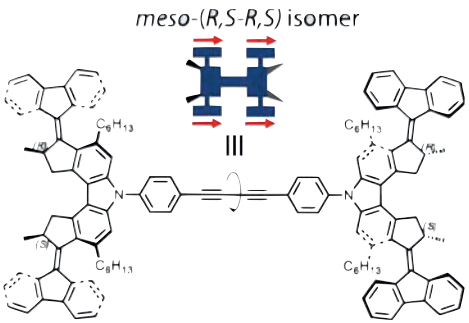

Fig. 2. *A molecular four-wheeler for unidirectional translation. Four helically overcrowded rotors are designed such excitation will all of them rotate into identical directions. The excitation requires in a first step a cis-trans isomerization, leading to a less-favoured configuration, which then relaxes back into the low-energy configuration by vibrational excitation.*

concept towards higher rotation speed, but also addressed the issue of surface-mounting of rotors [14]. The ultimate design included a large chassis and four rotors, whose stereochemical centers were carefully tuned in order to perform identical sense of rotation upon excitation. Figure 2 shows the structure of the molecule.

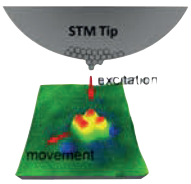

Fig. 3. *Electronic excitation by inelastic electron tunneling from an STM tip into the substrate via the molecule is expected to activate the rotor action. Because all rotors are designed to turn into the same direction, the molecule would perform a unidirectional motion on the surface.*

In order to activate propulsion, electronic excitations that causes a cis-trans isomerization a the C=C bonds is required. This is achieved only at higher voltages when tunneling from the tip into the substrate. Figure 4 shows a serious of images after exceeding 550 mV bias voltage. The molecule shows an almost linear movement and a different STM contrast appearance along the path. We attribute this to the motor action of the molecule that, as expected, led to linear unidirectional translation on the surface.

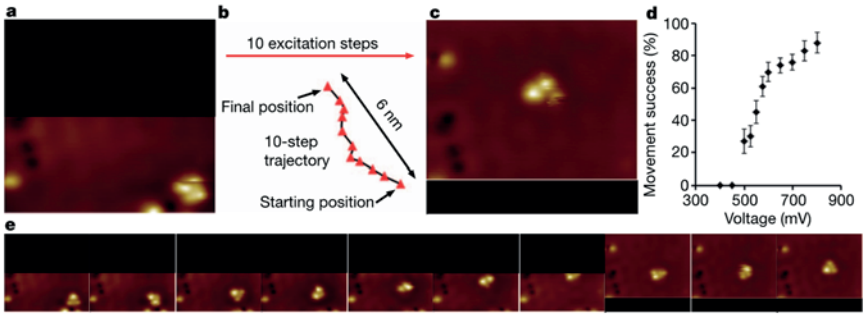

Fig. 4. *STM images taken after excitation at bias voltages corresponding to electronic excitations. The molecule moves along a basically linear trace. The threshold bias suggests tunneling into the LUMO orbital of the molecule.*

4. Conclusions and Outlook

After demonstrating the first proof of concept of unidirectional propulsion of a molecule after clever chemical design more insight into the molecular motor dynamics is required. Currently we perform experiments with two-motor unit

walkers (or ‘waddling ducks’; Fig. 5), which, besides unidirectionality, show identical behavior upon excitation by inelastic electron tunneling.

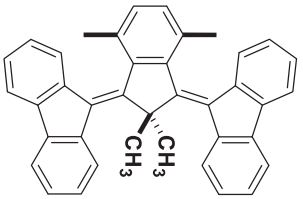

Fig. 5. *Molecule with two motor units*

References

[1] a) Schliwa, M. & Woehlke, G. Molecular motors. *Nature* **2003**, *422*, 759–765; b) van den Heuvel, M. G. L. & Dekker, C. *Science* **2007,** *317*, 333–336.
[2] M. Peplow, *Nature*, **2015**, *525*, 18.
[3] Eigler, D. M.; Schweizer, E. K. *Nature* **1990**, *344*, 524−526.
[4] Komeda, T. Prog. *Surf. Sci.* **2005**, *78*, 41−85.
[5] J. I. Pascual, N. Lorente, Z. Song, H. Conrad, H.-P. Rust, *Nature* **2003**, *423*, 525 – 528.
[6] P. A. Sloan, R. E. Palmer, *Nature* **2005**, *434*, 367–371; b) B. C. Stipe, M. A. Rezaei, W. Ho, S. Gao, M. Persson, B. I. Lundqvist, *Phys. Rev. Lett.* **1997**, *78*, 4410 – 4413.
[7] S. W. Hla, L. Bartels, G. Meyer, K.-H. Rieder, *Phys. Rev. Lett.* **2000**, *85*, 2777–2780; b) S. W. Hla, K.-H. Rieder, *Annu. Rev. Phys. Chem.* **2003**, *54*, 307–330.
[8] a) J. Gaudioso, L. J. Lauhon, W. Ho, *Phys. Rev. Lett.* **2000**, *85*, 1918–1921; b) F. Moresco, G. Meyer, K.-H. Rieder, H. Tang, A. Gourdon, C. Joachim, *Phys. Rev. Lett.* **2001**, *86*, 672 – 675.
[9] a) B. C. Stipe, M. A. Rezaei, W. Ho, *Phys. Rev. Lett.* **1998**, *81*, 1263 – 1266; b) T. Komeda, Y. Kim, M. Kawai, B. N. J. Persson, H. Ueba, *Science* **2002**, *295*, 2055 – 2058; c) B. C. Stipe, M. A. Rezaei, W. Ho, *Science* **1998**, *280*, 1732 – 1735.
[10] a) Perera, U. G. E. et al. *Nature Nanotech.* **2013** *8*, 46–51; b) Tierney et al. *Nature Nanotech.* **2011**, *6*, 625–629.
[11] Kudernac, T. et al. *Nature* **2011**, *479*, 208–211.
[12] Ernst, K.-H. *Nature Nanotech.* **2013**, *8*, 7–8.
[13] Koumura, N., Zijlstra, R. W. J., van Delden, R. A., Harada, N. & Feringa, B. L. Light- driven molecular rotor. *Nature* **1999**, *401*, 152–155.
[14] van Delden, R. A. et al. *Nature* **2005**, *437*, 1337–1340.

DNA Binding Radiosensitizers and Low Energy Electrons

Jaroslav Kočišek, Jiří Pinkas, Juraj Fedor and Michal Fárník
J. Heyrovský Institute of Physical Chemistry of the CAS, Dolejškova 3, 18223 Prague, CZ

Dan Reimitz, Marie Davídková
Nuclear Physics Institute of the CAS, Na Truhlářce 39/64, 180 00 Prague, CZ

During the interaction of ionizing radiation with living matter, a number of secondary species is formed. One of such species are low energy (0 eV - 10 eV) electrons. These electrons are formed in a large amount and exhibit energy dependent, resonant, breakage of DNA [1]. The resonant process that leads to the bond breaking at these low electron energies is called dissociative electron attachment (DEA). Several radio sensitizers exhibit large cross sections for the DEA, what was used as a base for the description of a synergistic effect of the combined chemo – radiation therapy. That is the higher combined effect of radiation and chemotherapy in comparison to the additive effect of individual treatments. The effect was studied for DNA binding chemotherapeutics such as cisplatin [2] or halo-uracils [3]. In this contribution, we present our experimental studies of cisplatin and halouracils in the effort to explain fundamentals of the synergistic effect.

Electron attachment to isolated halogen uracils leads to the formation of transient negative ion that dissociates to form Uyl radical or Uyl radical anion, which are highly reactive. Most of the studies so far were focused on the dissociation of the halouracil transient anions. Using the gas humidification method, we have been able to prepare single micro-hydrated molecules of uracil and its analogues that mimic biological conditions. In our study [4] we showed that the water environment is very effective in the stabilization of the transient anions and the dissociation is not effective. However, such stabilization results in the effective energy transfer to the solvent. We estimated this energy on the basis of our experiments with sequentially microhydrated molecules [5]. The energy is in the the range of eV and correlates with electron affinities of the microhydrated species. However, as we discuss in the work, scaling of the observation to real environments is not strightforward. Therefore, we are performing experiments on more realistic systems of plasmid DNA in solution.

The damage of DNA by different types of ionizing radiation is evaluated in the presence chemotherapeutics. To identify the effect of different secondary species created by ionizing radiation, we are using the method originally developed in the L. Sanche group for cisplatin [6]. We confirmed previous results for cisplatin and successfully implemented the method to study the combined effect of RAPTA C and gamma radiation on the plasmid DNA damage [7]. Clear detection of the synergism induced by secondary low energy electrons and chemotherapeutics requires suppression of the DNA damage induced by OH radicals and simultaneously high doses of ionizing radiation. In general, our studies show that direct effects of secondary low energy electrons are low and more complex chemical and bio-chemical models need to be developed to explain the chemo – radiation synergy observed in vivo.

Acknowledgment: This work was supported by the Czech Science Foundation (grant No.16-10995Y).

[1] Boudaiffa, B. et al., *Science* **287** (2000) 1658.
[2] Rezaee, M. et al., *Int. J. Radiat. Oncol. Biol. Phys.* **87** (2013) 847.
[3] Chomicz, L et al., *J. Phys. Chem. Lett.* **4** (2013) 2853.
[4] Kočišek, J. et al., *J. Phys. Chem. Lett.* **7** (2016) 3401.
[5] Poštulka, J. et al. *J. Phys. Chem. B* **121** (2017) 8965.
[6] Rezaee, M. et al. *Rad. Res.* **179** (2013) 323.
[7] Reimitz, D. et al., *Rad. Phys. Chem.* **141** (2017) 229.

Stereodynamics Coming in From The Cold

Sean D.S. Gordon[1], Juan J. Omiste[2], Junwen Zao[1], Silvia Tanteri[1], Paul Brumer[2] and Andreas Osterwalder[1*]
[1]*EPFL SB ISIC, LCPM Station 6, 1015 Lausanne, Vaud, Switzerland*
[2]*Department of Chemical Physics, University of Ontario, 80 St. George Street, Toronto, Ontario M5S 3H6*
**andreas.osterwalder@epfl.ch*

Introduction

The stereodynamics of the Penning and associative ionisation processes has recently been studied using a crossed molecular beam apparatus. [1] The experiment uses a curved magnetic hexapole to polarize a beam of incident metastable Ne($^3P_2$) [Ne*] atoms into an interaction region which features a set of magnets that adiabatically orient the Ne*. The beam of Ne* is crossed with neat Ar which allows us to determine the reactivities of each Ω state, where Ω is the projection of **J** onto the interatomic axis. The Penning and associative ionisation reaction channels both have Ω state specific cross sections which can be determined by scanning the ion yield of both channels, $I_{\mathrm{AI;PI}}$ as a function of the angle of the magnetic field with the relative velocity, $\theta_{\boldsymbol{kB}}$, which is related to the state dependent cross sections $\sigma^{\Omega}_{\mathrm{AI;PI}}$ by a simple equation in Ω

$$I_{\mathrm{AI;PI}}(\theta_{\boldsymbol{kB}}) \propto \sum_{\Omega=0}^{J} p_{\Omega}(\theta_{\boldsymbol{kB}})\sigma^{\Omega}_{\mathrm{AI;PI}}. \qquad (2)$$

The ratios of the state dependent reactivities, $\sigma^{\Omega}_{\mathrm{AI;PI}}$ obtained from fitting the experimental angle dependent ion yields can subsequently be compared with state of the art theory. [2,3] It is not possible to compare the state dependent reactivities directly as the experiment is measuring the ratio of the two reaction channels rather than the absolute cross sections of each channel independently. The state dependent reactivities are therefore obtained as a ratio of the AI and PI reactivities defined as

$$R_{\mathrm{AI/PI}}(\theta, E) = \frac{I_{\mathrm{AI}}(\theta_{\boldsymbol{kB}})}{I_{\mathrm{PI}}(\theta_{\boldsymbol{kB}})} = \frac{\sum_{\Omega=0}^{J} p_{\Omega}(\theta_{\boldsymbol{kB}})\sigma^{\Omega}_{\mathrm{AI}}}{\sum_{\Omega=0}^{J} p_{\Omega}(\theta_{\boldsymbol{kB}})\sigma^{\Omega}_{\mathrm{PI}}} \qquad (2)$$

Results

The experimental results shown in Figure 1 demonstrate that as the collision energy decreased, associative ionisation becomes preferred, at variance with long standing ideas of the long range nature of the Penning process. [1,4] The state dependent reactivities also change as a function of the collision energy becoming more similar as the collision energy decreases (right panel figure 1).

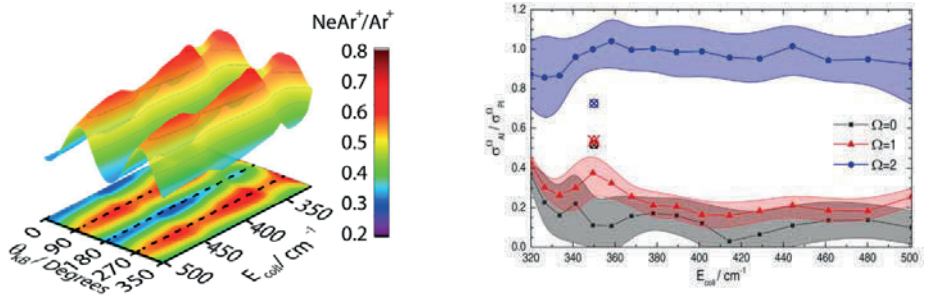

Figure 1. *Energy dependent stereodyanmics determined in a crossed molecular beam experiment. The left hand panel shows the steric effect as a function of orientation angle and collision energy from which the state dependent reactivities can be obtained (right panel).*

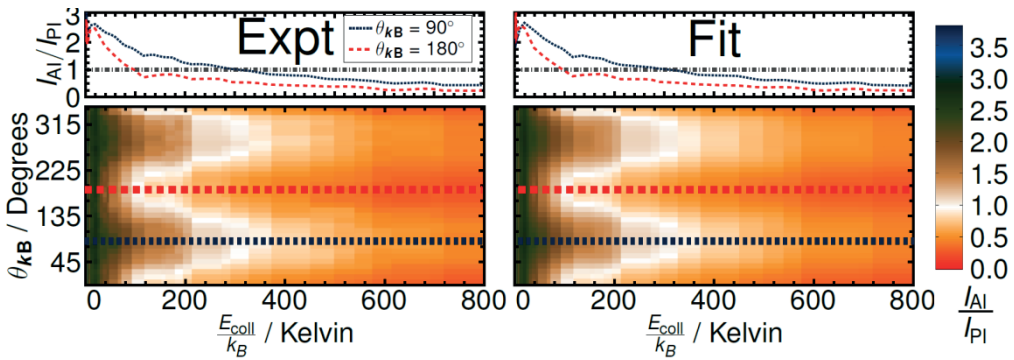

Figure 2*. Energy dependant Stereodynamics from 0.01K to 8000K for the Ne($^3P_2$)+Ar system. Green indicates the dominance of associative ionisation and red the dominance of Penning ionisation. The white area denotes the point the ion yield of AI and Pi are equal. Cuts as a function of collision energy along the red and blue lines are also shown.*

In order to investigate this phenomenon further, we use our merged beam setup [5] in a configuration where the Ne* beam is overlapped co-linearly with a beam of neat or seeded Ar. This setup is suitable for probing the steric effect at the lowest collision energies of a few millikelvin, but can also access very large collision energies. [6] We observe the complete dominance of the associative ionisation channel irrespective of the orientation direction and hence Ω state in the cold regime, as shown in Figure 2. We also observe the total loss of the Penning channel at these low collision energies, as can be seen in Figure 1. As the collision energy is slowly increased, the steric effect makes a return at approximately 10K, indicating a possible change of mechanism as the collision energy reaches this level. Newly calculated theory in the relevant collision energy range provided by Brumer *et al.* allows comparison to our experimental data across the energy regimes.

The state dependent reactivities obtained from the experiment are shown in Figure 3. Qualitatively the theory captures the rise in the cross sections as the collision energy is decreased, however, the quantitative agreement is not yet satisfactory. At low collision energy the steric effect is lost. The theory predicts that a residual steric effect should remain. At high collision energy, the Penning process dominates and the values of

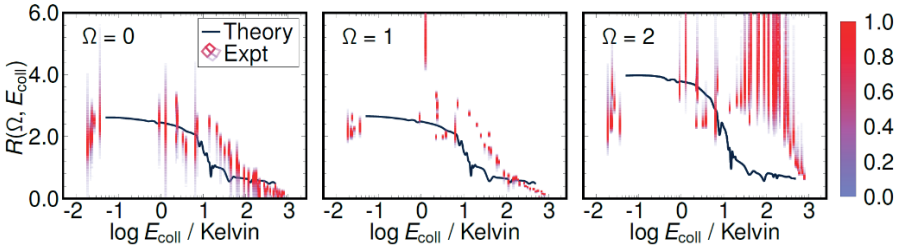

Figure 3. *State dependent reactivities obtained from the merged beam experiment (red colorbars) across the energy accessible range compared to state-of-the-art theory (blue). The colormap gives the probability density of the AI/PI state dependent reactivities having a certain value.*

The results presented give insight into the mechanism of the collision interaction. Morgner proposed that the reaction proceeds *via* two independent mechanisms, one in which a long range interaction causes the ionization of the Ar, leading to penning ionization and the other a short range interaction that leads to complexation and either AI or PI depending on the degree of internal

excitation.[7] In this picture, the long range mechanism would be thought to dominate at low collision energy when all reactions occur at long range. Given the PI cross section actually decreases at low collision energy, complexation must be preferred.

The raw signal intensities as a function of angle and collision energy, shown in Figure 4, demonstrate that the PI channel is mostly insensitive to the orientation of the magnetic field. The AI channel however responds strongly to the magnetic field. It appears that at lower Collison energy, the AI begins to dominate and the field direction no longer assists complex formation, this could indicate that the Ne* is positioning itself favourably for complex formation during the collision interaction itself and undergoing dynamical reorientation.

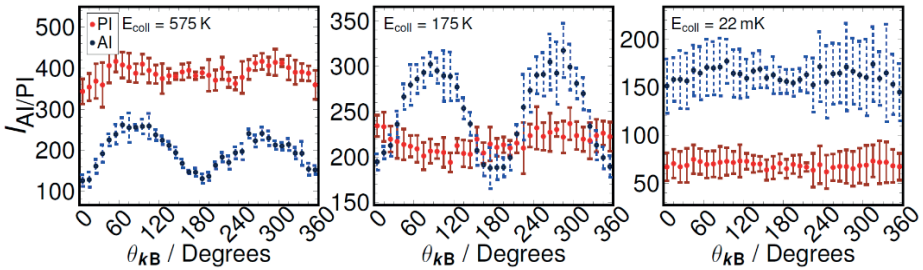

Figure 4. *The raw signal intensity at high (left), middle (middle) and low (right) collision energy. The AI channel (blue) responds strongly to the magnetic field in comparison to the PI channel (red).*

The collision energy being low causes few rovibrational states to be populated in the complex and thus it is more likely to auto-ionize rather than dissociatively ionize. This leads to a large reduction in the PI yield as more complexes are formed and more survive to form the AI products.

Conclusions

A merged beam experiment has been used to study the associative and Penning channels of the Ne*+Ar reaction. We have observed the increase in AI products as the collision energy is reduced and the coalescence of the state dependent reaction cross sections. The change in ion yield and the insensitivity to the magnetic field at low collision energy leads us to believe that the collision system is undergoing dynamical reorientation in order to maximize the chance of complex formation. At the low collision energies probed here, the complex forms almost entirely in the ground rotational states which lead to

autoionization and hence AI rather than dissociation and hence PI. A similar approach is being applied to molecular ionisation systems in order to observe the stereodynamics in the presence of exotic phenomena such as barrier resonances. In the presence of a resonance, the two reaction channels will drastically change leading to huge oscillations in the PI and AI channels.

References

[1] *Phys. Rev. Lett.* **119** (2017) 053001
[2] *Phys. Rev. Lett.* **97** (2006) 193202
[3] *J. Chem. Phys.* **125** (2006) 094315
[4] *J. Chem. Phys.* **82** (1985) 773
[5] *EPJTI*, **2** (2015) 10
[6] *J. Chem. Phys.* **142** (2015) 164305
[7] *J. Chem. Phys.* **67** (1977) 4923

A Molecular Quantum Switch Based on Tunneling in Meta-D-phenol C_6H_4DOH

Csaba Fábri,[1, 2, 3] Sieghard Albert,[1] Ziqiu Chen,[1] Robert Prentner[1] and Martin Quack[1]

[1]Physical Chemistry, ETH Zürich, CH-8093 Zürich, Switzerland
[2]Laboratory of Molecular Structure and Dynamics, Institute of Chemistry, Eötvös University, Pázmány Péter sétány 1/A, H-1117 Budapest, Hungary
[3]MTA-ELTE Complex Chemical Systems Research Group, P.O. Box 32, H-1518 Budapest 112, Hungary

We introduce the concept of a molecular quantum switch and demonstrate it with the example of m-D-phenol, based on recent theoretical and high-resolution spectroscopic results for this molecule. In the regime of tunneling switching with localized low-energy states and delocalized high-energy states the molecular quantum switch can be operated in two different ways, (i) a quasiclassical switching by coherent infrared radiation between the two isomeric structures syn- and anti-m-D-phenol; (ii) a highly nonclassical switch making use of bistructural quantum superposition states of the syn- and anti-structures, which can be observed by their time-dependent spectra after preparation.

Molecular switches and machines have received much attention over the last few decades (see Ref. [1] and references cited therein). Typical examples are provided by cis-trans isomerizations as in azobenzene derivatives [2] or in the retinal framework as used in bacteriorhodopsine or in vision [3], perhaps even prototypical for thought processes, the eye being part of the brain [4]. Chiral modifications of these or intrinsically chiral molecules can be used in chiroptical switches [5]. Molecular switches can be utilized to open and close molecular containers [6]. These switches are frequently driven by photoisomerisation employing visible or UV light, but more general chemical concepts have been applied and extensions exist to molecular motors and machines [7]. Common to all of these developments is the change of essentially “classical” molecular structures initiated by some external driving mechanism.

A different type of “switch” would be the change in the population of molecular quantum states driven by coherent radiation, as it occurs in a wide variety of situations ranging from the spin states in magnetic resonance (see Refs. [8] and [9]) or optically driven population transfers (see Refs. [10-13]). In these cases structural properties are irrelevant and the induced changes could refer

to spin states, rotation-vibration or electronic states of molecules or even single atoms or ions.

A simple one-dimensional model combining these two basic concepts has been proposed some time ago in terms of coherent quantum wavepacket motion showing transient chirality of a hypothetical chiral molecular quantum switch, however, without a realistic molecular background [14], and the principle of chiral molecular quantum switches has been discussed also in relation to parity violation in chiral molecules, with possible application towards experiments in fundamental molecular physics [11, 15, 16], but no immediately obvious application towards a possible molecular quantum technology.

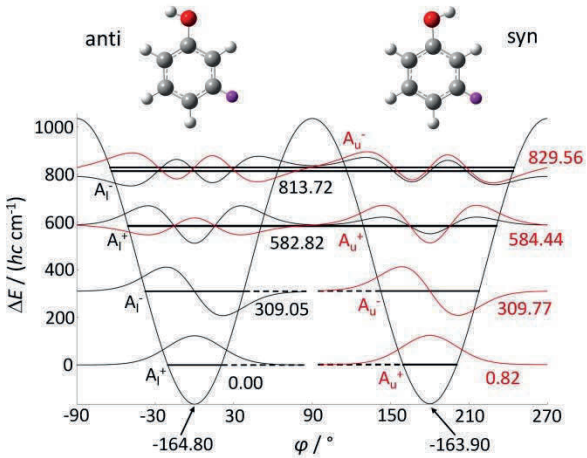

Figure 1. *The lowest adjusted adiabatic channel potential for meta-D-phenol including several torsional energy levels and wavefunctions. The two potential wells corresponding to the anti- and syn-structures are indicated by the two equilibrium structures (carbon atoms are shown in grey, hydrogen light grey, oxygen red and deuterium violet). The indices l and u refer to lower and upper levels, whose energies are referenced to the lowest quantum state as 0 and are given in terms of* E_k */(hc cm*$^{-1}$*). The exponents + and* − denote positive and negative parities. In the graphical representation the splittings can be seen only for the highest level but can be deduced from the energies given.

Here, we introduce a realistic prototypical example of a molecular quantum switch based on a conformation change in m-D-phenol, which was recently shown to exhibit the phenomenon of tunneling switching with excitation in the infrared spectral range [17, 18]. This molecule (Fig. 1) shows localized quantum states at low vibrational energies but can be switched between localized states when exciting to higher energies where tunneling switching

occurs, corresponding to delocalized, truly bistructural states. Using coherent excitation with electromagnetic radiation one can generate a genuine molecular quantum switch, which includes the possibilities of localized quasiclassical structure of low energy eigenstates, delocalized structures of excited torsional states and of quantum superposition states which are bistructural. The properties of such molecular quantum switches thus include both the properties of quasiclassical molecular structures and of quantum superposition states as they might find applications in quantum information and computing [19].

We treat the quantum dynamics of m-D-phenol with a purely vibrational model, as this contains the essence of the effects to be demonstrated. In the real system, rotation can be easily added using the usual rotation-vibration Hamiltonian and selection rules, which have been shown to provide an excellent representation of the high-resolution spectra of m-D-phenol [18] as also of phenol in this spectral range [17]. We follow Ref. [11] in the theoretical treatment, where the explicit inclusion of rotation had been discussed as well (for ClOOCl). The full-dimensional quantum dynamics is treated in two steps. First, we solve the time-independent vibrational Schrödinger equation (1) using the quasiadiabatic channel reaction path Hamiltonian approximation (RPH) treating the torsional coordinate as the large-amplitude reaction path [11, 20].

$$\hat{H}_0(x)\phi_k(x) = E_k\phi_k(x) \tag{1}$$

In the second step we solve the time-dependent Schrödinger equation

$$\mathrm{i}\frac{h}{2\pi}\frac{\partial\psi(x,t)}{\partial t} = \hat{H}(x,t)\psi(x,t) \tag{2}$$

with inclusion of the electric dipole interaction with a classical radiation field [10, 21, 22].

We report the wavepacket dynamics and the time dependent populations and spectra. The “wavepackets” are represented as probability proportional to probability density ($\left|\psi(\varphi,t)\right|^2 \mathrm{d}\varphi$ with a nominal value of $\mathrm{d}\varphi = 1°$). Figure 2 presents some exemplary results.

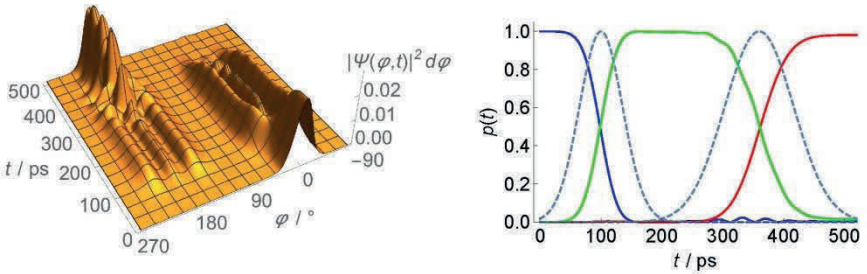

Figure 2. *Time-dependent wavepacket (reduced probability density as function of the torsional angle φ and time t) and populations ($|0_{anti}\rangle$: blue, $|0_{syn}\rangle$: red, $|2_{lower}\rangle$: green) for the two-pulse excitation scheme $|0_{anti}\rangle \rightarrow |2_{lower}\rangle \rightarrow |0_{syn}\rangle$. Two laser pulses, Gaussian envelopes, dashed lines: $\tau_P = 50\,\text{ps}$, $t_0 = 100\ \text{ps}$, $I_{max} = 150\ \text{MW/cm}^2$ and $\tilde{\nu}_0 = 582.82\ \text{cm}^{-1}$ (first pulse, resonant with the transition $|0_{anti}\rangle \leftrightarrow |2_{lower}\rangle$), and $\tau_P = 80\,\text{ps}$ $t_0 = 360\ \text{ps}$, $I_{max} = 150\ \text{MW/cm}^2$ and $\tilde{\nu}_0 = 582.00\ \text{cm}^{-1}$ (second pulse, resonant with the transition $|0_{syn}\rangle \leftrightarrow |2_{lower}\rangle$).*

Acknowledgments

Our work is supported financially by the Swiss National Science Foundation, ETH Zürich, an ERC Advanced Grant No. 290925, the COST project MOLIM and NKFIH (Grant No. PD124699). We thank Irina Bolotova, Attila G. Császár, Carine Manca Tanner, Roberto Marquardt, Ruth Schüpbach and Georg Seyfang for help and discussion.

[1] B. L. Feringa, W. R. Browne (Eds.), *Molecular Switches*, 2nd. ed., Wiley-VCH, Weinheim, **2011**.
[2] Y. Hirshberg, *Cr Hebd Acad Sci* **1950**, *231*, 903-904.
[3] D. Oesterhelt, P. Hegemann, P. Tavan, K. Schulten, *European Biophysics Journal with Biophysics Letters* **1986**, *14*, 123-129.
[4] M. Quack, *Time and Time Reversal Symmetry in Quantum Chemical Kinetics,* in *Fundamental World of Quantum Chemistry. Vol. 3* (Eds.: E. J. Brändas, E. S. Kryachko), Kluwer Adacemic Publishers, Dordrecht, **2004**, pp. 423-474.
[5] W. R. Browne, B. L. Feringa, *Chiroptical Molecular Switches,* in [1], pp. 121-179.
[6] V. A. Azov, F. Diederich, *Switching Processes in Cavitands, Containers and Capsules,* in [1], pp. 257-300.
[7] W. Szymański, J. M. Beierle, H. A. V. Kistemaker, W. A. Velema, B. L. Feringa, *Chem. Rev.* **2013**, *113*, 6114-6178.
[8] R. R. Ernst, G. Bodenhausen, A. Wokaun, *Principles of nuclear magnetic resonance in one and two dimensions*, Clarendon Press, Oxford, **1987**.

[9] A. Schweiger, G. Jeschke, *Principles of pulse electron paramagnetic resonance*, Oxford University Press, Oxford, **2001**.
[10] M. Quack, *Adv. Chem. Phys.,* **1982**, *50*, 395-473.
[11] R. Prentner, M. Quack, J. Stohner, M. Willeke, *J. Phys. Chem. A* **2015**, *119*, 12805–12822.
[12] P. Dietiker, E. Miloglyadov, M. Quack, A. Schneider, G. Seyfang, *J. Chem. Phys.* **2015**, *143*, 244305.
[13] N. V. Vitanov, A. A. Rangelov, B. W. Shore, K. Bergmann, *Rev. Mod. Phys.* **2017**, *89*, 015006, RMP.
[14] R. Marquardt, M. Quack, *Z. Phys. D* **1996**, *36*, 229-237.
[15] M. Quack, *Fundamental Symmetries and Symmetry Violations from High Resolution Spectroscopy,* in *Handbook of High Resolution Spectroscopy, Vol. 1*, Chap. 18. (Eds.: M. Quack, F. Merkt), Wiley, Chichester, New York, **2011**, pp. 659-722.
[16] M. Quack, *Molecular femtosecond quantum dynamics between less than yoctoseconds and more than days: Experiment and theory,* in *Femtosecond Chemistry,* , Chap. 27. (Eds.: J. Manz, L. Wöste), VCH, Weinheim, **1995**, pp. 781-818.
[17] S. Albert, P. Lerch, R. Prentner, M. Quack, *Angew. Chem. Int. Ed.* **2013**, *52*, 346-349.
[18] S. Albert, Z. Chen, C. Fábri, P. Lerch, R. Prentner, M. Quack, *Mol. Phys.* **2016**, *114*, 2751-2768.
[19] M. A. Nielsen, I. L. Chuang, *Quantum computation and quantum information*, Cambridge University Press, **2010**.
[20] B. Fehrensen, D. Luckhaus, M. Quack, *Chem. Phys.* **2007**, *338*, 90-105.
[21] S. Albert, K. Keppler Albert, H. Hollenstein, C. Manca Tanner, M. Quack, *Fundamentals of Rotation-Vibration Spectra,* in *Handbook of High-Resolution Spectroscopy, Vol. 1*, Chap. 3. (Eds.: M. Quack, F. Merkt), Wiley, **2011**, pp. 117-173.
[22] F. Merkt, M. Quack, Molecular Quantum Mechanics and Molecular Spectra, Molecular Symmetry, and Interaction of Matter with Radiation, in Handbook of High-Resolution Spectroscopy, Vol. 1, Chap. 1. (Eds.: M. Quack, F. Merkt), Wiley, Chichester, New York, **2011**, pp. 1-55.

Electron-impact induced ionization and fragmentation in hydrated biomolecule clusters

Xueguang Ren, Enliang Wang, Khokon Hossen and Alexander Dorn
Max-Planck-Institut für Kernphysik, 69117 Heidelberg, Germany

Electron-impact ionization of atoms and molecules is a fundamental process which is relevant to understand and interpret a wide range of scientific phenomenon and technological applications, including the physics and chemistry of planetary atmospheres, reactive plasmas, and more recently the medical radiation therapy. It is well known that primary ionizing radiation penetrating biological tissue produces large numbers of low-energy secondary electrons which effectively induce damages to the biological tissue [1].
In recent years it became apparent that for the transition from isolated molecules to clusters or the condensed matter, a wealth of new energy and charge transfer phenomena emerge which are absent for isolated molecules. One example is the intermolecular Coulombic decay (ICD) [2] where electronic excitation energy is transferred to a neighbour and the system decays by releasing ions and low-energy electrons. While ICD initially was found in noble gas dimers only recently it was also found in water which is ubiquitous on earth and surrounds all biological matter [3, 4]. Due to their importance in life and environmental sciences (see e.g. in [5]) water and hydrated (water-mixed) clusters are the subjects of intense research and our understanding of bio-systems could strongly profit from the discovery of hitherto unknown reaction mechanisms.
Electron-collisions with bio-relevant targets are regularly studied in the gas phase. In the present work, we report an experimental study on the electron-collision induced fragmentation and intermolecular processes in small clusters consisting of water and bio-relevant molecules like DNA constituents. Experimentally we employ a multi-particle coincidence technique, known as the reaction microscope [6, 7, 8] in which the momentum vectors and, consequently, the kinetic energies of all final state particles (electrons and ions) are measured in coincidence. In Figure 1 a schematic view of the reaction microscope is shown. Charged particles produced in the overlap region of a pulsed electron beam and a supersonic gas jet are extracted by means of homogenous electric and magnetic fields and projected onto time and position sensitive detectors. The data for each collision event are stored and evaluated in an offline analysis in order to determine the particle momentum vectors and the cross sections of interest.

We study tetrahydrofuran (THF, C_4H_8O) which is often regarded as being the simplest molecular analogue of deoxyribose, part of the DNA backbone. Figure 2 compares fragment ion time-of-flight spectra for the THF monomer and hydrated THF clusters obtained for 65 eV electron-impact ionization. The isolated monomer predominantly yields $C_3H_6^+$ as well as the parent ion $C_4H_8O^+$ and the parent with H secession. For the hydrated cluster target the line intensities change and new lines emerge. From this data and similar measurements using heavy water (D_2O) it can be concluded that H_2O allocates at the O-position in THF. Furthermore $(C_4H_8O)H^+$ originates from proton transfer from the neighbour either in an ionized THF dimer or in a THF-H_2O aggregate. Also $(C_4H_8O)(H_2O)H^+$ complexes are observed.

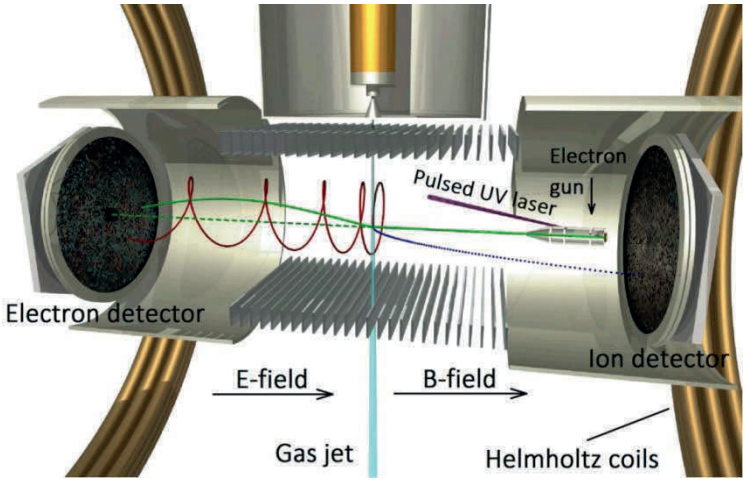

Figure 1. Schematic view of the employed reaction microscope for electron-scattering experiments.

From the measured kinetic energies of two outgoing electrons and one fragment cluster ion, the binding energy and, therefore, the ionized orbital for each fragmentation channel is obtained. By comparing the correlation spectra of binding energy and fragment species between clusters and the isolated molecule, we can investigate in detail the role of the neighbours for the modification of the biomolecular fragmentation.

In addition, we can identify ICD as predicted by theory [9] and other related processes in the THF-water dimer by the measurement of two fragment ions

in coincidence with ejected electrons. More detailed results will be presented at the conference.

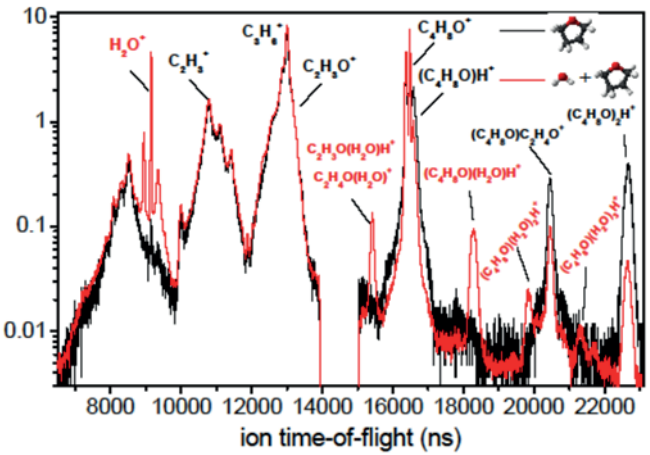

Figure 2. *Measured fragment ion time-of-flight spectra of THF and hydrated THF clusters induced by electron-impact (E_0 = 65 eV)*

References

[1] Alizadeh E et al *Annu. Rev. Phys. Chem.* (2015) **66** 379
[2] Cederbaum L S et al *Phys. Rev. Lett.* (1997) **79** 4778
[3] Jahnke T et al *Nat. Phys.* (2010) **6** 139
[4] Mucke M et al *Nat. Phys.* (2010) **6** 143
[5] Stumpf V et al *Nat. Chem.* **8** (2016) 237
[6] Ullrich J et al *Rep. Prog. Phys.* (2003) **66** 1463
[7] Ren X et al *J. Chem. Phys.* **141** (2014) 134314
[8] Ren X et al *Nat. Commun.* **7** (2016) 11093
[9] Stoychev S D et al *J. Am. Chem. Soc.* (2011) **133** 6817

Effect of vibrational excitation on HBr clusters: Velocity map imaging with action spectroscopy

Kateryna Grygoryeva, Jozef Rakovský, Viktoriya Poterya and Michal Fárník
J. Heyrovský Institute of Physical Chemistry, Prague, Czech Republic

1. Introduction

The role of hydrogen bonding is undoubtedly essential for all living matter. Hydrogen-bonded clusters therefore represent an interesting tool for studying of their properties. There still are questions to be answered: What impact does vibrational excitation of one subunit have on the dynamics of the whole cluster? How does the energy redistribute? Hydrogen halide clusters, especially the smallest ones, serve as prototypical hydrogen-bonded systems. Therefore, their intermolecular dynamics is of particular interest.

In this work, we investigate the effect of vibrational excitation on hydrogen bromide clusters and on their photodissociation dynamics. In particular, we excite one quantum of HBr stretch at the wavelengths corresponding to various clusters and, for comparison, to bare molecules [1]. Subsequently, the HBr molecules are dissociated with one 243nm UV photon, and the resulting hydrogen fragments are REMPI-ionized and detected by velocity map imaging. For bare molecules, IR excitation increases the Franck-Condon overlap of the subsequent electronic transition [2], and the increased hydrogen yield can serve for a measurement of action spectra. In the case of clusters, IR-excitation also leads to the H-signal enhancement, but there are several mechanisms possibly explaining the effect, which will be discussed in the following sections.

2. Experiment

The present experiments were conducted on the Apparatus for Imaging (AIM), which combines a pulsed molecular beam with a velocity map imaging setup (VMI) in a perpendicular arrangement. The system was first described in [3], and some more experimental details can be found in our recent study [4].

A mix of HBr and helium or argon was supersonically expanded through a pulsed solenoid valve and skimmed (see Tab. 1 for expansion conditions). The resulting molecular beam was crossed with UV and IR laser beams in the center of an electrostatic lens system, which approximately followed the original VMI setup by Eppink and Parker [5].

***Tab. 1**: Expansion conditions exploited in the present work. Nozzle parameters: diameter 0.6 mm, pulse length 300 μs.*

	Carrier gas	Concentration	Exp. pressure	Generated species
1	He	5 %	1 bar	bare molecules
2	He	20 %	3 bar	pure HBr clusters
3	Ar	6.5 %	3 bar	mixed HBr&Ar clusters

The IR wavelength was either scanned to obtain action spectra, or it was set to positions of the desired (ro)vibrational transitions for VMI measurements. The UV laser provided 243nm photons for photodissociation and 2+1 REMPI ionization of the resulting H-atoms. The H-ions were then detected via the classical VMI, and their signal was recorded as images, or it was integrated for each laser shot and recorded as a function of the IR wavelength. In the end, the velocity map images were transformed using Hankel algorithm, and kinetic energy distributions (KEDs) of H-atoms were obtained. The KEDs shown here represent difference spectra: KEDs obtained from measurements without IR irratiadion were subtracted from KEDs obtained with IR laser on.

3. Results and discussion

Fig. 1 a–c shows action spectra recorded at expansion conditions 1, 2, and 3. You can see rovibrational transitions of pure molecules present in spectra a and b, whereas the broad feature between 2400–2510 cm^{-1} in spectra b and c can be assigned to the cluster response. Unlike Haber et al. [1], we were not able to obtain spectra with distinct dimer, trimer or tetramer transitions, possibly due to the detection scheme executed here.

Right side of Fig. 1 shows kinetic energy distributions (KEDs) of hydrogen atoms recorded at different IR wavenumbers (difference spectra). Panel e contains a KED of bare molecules excited via R(0) transition. For comparison, a KED of unexcited molecules (recorded with the IR beam off) is displayed in a red dashed line. Panel f demonstrates KED from pure clusters (in He expansion) excited at 2497.4 cm^{-1}, which corresponds to HBr vibration in trimer. However, small negative feature at 0 eV indicates a contribution from larger HBr clusters. We attribute it to a caging effect, which was first observed for Ar coated clusters and which manifests as a sharp peak at 0 eV [6]. Here, vibrational excitation must fragment the cluster, which leads to the decrease of caged hydrogens. The same is observed for clusters in Ar expansion (f).

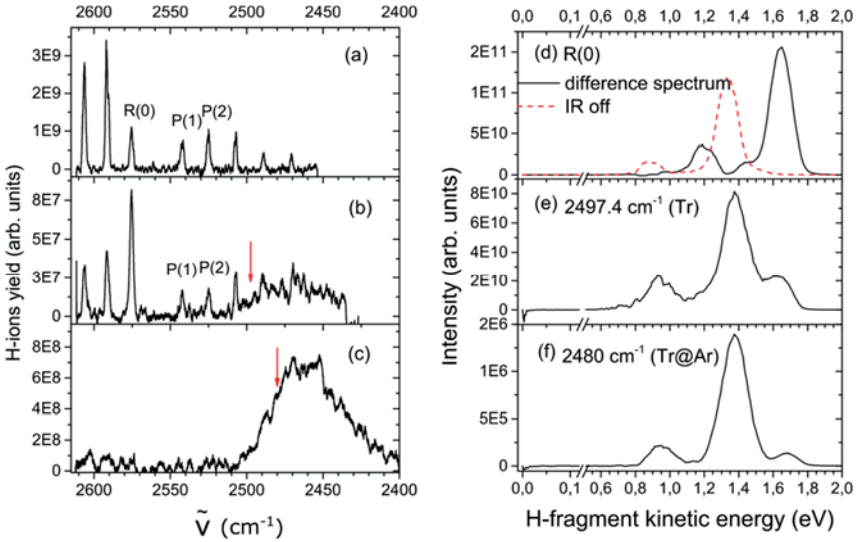

***Fig. 1**: Action spectra and KEDs of H-fragments obtained at expansion conditions 1–3 (top to bottom). Red arrows indicate IR-photon energy, at which the KEDs were measured.*

Peaks between 0.7–1.5 eV in spectra 1 e, f resemble the spectrum of IR-unexcited bare molecule. They may result from the following mechanism: one of the cluster subunits is vibrationally excited, and energy is dissipated in cluster, which leads to its dissociation. A liberated molecule is then UV-dissociated. A similar process was observed for HCl small clusters by [7].
Remarkable is a peak at 1.65 eV, which appears not only in the case of bare molecules, but also for pure and mixed clusters. This peak corresponds to Hfragments from HBr molecules that were vibrationally excited at the moment of photodissociation. Possible explanations include: (i) one cluster subunit is vibrationally excited and is UV-dissociated before any relaxation could occur. Vibrational excitation is then localized at the dissociating molecule and the dissociation proceeds directly in the cluster. (ii) One IR photon causes vibrational excitation of one cluster subunit, while another IR photon causes cluster fragmentation. However, we investigated the IR-photon flux dependence of this peak, which showed to be linear with a smaller slope than the dependence of peak at 1.4 eV; therefore, we exclude an IR-multiphoton process.

Acknowledgments

We acknowledge the financial support of Czech Science Foundation grant No 1704068S.

References

[1] T. Haber, Physical Chemistry Chemical Physics, 2003, 5(7), 1365–1369.
[2] S. Rosenwaks, Vibrationally Mediated Photodissociation, The Royal Society of Chemistry, Cambridge, 2009.
[3] J. Fedor, J. Kocisek, V. Poterya, O. Votava, A. Pysanenko, M. L. Lipciuc, T. N. Kitsopoulos, and M. Fárník, The Journal of chemical physics, 2011, 134(15), 154303.
[4] K. Grygoryeva, J. Rakovský, O. Votava, and M. Fárník, Journal of Physical Chemistry A, 2017, 147(1), 013901.
[5] D. H. Parker and A. T. J. B. Eppink, The Journal of Chemical Physics, 1997, 107(7), 2357–2362.
[6] U. Buck, Journal of Physical Chemistry A, 2002, 106(43), 10049–10062.
[7] A. K. Samanta, G. Czakó, Y. Wang, J. S. Mancini, J. M. Bowman, and H. Reisler, Accounts of Chemical Research, 2014, 47(8), 2700–2709.

Low-Temperature Chemistry of Gold

Marcelo Goulart, Martin Kuhn, Paul Martini, Lorenz Kranabetter, Monisha Rastogi, Johannes Postler, Paul Scheier
Institute for Ion Physics and Applied Physics, University of Innsbruck, A-6020 Innsbruck, Austria

Bilal Rasul
Univ Sargodha, Sargodha 40100, Pakistan

Andrew M. Ellis
Department of Chemistry, University of Leicester, LE1 7RH Leicester, United Kingdom

Olof Echt
Department of Physics, University of New Hampshire, NH 03824, New Hampshire, United States

Diethard Bohme
Department of Chemistry, York University M3J 1P3, Toronto, Ontario, Canada

Gold, the noblest of all metals, exhibits an interesting chemistry at the nanoscale level with many applications in fields like diagnosis, drug delivery systems, catalysis, solar energy conversion, molecular detection and anti-cancer therapeutics, among others. Many of gold's properties are attributed to relativistic effects [1] that arise as a consequence of electrons moving with relativistic velocities in a field of high nuclear charges. In this scenario, gold clusters arouse interest as they serve as models for structure and bonding of cluster compounds.

Superfluid helium nanodroplets [2] (HND) are formed by supersonic expansion of gaseous helium through a nozzle achieving a final temperature of 0.37 K. They are capable of picking up virtually any atom or molecule, which then aggregate and form clusters on the surface or within an HND. The sequential addition allows for the construction of clusters that cannot be synthesized by other methods. HND are a powerful experimental technique that has been extensively used in studies of atoms, molecules and nanoparticles for cryogenic isolation.

Herein we report mass spectrometric studies of mixed clusters containing gold and other species, focusing on the chemical character of the metal. The mixed clusters were formed inside HNDs via individual pickup. The neutral doped HNDs were ionized by an electron beam and then accelerated through a set of electrostatic lenses to a TOF analyzer, where the ion yield was recorded as a function of the mass per charge ratio. Anomalies in the yield, colloquially known as “magic numbers”, indicate the most stable structures after ionization. Some of these structures strongly indicate a covalent character of gold.

[1] P. Schwerdtfeger, *Heteroatom Chem.*, 2002, **13**, 578.
[2] J. P. Toennies and A. F. Vilesov, *Angew. Chem. Int. Ed.*, 2004, **43**, 2622.

Contributed Papers

Posters

Positive and negative ion formation upon collision induced dissociation of 2-Formylphenylboronic acid

J. Ameixa, J. Khreis, S. Denifl
Institut für Ionenphysik und Angewandte Physik, Leopold-Franzens-Universität Innsbruck, Technikerstraße 25, 6020 Innsbruck, Austria

F. Ferreira da Silva
Laboratório de Colisões Atómicas e Moleculares, CEFITEC, Departamento de Física, Faculdade de Ciências e Tecnologia, Universidade NOVA de Lisboa, Campus de Caparica, 2829-516 Caparica, Portugal

1. Introduction

Boronic acids are boron containing organic compounds that possess one carbon-based substituent and two hydroxyl groups. They are important compounds in organic chemistry due to their stability and ease of handling [1]. For instance, boronic acids have been extensively used as synthetic intermediates, namely in the Suzuki-Miyaura cross-coupling reaction (Chemistry Nobel Prize, 2010) [2]. Boronic acid derivatives have a significant variety of applications ranging from medicinal chemistry, namely in the synthesis of boron-based drugs, up to material science [3].

Recently, a concerted effort in understanding the use of boronic acids in labelling and functionalization of proteins is noticeable [3][4]. For instance, P.M.P. Gois and co-workers have demonstrated that 2-formylphenylboronic acid (2-FPBA) plays a main role in selectively functionalizing biomolecules. These findings unravel a new and potential tool for the synthesis of bioconjugates, such as drug-protein conjugates [5] [6]. In order to investigate the stability of 2-FPBA ions formed by electrospray ionization (ESI), we assessed the formation of positive and negative ions upon collision induced dissociation (CID). Moreover, we calculated kinetic energy release (KER) values for the most favourable dissociation channels.

2. Experimental Methods

A home built ESI source coupled to a double focusing mass spectrometer in reversed geometry was used in the present study. Briefly, the ESI source consists of a spray needle, an inlet capillary, an ion funnel, an octupole ion guide as well as an einzel lens setup. The ions were accelerated to 6 kV, followed by momentum analysis by a magnetic sector and energy analysis by an electrostatic sector. Finally, the ions were detected by a

secondary electron multiplier. We performed CID studies by placing a collision cell before the electrostatic sector. Helium was used as a collision gas. All the experiments were carried out using a 10 mM solution of 2-FPBA (purity ≥ 95,0%, Sigma-Aldrich, Austria) dissolved in methanol/water/acetic acid (50/50/1).

3. Results and Discussion

We recorded the formation of positive and negative ions using ESI mass spectrometry. In the former case, we observed $[(2\text{-FPBA})\text{-OH}]^+$ at m/z=133 as the most abundant cation. The protonated parent cation, at m/z=151, is the second most abundant cation. In the latter case, the formation of the dehydrogenated parent anion arises as the most abundant anion, at m/z=149. Thereafter, we studied the CID of the aforementioned ions. As example, the high-energy energy CID mass spectrum of $[(2\text{-FPBA})+H]^+$ is shown in Figure 1. The protonated cation (m/z=151) dissociates efficiently into a wide assortment of fragments. The loss of a hydroxyl group represents the most favourable dissociative channel, leading to a fragment cation at m/z=133.

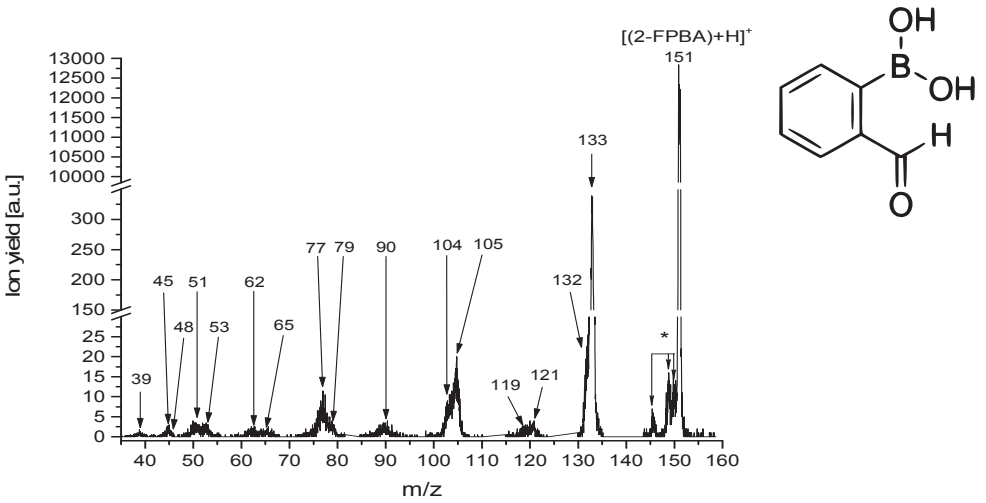

Figure 1 *– Collision-induced dissociation mass spectrum of $[(2\text{-FPBA})+H]^+$. The peaks labelled with * are artifacts.*

4. Acknowledgments

JA and FFS acknowledge the Portuguese National Funding Agency FCT-MCTES through grants PD/BD/114447/2016 and researcher position IF-FCT IF/00380/2014, respectively, and the research grant UID/FIS/00068/2013. S.D. acknowledges support from the FWF (I1015). This work was supported by Radiation Biology and Biophysics Doctoral Training Programme (RaBBiT, PD/00193/2012); UID/Multi/04378/2013 (UCIBIO).

5. References

[1] D. G. Hall, in *Boronic Acids* (Wiley-VCH Verlag GmbH & Co. KGaA, Weinheim, Germany, 2011), pp. 1–133.
[2] N. Miyaura, K. Yamada, and A. Suzuki, Tetrahedron Lett. **20**, 3437 (1979).
[3] D. B. Diaz and A. K. Yudin, Nat. Chem. **9**, 731 (2017).
[4] C. B. Rosen and M. B. Francis, Nat. Chem. Biol. **13**, 697 (2017).
[5] H. Faustino, M. J. S. A. Silva, L. F. Veiros, G. J. L. Bernardes, and P. M. P. Gois, Chem. Sci. **7**, 5052 (2016).
[6] P. M. S. D. Cal, J. B. Vicente, E. Pires, A. V. Coelho, L. F. Veiros, C. Cordeiro, and P. M. P. Gois, J. Am. Chem. Soc. **134**, 10299 (2012).
[7] J. M. Khreis, J. Reitshammer, V. Vizcaino, K. Klawitter, L. Feketeová, and S. Denifl, Rapid Commun. Mass Spectrom. Accepted (2017), DOI: 10.1002/rcm.8027

BeD Compounds formed in an Ion-Surface Collision

Lorenz Ballauf
Institute for Ion Physics and Applied Physics, University of Innsbruck, Technikerstrasse 25, 6020 Innsbruck, Austria

Faro Hechenberger, Lorenz Kranabetter, Paul Scheier
Institute for Ion Physics and Applied Physics, University of Innsbruck, Technikerstrasse 25, 6020 Innsbruck, Austria

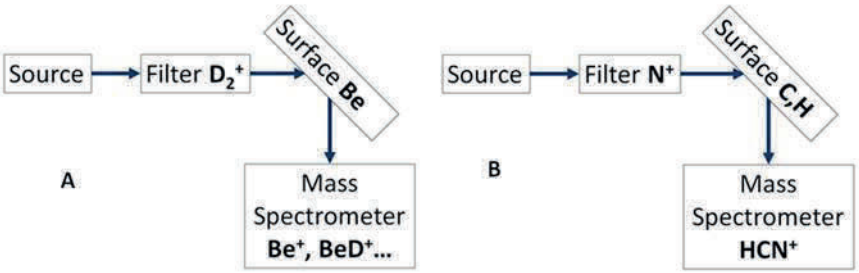

Fig. 1 *Sketch of Ion-Surface Investigation with focus on Tritium retention in (A) and HCN^+ formation in (B).*

The experimental work described focuses on reactive ion-surface collisions and their ionic products. There are two main fields of investigation. First, in context of thermonuclear fusion, is the Tritium retention – radioactive Tritium accumulates in the Tokamak. The aim is to understand the underlying mechanisms in order to control them.

Current research indicates that tritium retention is driven by co-deposition with Beryllium (Be) eroded from the first wall [1]. In order to investigate possible compounds of Be and H, D and T, a Be surface is bombarded with Deuterium molecular ions and Ar^+ ions (compare Fig 1 (A)). Our experiments reveal that indeed BeH^+ and BeD^+ compounds are formed. The chemical nature of their binding indicates that a BeT^+ compound should form in the same way.

Especially this chemical character is of particular interest, because a removal from the Tokamak requires different techniques compared to simple adsorption – binding energies are very different.

In measurements it is well shown, that the formation of BeH^+ is efficient at all energies that we used (110 eV to 426 eV). It was also efficient with very different projectiles, i.e. D_2^+ and Ar^+.

Second field of investigation is the formation of HCN^+ and other bio-relevant molecules in a collision of a N-containing projectiles (N_2^+, N^+, NH^+ NH_2^+…) and hydrocarbon surfaces (compare Fig 1 (B)).

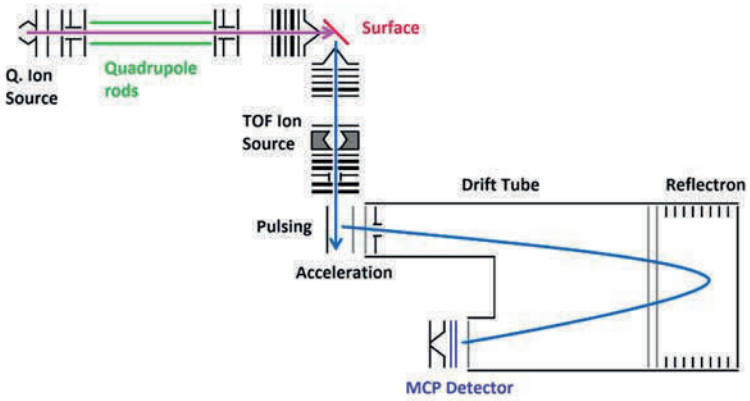

Fig. 2. *Sketch of the tandem mass spectrometer constructed and used for the measurements.*

1. In-Situ Surface cleaning

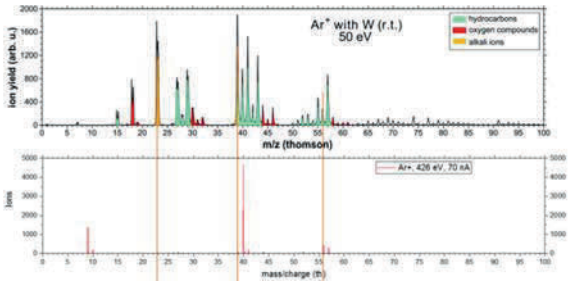

Fig. 3. *Comparison of the old spectra [3] (top, Ar^+ impacting W, 50 eV) with the new spectra (bottom, Ar^+ impacting Be, 426 eV).*

As visible in Fig 3, the spectra obtain at the new setup are free of hydrocarbons. That is remarkable, as the pressure in the corresponding chamber is usually 2×10^{-8} mbar – it is achieved by in-situ sputter cleaning of the surface by the very intense projectile beam (15-80 nA), which works throughout the whole energy range. Hence, the products measured are normally only compounds of the projectile, the surface and likely water, as it is

very abundant in the residual gas and sticks to surfaces due to its dipole moment.

2. Product ions detected from a Be surface

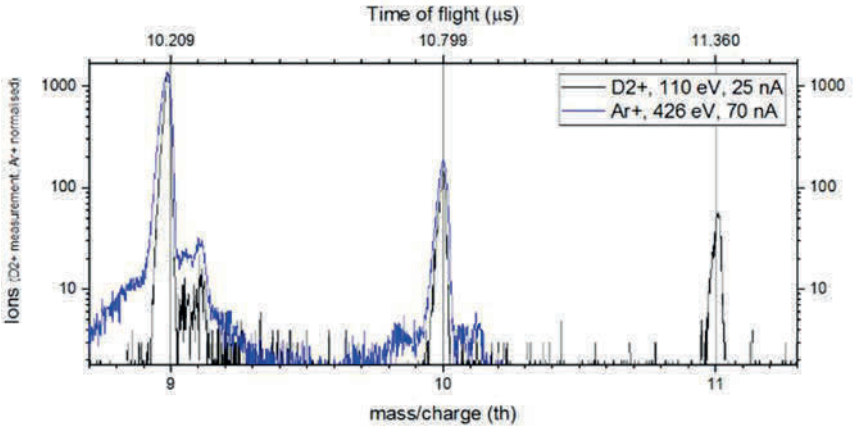

Fig. 4. *The comparison of products created by D_2^+ (black) and Ar^+ (blue). Be^+ has a mass to charge ratio of 9 Th, BeH^+ 10 Th and BeD^+ with 11 Th. There is a peak shape issue caused by improper focusing into the orthogonal extraction region, which has no physical meaning, it repeats on every peak, but is not easily visible e.g. on the BeD^+ peak because of the logarithmic scale.*

As seen in Fig 4, the BeH^+ compound is easily formed in almost any condition concerning projectile energy, projectile type and projectile current. This is surprising, as for example, performing an Ar^+ on Be impact, there is no obvious source for H. We assume, that H_2O adsorbs on the surface and is split by the projectile. This will be checked by measurements on elevated temperature and also by introducing D_2O into the vacuum chamber in the collision region and checking the creation of BeD^+ by Ar^+ impact.
Fig 5 shows again that the surface is sputter cleaned from oils. Also, neither N^+, O^+ nor O_2^+ appear in this spectrum. Interestingly the 18 Th peak, usually water, must have a different contribution as well, as OH^+ on 17 Th is lower than the ratio created by water dissociation. On these high energy, contribution of Be_2^+ to the 18 Th peak is assumed, with Be_2H^+ on 19 Th. Accordingly Be_3^+ with 27 Th and Be_3H^+ on 28 Th. So creation of small Be Clusters is observed.

26 Th is assigned to BeOH. What cannot be seen here is that for lowest (110 eV) impact energies, this peak remains the highest. This is the effect of chemical sputtering, the compound BeOH has a lower surface binding energy and is hence sputtered more efficiently.

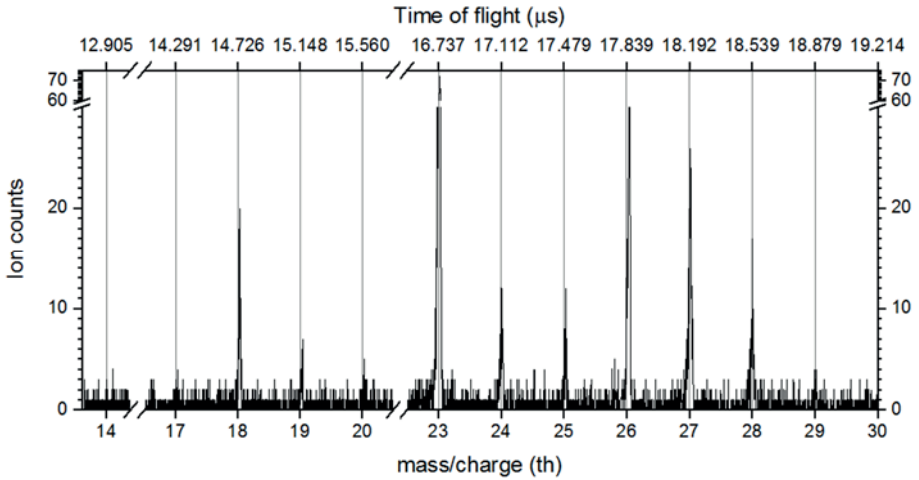

Fig. 5. *After a few minutes and 80 nA of surface current created by projectile neutralisation, 426 eV impacting mainly D2+ and little contribution of D+ and D3+ (quadrupole not used here in favour of Surf. current).*

3. Projectile Energy scan

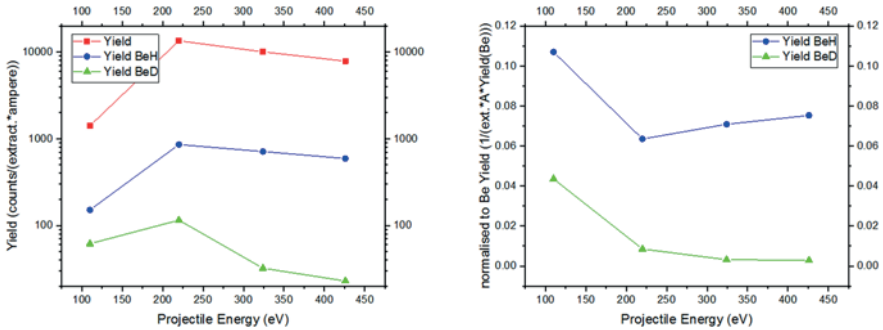

Fig. 6. *Left: Be^+, BeH^+ and BeD^+ peaks integrated and normalised and background-corrected at 4 different projectile energies (absolute yield). Right:* the same, but normalised to the Be^+ yield of each spectrum. i.e. the green curve shows how many BeD^+ ions are sputtered per Be^+ ion sputtered (relative yield).

The energy scan (Fig 6) shows qualitative agreement with theory. On the absolute yield, one can see that in general more molecules are sputtered at higher energies. On top of that, the ionisation probability per product is likely rising, so a mixture of both is measured here. The statistical errors are very small, usually smaller than the symbols used – but systematic errors by different transmission of the ion optics at different product kinetic energies are difficult to estimate. Hence, the highest product ion yield at 210 eV could be influenced by such effects.
The relative yield cancels such errors, as it can be safely assumed, that a Be^+ is transmitted as good by the optics as BeH^+ and BeD^+
are. If similar ionisation probabilities are assumed as well, this also represents the neutral behaviour.
The measured BeD^+ behaviour can safely be explained with a better adsorption of neutral D_2 from the projectile beam to the surface, which agrees nicely with MD simulations [2]. Unfortunately, it is so far experimentally impossible to access even lower energies, where the neutral sputtering should be even more effective.
The BeH^+ is more difficult to explain as the source of H is still to be identified more surely. Ongoing measurements indicate a strong temperature dependence towards lower BeH^+ at higher Surface temperatures. The results will be available and discussed at SASP 2018.

4. References

[1] De Temmerman, G. et al. Efficiency of thermal outgassing for tritium retention measurement and removal in ITER. Nuclear Materials and Energy (2017). doi:10.1016/j.nme.2016.10.016
[2] Björkas, C. et al. Molecules can be sputtered also from pure metals: sputtering of beryllium hydride by fusion plasma–wall interactions. Plasma Physics and Controlled Fusion 55, 074004 (2013).
[3] Harnisch M. et al. Ion-surface collisions of slow ions with fusion-relevant surfaces [Phd]. University of Innsbruck; 2015

Reactivity of $M(CO_2)(H_2O)_n^+$ cations; M=Co, Mg

Erik Barwa, Tobias Pascher, Milan Ončák, Thomas Taxer,
Christian van der Linde, Martin K. Beyer
Institut für Ionenphysik und Angewandte Physik, University Innsbruck, Technikerstraße 25/3, 6020 Innsbruck, Austria

Hydrated singly charged metal ions doped with carbon dioxide, $M(CO_2)(H_2O)_n^+$ (M=Co, Mg; n<50), in the gas phase are valuable model systems for the electrochemical activation of CO_2. These systems are studied on a modified 4.7 T Fourier transform ion cyclotron resonance (FT-ICR) mass spectrometer Bruker/Spectrospin CMS47X with an external laser vaporization source combined with laser spectroscopy [1,2]. Since mass spectrometry does not yield direct structural information, the presence of an intact CO_2 molecule was tested via the exchange against O_2. For both metals, the exchange is efficient, as seen in Figure 1. In contrast, exchange of CO against O_2 is observed for the negatively charged species $Co(CO_2)(H_2O)_n^-$, which suggests that Co^- is inserting into the C-O bond to yield $OCCoO(H_2O)_n^-$. Reaction rate constants k_{abs} and thermochemical information are extracted from the data in a nanocalorimetric analysis where the average cluster sizes and integrated intensities of reactants and products are modelled with differential equations [3]. Furthermore, absorption spectra from the ultraviolet all the way to the infrared region of the electromagnetic spectrum are measured with the combination of tuneable OPO laser systems. As seen in Figure 2, the absorption of visible light by $Co(CO_2)(H_2O)_n^-$ (n≤5) and the subsequent detection of $CoO(H_2O)_m^-$ (m≤n) supports the assumption that the C-O bond was broken and CO_2 is inserted to yield $OCCoO(H_2O)_n^-$. Structural calculations for $Co(CO_2)(H_2O)_n^-$ (n=0, 1, 2) also yield the separation of the CO_2 molecule for n≥1 as seen in Figure 3. The structure was optimized on the B3LYP/ECP10MDF/cc-pVTZ level of theory. In the case of $MgCO_2^+$ the absorption is much weaker and narrower as shown in Figure 4. Whereas in the first case for $CoCO_2^-$, the carbon atom is directly bound to the metal, in the case for $MgCO_2^+$ the molecule is calculated to be linear at the B3LYP/6-31++g** theory level. A UV photon may break the C-O bond, resulting in the release of a neutral CO molecule. The only case where the absorption was detected was for species without water, most probably because the cross section of this species is much higher than for hydrated systems, as derived from the calculations.

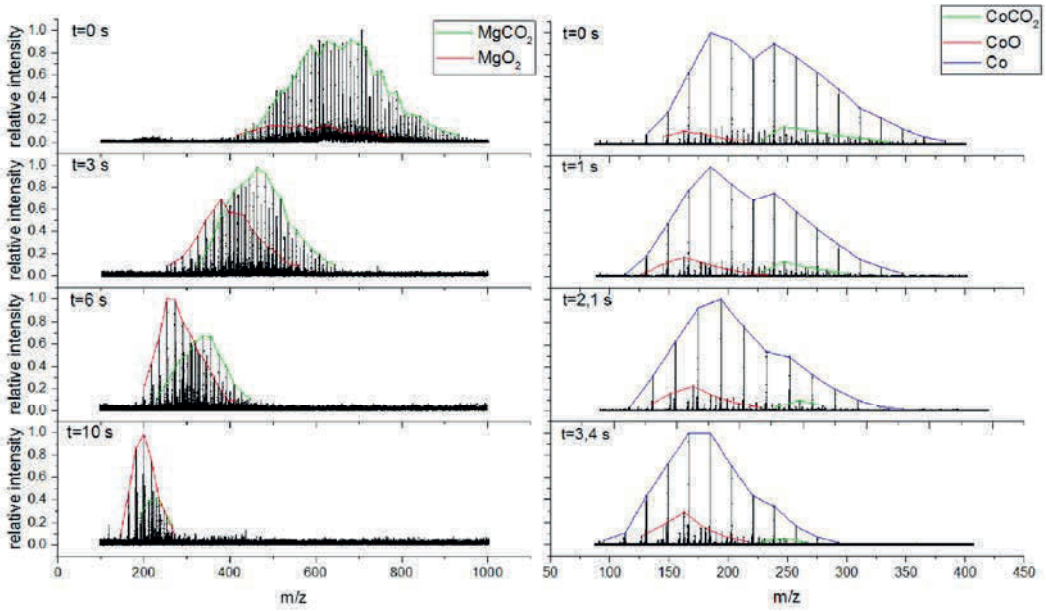

Figure 1: *Mass spectra at different reaction delays. Left the reaction of* $Mg(CO_2)(H_2O)_n^+ + O_2 \rightarrow Mg(O_2)(H_2O)_n^+ + CO_2$, *right the reaction of* $Co(CO_2)(H_2O)_n^+ + O_2 \rightarrow Co(O_2)(H_2O)_n^+ + CO_2$.

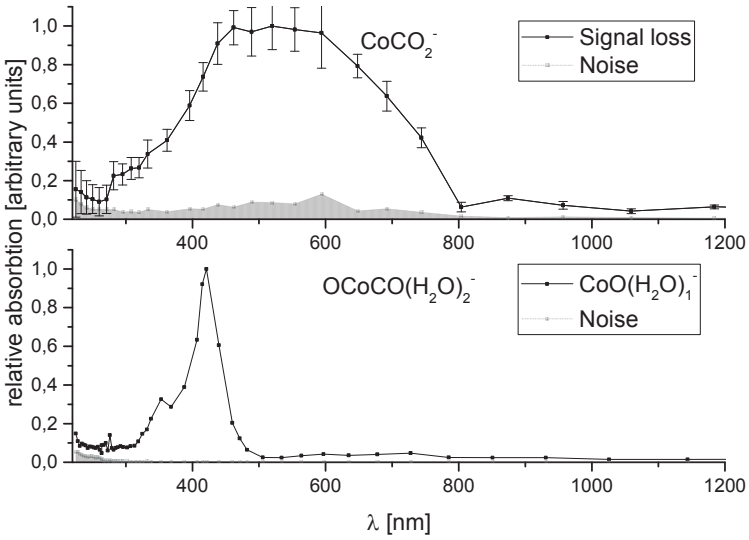

Figure 2: *Absorption spectra of $Co(CO_2)(H_2O)_n^-$ for n≤5. The more water molecules are bond to the CoO, the further the absorption peak is blue shifted.*

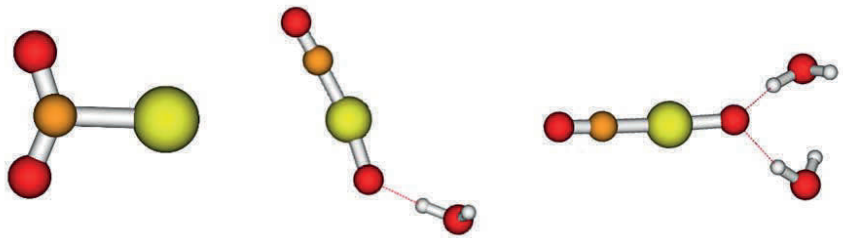

Figure 3: *Structures of $Co(CO_2)(H_2O)_n^-$ for n = 0 – 2, optimized at the B3LYP/ECP10MDF/cc-pVTZ level of theory.*

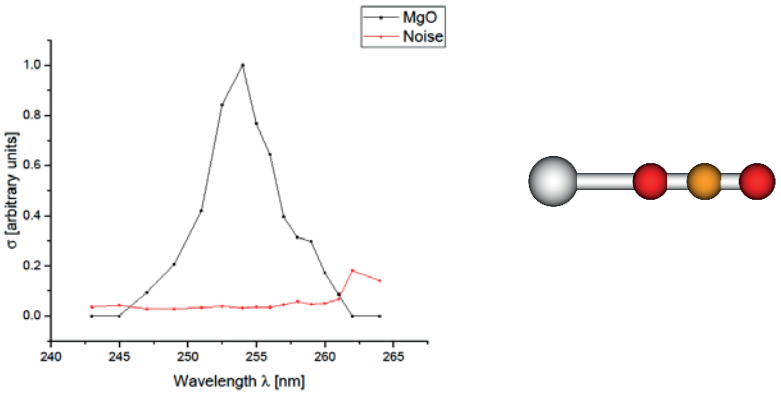

Figure 4: *Absorption spectrum of $MgCO_2^+$ without water and the calculated structure (optimized at the B3LYP/6-31++g** level).*

References:

[1] C. van der Linde, A. Akhgarnusch, C.-K. Siu, M.K. Beyer. *J. Phys. Chem. A* **2011**, *115*, 10174–10180.

[2] C. van der Linde, S. Hemmann, R.F. Höckendorf, O.P. Balaj, M.K. Beyer. *J. Phys. Chem. A* **2013**, *117*, 1011–1020.

[3] R.F. Höckendorf, O.P. Balaj, C. van der Linde, M.K. Beyer, *Phys. Chem. Chem. Phys.* **2010**, *12*, 3772–3779.

Disentangling the Excess Proton Contribution to a Sea of Broad OH Bands in Protonated Water Clusters

Chinh H. Duong, Nan Yang, Olga Gorlova, Patrick J. Kelleher, and Mark A. Johnson
Sterling Chemistry Laboratory, Yale University, New Haven, CT 06525, USA

Steffen Spieler
Institute of Ion Physics and Applied Physics – Molecular Systems, Universität Innsbruck, 6020 Innsbruck, Austria

Qi Yu and Joel M. Bowman
Department of Chemistry and Cherry L. Emerson Center for Computational Science, Emory University, Atlanta, GA 30322, USA

Anne B. McCoy
Department of Chemistry, University of Washington, Seattle, Washington 98195, USA

Abstract:
Cryogenic "messenger tagging" vibrational spectroscopy provides a microscopic picture into the mechanics of proton accommodation and the dynamics of charge translocation. We present predissociation spectra of the protonated water trimer, tetramer, and their isotopologues to systematically isolate the contributions of the excess proton to the complex band pattern occurring near the intramolecular bending mode of a water molecule. This is accomplished with a series of two-color, IR-IR photodissociation experiments. The diffuse bands in the red-shifted OH stretching region are traced to the behaviour of a single proton embedded in the hydronium ion core within the protonated water tetramer. The major bands associated with the inter-water hydrogen bond in the protonated trimer are particularly strongly mixed, and are not assignable by harmonic or perturbative theories. The isotope dependence of the bands in protonated trimer are, however, consistent with a new model developed by Joel Bowman's group based on extensive (18) mode-couplings on a realistic potential energy surface. These measurements were taken using a new background free, dual laser, triple focusing cryogenic ion mass spectrometer recently commissioned at Yale.

Electron impact induced continuum radiation of H_2

Michal Ďurian, Marián Danko, Anita Ribar, Juraj Országh
and Štefan Matejčík
Faculty of Mathematics, Physics and Informatics,
Comenius University in Bratislava, Slovakia

1. Synopsis

We report our current experimental data regarding electron induced H_2 continuum radiation of the $a^3\Sigma_g^+ \rightarrow b^3\Sigma_u^+$ transition in the spectral range of 180 – 900 nm at near-threshold electron impact energies. In contrast to earlier studies, present measurements indicate that H_2 continuum radiation is detectable above 500 nm. To supplement this, we present a comparison of relative excitation-emission cross-sections (EECS) of H_2 continuum measured at various wavelengths, with precautions taken to rule out other possible signal sources.

2. Introduction

Hydrogen and deuterium range among the most widely studied molecules in modern science [1, 2]. High-quality kinetic data of processes involving H_2 are crucial for modelling of fusion and other plasmas. We are using the electron induced fluorescence (EIF) technique, where precise control of electron kinetic energy and high photon detection sensitivity allows to obtain high-quality spectral and kinetic data. The experiment is capable of measuring emission spectra excited by electron impact and their corresponding photon efficiency curves. These can be subsequently calibrated to obtain electron excitation-emission cross-sections.

In this abstract we present results of our recent experiments involving H_2 continuum radiation spectra originating from the $a^3\Sigma_g^+ \rightarrow b^3\Sigma_u^+$ transition. The hydrogen continuum spectrum is a superposition of narrower continua (Fig. 1) corresponding to excitation of different vibrational states in the upper electronic state and their subsequent radiative decay to the lower unbound state [1, 3].

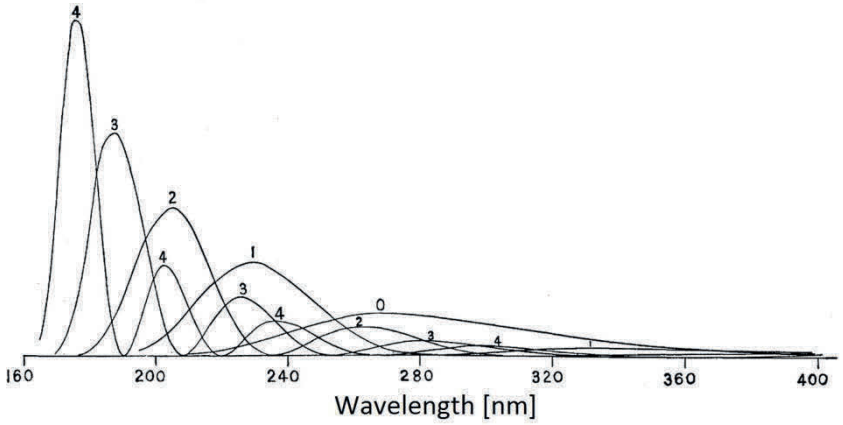

Fig. 1: *Theoretical view of the H_2 continuum.*

3. Experiment

The EIF apparatus is described in detail in [4]. The core of the experiment are crossed molecular and electron beams. Heated tungsten hairpin filament and a trochoidal electron monochromator (TEM) are used to create the electron beam, which in present experiment had electron energy resolution of 0.5 eV FWHM, electron current of a few hundred nA and with electron kinetic energy ranging from 5 to 100 eV. Photon emission is measured using an optical system comprising of Cornerstone 260 grating monochromator, focusing optics and a cooled Hamamatsu R3896 PMT tube, with spectral range from 180 to 900 nm. Typical signal intensities are in 10^0 – 10^1 order of magnitude. Spectral sensitivity calibration is performed using tungsten filament emission, taking grey body radiation model for wavelengths above 500 nm and using known H_2 continuum radiation shape for wavelengths above 200 nm [5].

4. Results

Fluorescence spectra of H_2 were taken first in 180 – 500 nm spectral range (Fig. 2) and then in 420 – 900 nm range, while using an optical filter with 420 nm cut-off wavelength to rule out higher order grating diffractions (Fig. 3). Traces of electron source filament radiation in the 500 – 700 nm region were measured and subtracted from the H_2 spectrum. Distinct spectral features, such as the continuum maximum and Fulcher bands were visible. Uniqueness of these spectra lies in observation of the continuum radiation up to 900 nm, which is much higher than the commonly reported 500 nm limit. To prove the origin of the longer wavelength radiation is in the $a^3\Sigma_g^+ \rightarrow b^3\Sigma_u^+$ transition, we

have measured relative EECS of H_2 continuum at 670 nm and 900 nm and compared their shape and thresholds to relative EECS measured at 230 nm (Fig. 4).

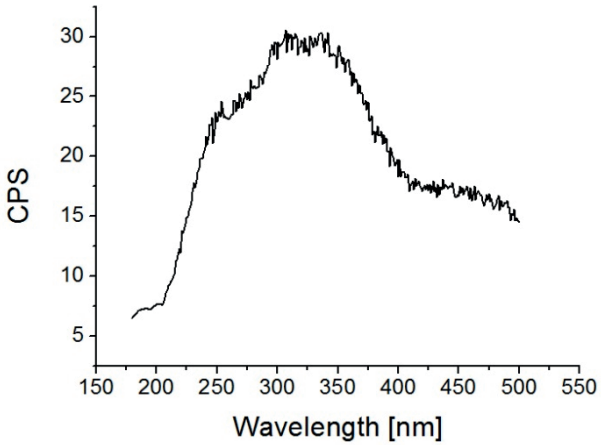

Fig 2: *H_2 continuum radiation in the 180 – 500 nm spectral region measured at 14 eV of electron energy.*

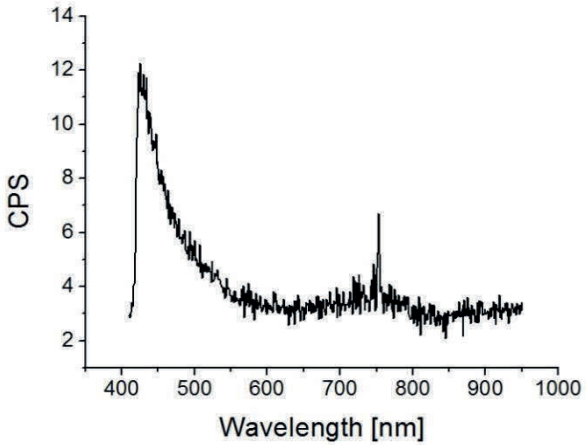

Fig 3: *H_2 spectrum in the 420 – 900 nm region measured at 12.5 eV of electron energy.*

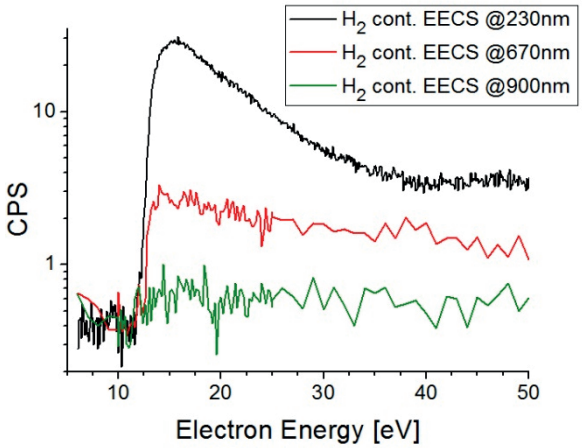

Fig 4: *Relative EECS of H_2 continuum measured at various wavelengths.*

Acknowledgements

This work was supported by the Slovak Research and Development Agency, project Nr. APVV-15-580 and the grant agency VEGA, project Nr. VEGA-15-089. This project has received funding from the European Union's Horizon 2020 research and innovation programme under grant agreement number 692335.

References

[1] B. P. Lavrov et al. 1999 *Phys. Rev. E* **59** 3526
[2] M. Ajello, D. E. Shemansky 1993 *ApJ* **407** 820
[3] H. M. James et al. 1939 *Phys. Rev.* **55** 184
[4] M. Danko et al. 2013 *J. Phys. B* **46** 045203
[5] G. K. James et al. 1998 *J. Geophys. Res.* **103** 20113

Gold clusters in helium nanodroplets

Michael Gatchell, Marcelo Goulart, Lorenz Kranabetter, Martin Kuhn, Paul Martini, Norbert Gitzl, Johannes Postler, Paul Scheier
Universität Innsbruck, Institüt für Ionenphysik und Angewandte Physik, Technikstraße 25, 6020 Innsbruck, Austria

Andrew Ellis
University of Leicester, Department of Chemistry, University Road, Leicester, LE1 7RH, United Kingdom

Gold is the poster-child of chemical stability. However, gold at the molecular level has chemical properties that stand out compared to the bulk material and can be quite reactive. Relatively little work has been carried out on organometallic complexes containing gold, especially when compared to systems with other transition metal. In this work we have performed experiments with helium nanodroplets doped with gold atoms in order to identify the structures of small gold clusters. By additionally doping the droplets containing gold with molecules such as benzene and imidazole, we have studied the chemical properties of the gold clusters, identifying characteristic “magic” combinations of gold and the aromatic rings. These experimental results are interpreted with the aid of quantum chemical structure calculations.

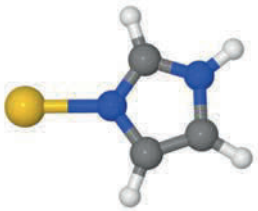

The lowest energy structure of the cationic Au + imidazole complex from DFT calculations.

This work was supported by the Austrian Science Fund FWF (projects P26635 and M1908-N36) and the Swedish Research Council (Contract No. 2016-06625) and the European Commission (Grant Agreement number: 692335 — ELEvaTE).

Observation of different reactivities of *para*- and *ortho*-water towards cold diazenylium ions

Ardita Kilaj, Hong Gao, Daniel Rösch, Uxia Rivero and Stefan Willitsch
Department of Chemistry, University of Basel, Klingelbergstrasse 80, 4056 Basel, Switzerland

Jochen Küpper
Center for Free-Electron Laser Science, DESY, Notkestrasse 85, 22607 Hamburg, Germany; Department of Physics and The Hamburg Center for Ultrafast Imaging, University of Hamburg, Luruper Chaussee 149, 22761 Hamburg, Germany; Department of Chemistry, University of Hamburg, Martin-Luther-King-Platz 6, 20146 Hamburg

Water, H_2O, is one of the fundamental molecules in chemistry, biology and astrophysics. It exists as two distinct nuclear-spin isomers, *para*- and *ortho*-water, which do not interconvert in isolated molecules. The experimental challenges in preparing pure samples of the two isomers have thus far precluded a characterization of their individual chemical behaviour.

Recent progress in manipulating polar molecules using electrostatic fields has made it possible to select and spatially separate different conformers and rotational states of molecules in supersonic molecular beams [1, 2]. By combining this technology with a stationary reaction target of Coulomb-crystallized ions in a linear quadrupole ion trap [3] we have recently studied conformer-selected molecule-ion reaction dynamics and observed that reaction-rate constants can strongly depend on molecular conformation [4, 5].

Here, we extend this method to the separation of different nuclear-spin isomers for studies of ion-molecule reactions with control over the rotational and nuclear-spin state of the neutral reaction partner. We have studied the proton-transfer reaction of the spatially separated ground states of *para*- and *ortho*-water with cold ionic diazenylium (N_2H^+), an important molecule in astrochemistry. We found a 23(9)% higher reactivity for the *para* nuclear-spin isomer which we attribute to the smaller degree of rotational averaging of the ion-dipole long-range interaction compared to the *ortho*-species. This finding is in quantitative agreement with a modelling of the reaction kinetics using rotationally adiabatic capture theory [6]. The present results highlight the subtle interplay between nuclear-spin and rotational symmetry and its ramifications on chemical reactivity.

[1] D. A. Horke, Y.-P. Chang, K. Dlugolecki, and J. Küpper, Angew. Chem. Int. Ed. **53**, 11965 (2014).
[2] Y.-P. Chang, D. A. Horke, S. Trippel, and J. Küpper, Int. Rev. Phys. Chem. **34**, 557 (2015).
[3] S. Willitsch, Int. Rev. Phys. Chem. **31**, 175 (2012).
[4] Y.-P. Chang, K. Dlugolecki, J. Küpper, D. Rösch, D. Wild, and S. Willitsch, Science **342**, 98 (2013).
[5] D. Rösch, S. Willitsch, Y.-P. Chang, and J. Küpper, J. Chem. Phys. **140**, 124202 (2014).
[6] D. Clary, J. Chem. Soc., Faraday Trans. 2, **83**, 139 (1987).

Resonant electron attachment to mixed hydrogen/oxygen and deuterium/oxygen clusters

Michael Renzler, Lorenz Kranabetter, Erik Barwa, Lukas Grubwieser, Siegfried Kollotzek, Paul Scheier
Institut für Ionenphysik und Angewandte Physik, Universität Innsbruck, Technikerstr. 25, A-6020, Austria

Michael Renzler
Institut für Mechatronik, Universität Innsbruck, Technikerstr. 13, A-6020, Austria

Andrew M. Ellis
Department of Chemistry, University of Leicester, University Road, Leicester LEI 7RH, United Kingdom

1. Introduction

Dissociative electron attachment (DEA) has been extensively studied over several decades. It is of fundamental importance in developing an understanding of how electrons interact in collisions with molecules. The following studies did investigate low energy electron attachment to mixed $(H_2)_x/(O_2)_y$ clusters and their deuterated analogs for the first time. The experiments were carried out using liquid helium nanodroplets to form the clusters, and the effect of the added electron was then monitored via mass spectrometry. A particularly notable feature is the formation of HO_2^- and H_2O^- ions from an electron-induced chemical reaction between the two dopants. The electron resonances for H_2 can lead to dissociative electron attachment (DEA), just as for the free H_2 molecule. However, there is evidence that the resonance in H_2 can also lead to rapid electron transfer to O_2, which then induces DEA of the O_2. This kind of excitation transfer has not, as far as we are aware, been reported previously [1].

2. Experimental

Helium nanodroplets were produced by expanding gaseous helium (Messer, purity 99.9999%) at a stagnation pressure of 20 bars through a 5-µm nozzle, which was cooled by a closed-cycle refrigerator (Sumitomo Heavy Industries Ltd., model RDK-415D). The nozzle temperature was measured as 9.4 K for the experiments with hydrogen and 9.6 K for the experiments with deuterium, respectively, resulting in both cases in an average droplet size of roughly 5×10^5

helium atoms [2]. A beam of helium droplets was created by the passage of the helium expansion through a conical skimmer with a 0.8-mm diameter aperture. The droplet beam then traversed two differentially pumped pickup chambers: oxygen was introduced in the first chamber and hydrogen (or deuterium) in the second. The doped droplets were subsequently crossed with an electron beam at energies ranging from 0 to 30 eV. The resulting anions were accelerated to 40 eV into the extraction region of a commercial orthogonal reflectron time-of-flight mass spectrometer (Tofwerk AG, model HTOF) with a resolution (m/Δm) of ~3000. The data were analysed using a custom-built software package, IsotopeFit,[3] which makes it possible to deduce ion abundances from the raw mass spectra. This software takes all possible isotopologs into account and can be used to subtract contributions from background impurities.[1]

3. Results

With the focus on D_2 instead of H_2, the principal anionic products are mixed clusters of the form $D_nO_m^-$. Figures 1 shows how the ion yield varies with *n* for some selected even values of *m*. These data were recorded at an electron energy of 12 eV. All of the plots show odd-even intensity oscillations as a function of *n*, particularly for large *n*. Most striking of all is the large ion abundance seen for *n* = 1 in the even *m* case.[1]

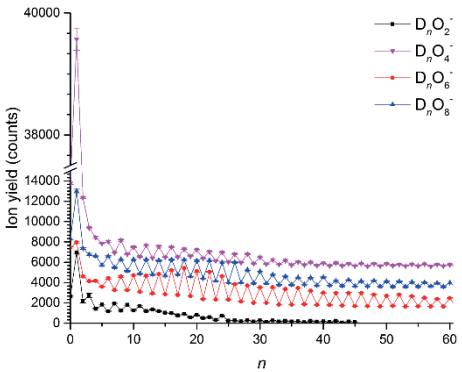

Figure 1: *Ion yields as a function of n for $D_nO_m^-$ ions with several different even values of m.*[1]

We next consider ion yields as a function of electron kinetic energy. Figure 2 shows data for the production of O_2^- and O_4^-, both with and without added D_2 (upper and lower traces, respectively). Resonances are seen, i.e., maxima in

the ion yield at certain electron energies. The signal-to-noise ratios for the O_2^- and O_4^- data when D_2 is also present in the helium droplet are relatively low, but it is nevertheless clear that there are major differences in the ion yield profiles for O_2^- and O_4^- formations in the presence and absence of D_2.[1]

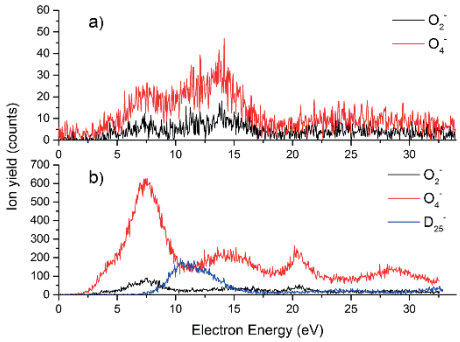

Figure 2: *(a) Dependence of the yields of O_2^- and O_4^- on electron energy for droplets containing a mixture of D_2 and O_2 in helium nanodroplets. (b) The ion yield curves for O_2^- and O_4^- obtained from pure oxygen clusters in helium droplets, and the ion yield curve for D_{25}^- obtained from pure deuterium clusters in helium nanodroplets.*[1]

Additionally, the production of DO_4^- was investigated to be able to compare all ion yield graphs and find resemblances of resonances of any kind.

4. Conclusion

Importantly, the findings from these experiments are not simply a superposition of the expected behavior for the individual hydrogen and oxygen clusters. Instead we find that the electrons can initiate chemistry, and very strong signals from the deuteroperoxy (DO_2^-) and deuterated water (D_2O^- ions) are seen. In the latter case, the bare D_2O^- ion does not survive because of rapid autodetachment but does survive when combined with at least one D_2 or O_2 molecule to form a cluster. The resonance behavior seen for the hydrogen/oxygen clusters is particularly surprising. The observation of high probabilities for anionic reactions at electron energies near 12 and 14 eV is interpreted in terms of resonances of D_2, since O_2 should have no strong resonances in this region. D_2 would normally undergo dissociative electron attachment at these energies and can then react with O_2 to yield the DO_2^- ion. However, explaining the formation of D_2O^- is more challenging. Our best explanation at present is that an electron initially undergoes resonant attachment to D_2 but that electron is then transferred to O_2 before the DEA of

the former can occur. If correct, then there is a competition between the DEA of D_2 and the rapid electron transfer to O_2. When the latter occurs, it sets in motion a process which can lead to efficient D_2O^- production.[1]

5. Acknowledgments

The authors are grateful for a grant from the Austrian Science Fund, FWF No. P26635, in support of this work.

6. References

[1] Michael Renzler, Lorenz Kranabetter, Erik Barwa, Lukas Grubwieser, Paul Scheier, and Andrew M. Ellis: *The Journal of Chemical Physics* **147** (2017) 194301

[2] L. F. Gomez, E. Loginov, R. Sliter, and A. Vilesov, *J. Chem. Phys*. **135** (2011) 154201

[3] S. Ralser, J. Postler, M. Harnisch, A. M. Ellis, and P. Scheier, *Int. J. Mass Spectrom*. **379** (2015) 194

Photo fragmentation of charged cluster complexes

L. Kranabetter, M. Kuhn, P. Martini, J. Postler, F. Laimer, M. Ončák, M. Beyer, P.Scheier
Institut für Ionenphysik und Angewandte Physik, University of Innsbruck, 6020 Innsbruck, Austria

Helium nanodroplets (HNDs) have unique properties that facilitate the growth of clusters and nanoparticles [1,2,3]. The ClusTof experiment uses these properties to produce cold cluster ions to analyze them via a high-resolution reflectron time of flight mass spectrometer (TOF MS). After production by means of a supersonic jet expansion, the droplets pick up dopant atoms or molecules. Trapped inside a small potential well on the surface or inside the HNDs, the single particles will assemble into the cluster. Almost the complete binding energy of the dopant cluster will be dissipated into the helium droplet and leave the droplet via the evaporation of helium atoms. Subsequent ionization of the cluster via different indirect ionization mechanisms is triggered by electron bombardment of the HNDs. These reaction chains create cold charged clusters, sometimes with a small number of helium atoms attached to them. Product ions are then guided by a set of electrostatic lenses to the extraction region of the orthogonal time of flight mass spectrometer where they are pulsed into the analyzing section of the instrument that measures the ion yield as a function of the flight time to the detector [4].
Recent measurements investigate the ion yield depletion of pristine or He tagged cluster ions when exposed to laser light radiation of a certain wavelength [5]. A Q-switched optical parametric oscillator light source (EKSPLA NT240-SH-K1) generates the laser pulses synchronized to specific extraction pulses of the TOF MS. This allows the setup to record an irradiated spectrum with the lasers repetition rate of 1 kHz while every extraction with a phase shift is used to record an unperturbed spectrum. The fast duty cycle of this indirect detection method of adsorption lines enables survey scans over a broad laser frequency range. First measurements of the photodissociation of Cs cluster cations are shown.

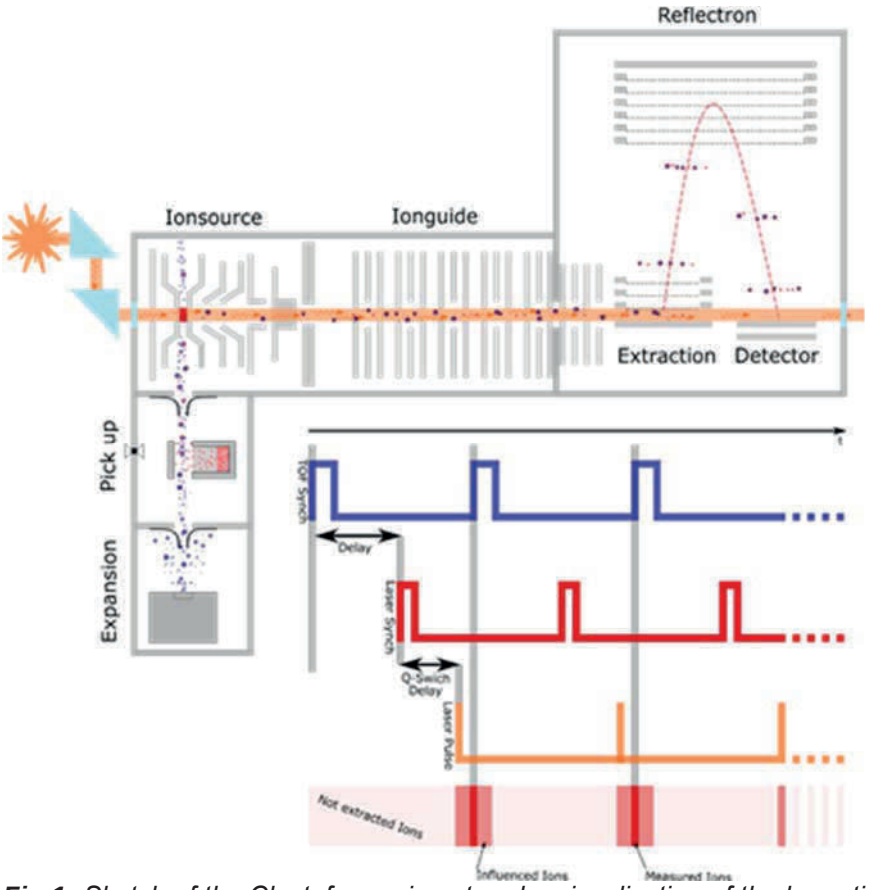

Fig 1: *Sketch of the Clustof experiment and a visualization of the laser-timing layout. Adapted from M. Kuhn (unpublished).*

References

[1] M.Farnik and J.P.Toennies; *JCP* **122** (2005) 014307; doi: 10.1063/1.1815272
[2] V.Mozhayskiy et al; *JCP* **127** (2007) 094701; doi: 10.1063/1.2759927
[3] A.W. Hauser et al; *PCCP* **17** (2015) 01805; doi: 10.1039/C5CP01110H
[4] L.Kranabetter et al; *JCP C* **121** (2017) 10887; **doi:** 10.1021/acs.jpcc.6b12057
[5] M.Kuhn et al; *Nat.Com.* **7** (2016) 13550; doi: 10.1038/ncomms13550

Acknowledgments

This work was supported by the FWF (Project numbers P26635 and M1908-N36), XLIC and the European Commission (ELEVATE, Horizon 2020 research and innovation program under grant agreement No. 692335).

SNOWBALL - Investigation of droplet size distribution and charge induced fragmentation of large suprafluid ^{4}He droplets

F. Laimer, L. Kranabetter, M. Rastogi, A. Ritsch, A. Huber, L. Kaserer, M. Renzler and P. Scheier
Institut für Ionenphysik und Angewandte Physik, University of Innsbruck, Austria
E-mail: felix.laimer@student.uibk.ac.at

In the SNOWBALL setup, charged ^{4}He droplets with a size of up to $3x10^7$ atoms are produced via supersonic expansion of precooled helium into ultra-high vacuum followed by electron impact ionization. To measure size distributions the ionized droplets are deflected by an electrostatic sector and detected by a channel electron multiplier.

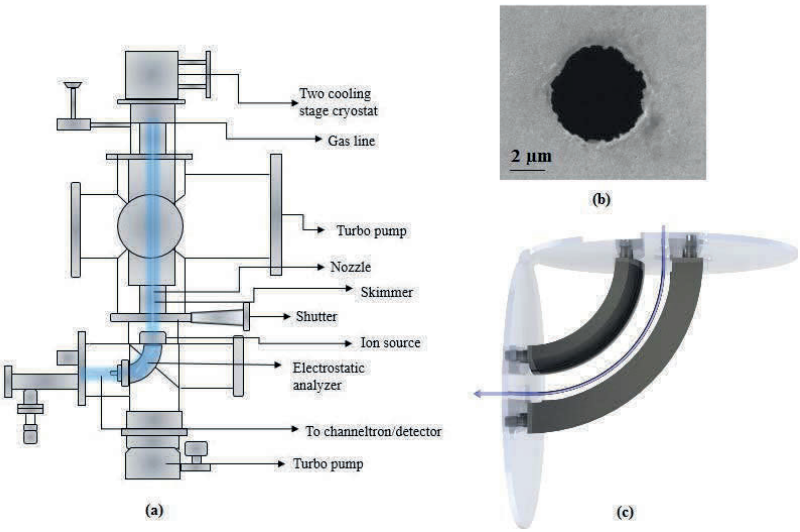

Figure 1: *(a) Schematics of the SNOWBALL experiment for the investigation of droplet size distributions. (b) SEM image of the droplet source nozzle. (c) Electrostatic sector analyzer used to deflect mass selected helium droplets. Adapted from M. Rastogi et al. [1].*

Preliminary results suggest that the size distribution of produced singly charged cationic droplets at temperatures between 5 and 9.5 Kelvin can be

described by a log-normal distribution. The same behavior has been observed and reported for smaller ^{4}He droplets at temperatures from 14 to 24 Kelvin by M. Lewerenz et al. [2].

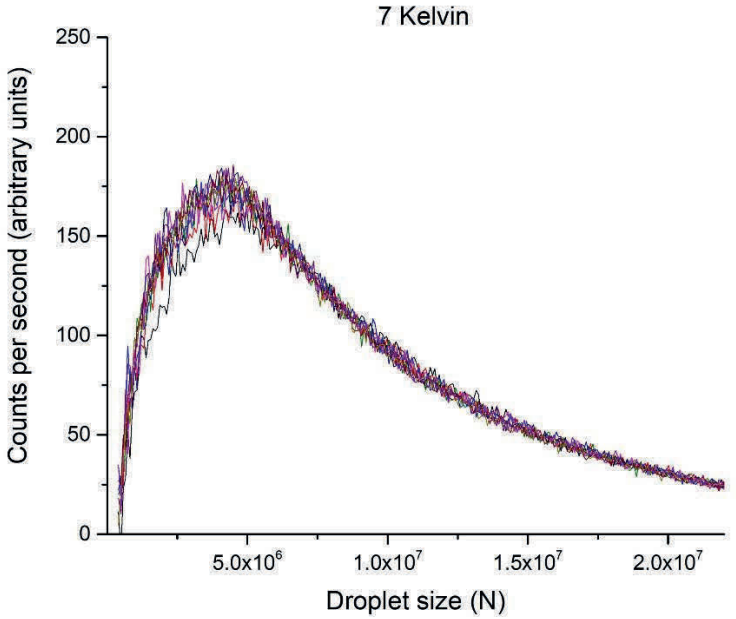

Figure 2: *First results of cluster size distributions for ^{4}He cationic droplets in relation to nozzle temperature. The measurement was done at 20 bar helium stagnation pressure and electron impact ionization by 5 µA electron current at 40 eV.*

Measurements at higher electron energies and electron currents lead to narrower distributions indicating charged induced fragmentation. For the investigation of fragmentation behavior of ^{4}He droplets, the SNOWBALL setup will be expanded by a further section containing a second ion source and an electrostatic sector. Future results will be presented.

This work was supported by the FWF, Wien (projects P26635 and W1259).

[1] M. Rastogi et al., *A new route to control the size of helium nanodroplets* (to be published)

[2] M. Lewerenz et al., *A new scattering deflection method for determing and selecting the sizes of large liquid clusters of ^{4}He,* Chem. Phys. Lett., 206 (1993), p. 381

A new 1u state in Cu_2: High resolution RFWM experiments and high level ab initio calculations

B. Visser[1], M. Beck[1], P. Bornhauser[1], G. Knopp[1], J.A. van Bokhoven[1,2], R. Marquardt[3], C. Gourlaouen[3], and P. P. Radi [1]

[1)] *Paul Scherrer Institute, CH-5232 Villigen, Switzerland*

[2)] *Institute for Chemical and Bioengineering, ETHZ, Zurich, Switzerland*

[3)] *Institut de Chimie, UMR 7177 CNRS/Université de Strasbourg, F-67081 Strasbourg, France*

The low energy electronic structure of the copper dimer has been re-investigated using non-linear four-wave mixing spectroscopy and high level *ab initio* calculations.

In addition to the measurement of the previously reported A, B and C electronic states [1], a new state denoted A′ is identified with T_0 = 20100.3992(12) cm^{-1} ($^{63}Cu_2$), see Figure 1. Rotational analysis of the A′-X (0,0) and (1,0) transitions leads to the assignment of A′ 1_u (see Figure 2).

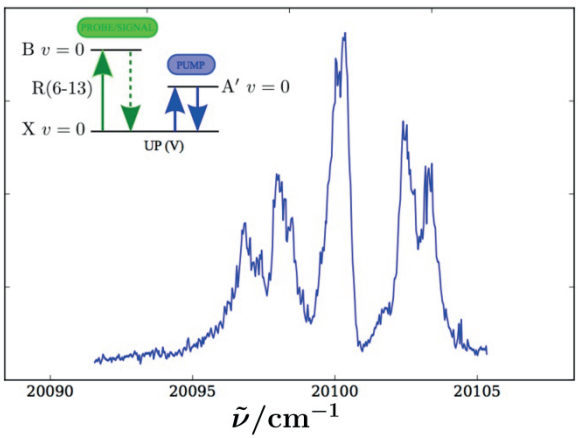

Figure 1. *Low resolution survey scan of the (0,0) A′-X $^1\Sigma_g^+$ band using the UP (or hole-burning) scheme of the two-color resonant four-wave mixing technique (see [2, 3] for further details).*

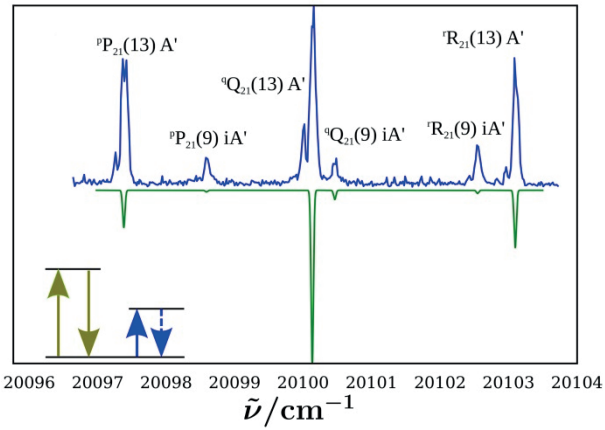

***Figure 2**. High-resolution detail of the (0,0) A'-X $^1\Sigma_g^+$ showing individual P(J") and Q(J") lines for the $^{63}Cu_2$ (A') and $^{63}Cu^{65}Cu$ (iA'). The inverted spectrum is a simulation (see [2, 3] for further details).*

The *ab initio* calculations at the internally contracted multi-reference configuration interaction level of theory using Douglas-Kroll and Breit-Pauli hamiltonians, and a basis set of quadruple ζ quality present the first theoretical description of the low energy states of the copper dimer in Hund's case (c) and confirms with unprecedented accuracy the experimental assignment. Figure 3 below shows, on the left hand side, a survey of low lying potential energy functions for the Cu_2 molecule obtained from the present *ab initio* calculations, while on the right hand side details of the potentials are shown around the equilibrium.

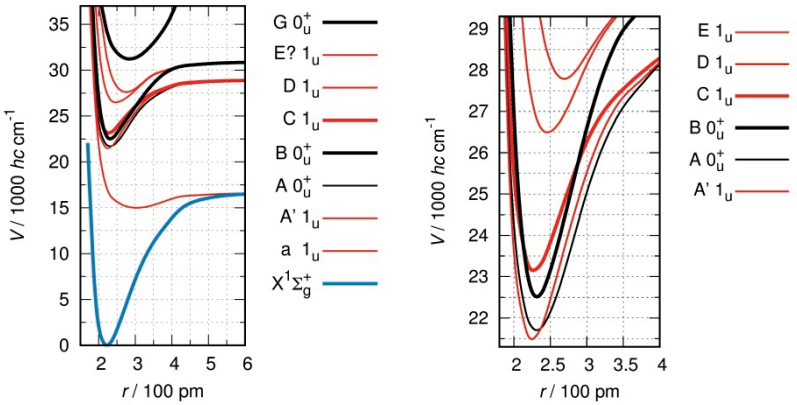

Figure 3. *Some potential energy functions for the Cu_2 from MRCI+Q calculations including spin-orbit couplings. The right hand side shows details of some spectroscopically relevant ungerade states in Hund's case (c) notation, putting in evidence the newly measured A' 1_u state, as well as the previously measured A, B, C and D states (see ref. [3]).*

The present results solve a more than 40 year old mystery in the initial experimental assignment of the A state [3].

Acknowledgments
Our work is supported financially by the Swiss National Science Foundation (#200021 153170), as well as by the Centre national de la recherche scientifique (CNRS) and the Université de Strasbourg.

[1] M. D. Morse, *Chem. Rev.* **86**, 1049 (1986).
[2] B. Visser *et al.*, *J. Raman Spec.* **47**, 425 (2016).
[3] B. Visser *et al.*, *J. Chem. Phys.*, 00, 000 (2017).

Stability of mixed gold and benzene clusters embedded in helium nano droplets

P.Martini, M,Goulart, L.Kranabetter, M.Kuhn, J.Postler, P.Scheier
Institut für Ionenphysik und Angewandte Physik,
University of Innsbruck, 6020, Austria

Synopsis Gold and benzene clusters embedded in helium nano droplets were studied using a high-resolution mass spectrometricmethod.

Gold and benzene clusters embedded in helium nano droplets were analyzed using a mass spectrometric method. Previous results about mixed gold and adamantane aggregates as well as gold and imidazole clusters raised some questions about the structure of these adducts and the bonds between the gold atoms and those molecules. To solve this questions measurements with mixed gold and benzene clusters were performed.

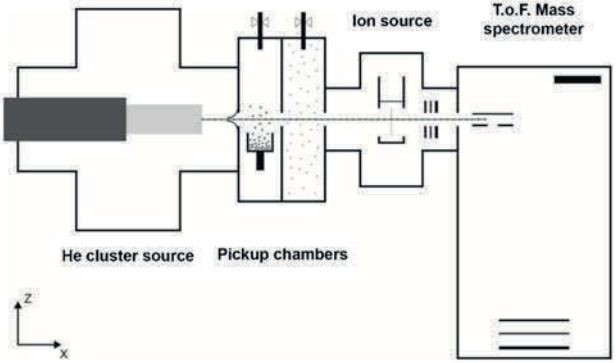

(a) Graphical illustration of the experimental setup.

Superfluid helium nano droplets (HND) can be used to simulate the cluster formation in ultra-cold conditions like in the interstellar medium. Their special properties e.g. to pick up virtually any atom or molecule and cool them down to 0.4 K [1], makes this cryogenic matrix a perfect laboratory to study the gold and benzene aggregates. In order to look into the behavior and possible aggregation patterns, a well known method was used [2]. Anomalies in the intensity of the mass spectra peaks, known as magic numbers, are used to identify the most likely formed adducts of the positively charged $Au_n(C_6H_6)_m$ clusters.

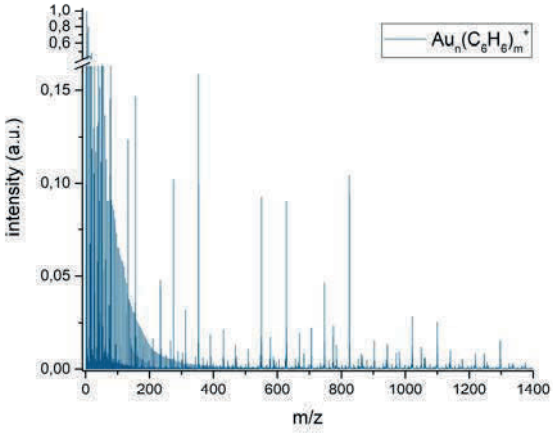

(b) Measured mass spectrum of the $Au_n(C_6H_6)^+_m$ cluster series.

References

[1] Toennies, J.P. and A.F. Vilesov, Superfluid helium droplets: A uniquely cold nanomatrix for molecules and molecular complexes. Angewandte Chemie-International Edition, 2004.43(20):p.2622-2648.

[2] Schöbel, H., Bartl, P., Leidlmair, C., Denifl, S., Echt, O., Märk, T. D. and Scheier, P., High-resolution mass spectrometric study of pure helium droplets, and droplets doped with krypton. The European Physical Journal D-Atomic, Molecular, Optical and Plasma Physics, 2011. 63(2):p.209-214.

This work was supported by the FWF, Wien (projects P26635 and M1908-N36) and the European Commision (grant agreement number 692335).

Low Energy Electron Interactions with Nimorazole

Rebecca Meißner, Stephan Denifl
Institute of Ion Physics and Applied Physics and Center for Molecular Biosciences Innsbruck (CMBI), Leopold-Franzens University Innsbruck, Technikerstraße 25/3, 6020 Innsbruck, Austria

Linda Feketeová
Université de Lyon, Université Claude Bernard Lyon 1, Institut de Physique Nucléaire de Lyon, CNRS/IN2P3 UMR 5822 43 Bd du 11 novembre 1918, 69622 Villeurbanne Cedex, France

1. Introduction

In radiotherapeutic treatment, radiosensitisers can be administered to enhance the ratio of cell survival of healthy cells towards malignant cells. Nimorazole is one example of such a compound, see Fig. 1. It is based on imidazole which is omnipresent in nature as a building block of amino acids and purine nucleobases. In Denmark, nimorazole is already clinically tested in head and neck cancer treatment to enhance tumour control of radio-resistant hypoxic tumours [1].

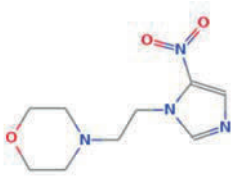

Figure 1 *Chemical structure of nimorazole. Taken from NIST database.*

Within radiotherapy, high energetic particles traverse the human body and interact with the constituents of the cells. As a consequence, secondary low energy electrons (LEEs) are formed [2]. The most probable energy of those electrons is about 10 eV for liquid water [3]. LEEs can induce DNA damage and therefore kill the cell [4]. Radiosensitisers enhance the response towards radiation and thus increase the likeliness of DNA damage. They are designed to favourably attach to malignant cells.

The physical process responsible for the DNA damage is mainly dissociative electron attachment (DEA). Here, the LEEs interact with the molecule, e.g. the

DNA nucleobase, forming a transient negative ion (TNI). Subsequently, the TNI can either relax back to the neutral state or decompose into fragments, thus causing DNA strand breaks [4]. Nimorazole was suggested as drug to increase the magnitude of electron capture in malignant cells [5]. Thus, either the direct decomposition of DNA strands is induced or radicals can be produced causing DNA damage as a secondary reaction.

In the present study, the decomposition of nimorazole upon DEA in the gas phase is studied by means of mass spectrometry. The focus lies on the investigation of the stability of the compound upon DEA and the determination of the ion yields as a function of the initial electron energy for the most important product anions.

2. Experimental Setup

The mass spectrometer used in this study is shown in Fig. 2.

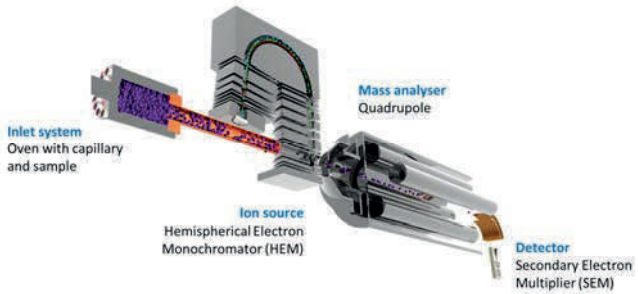

Figure 2 *The mass spectrometer used for the present study comprising an oven filled with nimorazole, a hemispherical electron monochromator, a quadrupole mass analyser and a channeltron detector.*

The nimorazole is stored in a heatable oven inside of the vacuum chamber and a capillary ensures that the molecules are guided towards the interaction point with the electron beam. The electrons are produced by the ion source which combines a hairpin filament with a hemispherical electron monochromator, focussing the beam both energetically and spatially. After the electron attachment and fragmentation process, the anions are extracted into a quadrupole mass analyser and detected with a channeltron. A discriminator and a subsequent counting and readout unit enable signal processing. The setup is described in more detail in [6].

3. Results

The DEA to nimorazole (NIMO) results in the observation of both the parent anion and various fragment anions. The parent anion is formed by the attachment of about 0 and 0.25 eV electrons, although the contribution of the latter ones account for a significantly smaller amount, see Fig. 3 (left). That channel possesses the highest observed production cross section. The fragment anions show maximal production rates at electron energies between 2 and 6 eV, and smaller efficiencies between 0 and 2 or 6 and 10 eV. An example measurement is shown in Fig. 3 (right). The fragmentation products can be compared to former measurements performed with nitroimidazole (NITRO) [7], which was also suggested as a radiosensitiser on the basis of an imidazole ring [8]. Interestingly, the observed fragments differ noticeably. For the nitroimidazoles, the loss of $OH^{\bullet}$, H_2O and $NO^{\bullet}$ form the dominant channels. In contrast, in case of the nimorazole mainly the NO_2^- fragment anion is observed while the other fragmentation channels are deprived. Furthermore, for nitroimidazoles the loss of a hydrogen atom (NITRO-H) has a large cross section. For nimorazole, this channel (NIMO-H) is observed only with a low cross section. Additionally, the imidazole and the morpholine ring anions with the loss of in between one and three hydrogen atoms feature pronounced energy resonances for nimorazole.

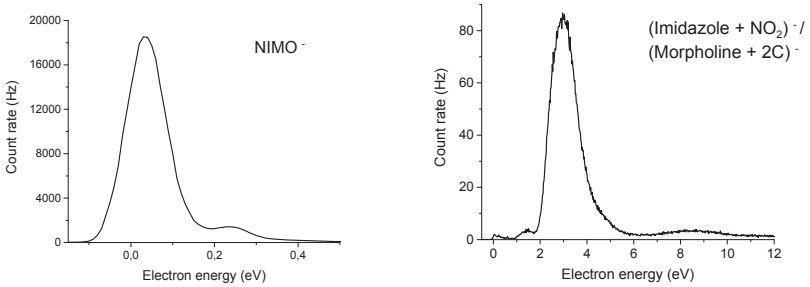

Figure 3 *Ion efficiency curve of the parent anion (226 u, left) and the 112 u fragment (right) which can result either from the imidazole ring with attached NO_2 group or the morpholine ring with attached carbon chain.*

Acknowledgements

This work was supported by FWF (P30332) and by Fundação para a Ciência e a Tecnologia (FCT-MCTES), Radiation Biology and Biophysics Doctoral Training Programme (RaBBiT, PD/00193/2012); UID/FIS/00068/2013 (CEFITEC); and scholarship grant number PD/BD/114452/2016 to RM.

References

[1] J. Overgaard, *Radiother. Oncol.* **100** (2011) 22
[2] Y. Zheng and L. Sanche, *RNN* **2(1)** (2013) 1
[3] S. M. Pimblott *et al., Radiat. Phys. Chem.* **76** (2007) 1244
[4] L. Sanche, *Nature* **461(17)** (2009) 358
[5] G.E. Adams *et al., Radiat. Res*. **178** (2012) AV183
[6] S. Denifl *et al., J. Chem. Phys.* **123** (2005) 104308
[7] A. Ribar *et al*., *Phys. Chem. Chem. Phys.* **19** (2017) 6406
[8] M. R. Horseman, *Basic Clinical Radiobiology, 4th edition* (2009) 233

Recent results in imaging S_N2 and E2 reaction dynamics

Tim Michaelsen, Eduardo Carrascosa, Martin Stei, Björn Bastian,
Jennifer Meyer and Roland Wester
Institut für Ionenphysik und Angwandte Physik, Universität Innsbruck, Austria

We study ion molecule reaction dynamics using a combination of crossed beams and velocity map imaging. An interesting model system for nucleophilic substitution reactions (S_N2) are the reactions of halide anions with methylhalides [1]. In the past we were able to identify dynamic fingerprints for various reaction mechanisms in these systems in the obtained energy- and angle-differential cross sections. In comparison with theory the reaction mechanism can be unambiguously assigned to such dynamic features [2].

Here, we present recent results on two different approaches to further this insight. On the one side we extended the study from reactions with methyl halides to larger systems. Already in the reaction with ethyl halides a new reaction pathway is possible, namely base induced elimination (E2). The S_N2 and E2 reaction pathways almost always appear in competition and a lot of studies have been undertaken to gain more insight into it. One of the main challenges here is that they both lead to the same product ion, making mass spectrometry alone unsuited to differentiate the pathways. We instead looked at the difference in the reaction dynamics of both pathways.

By stepwise methylation, from the methyl- to the tert-butyl-halide case, the S_N2 channel gets more and more suppressed by steric hindrance. By comparing the obtained velocity distributions for various stages of methylation and by varying the attacking anions as well as leaving groups, we were able to identify a dynamic fingerprint of the E2 reaction mechanism. [3]

In a second approach, we study the influence of vibrational excitation on the outcome of reactions both in the branching ratios of competing reaction pathways as well as the dynamics.

Here, we present results obtained for the reaction of F^- with CH_3I [4]. There are two reaction pathways of interest to us, the exothermic nucleophilic substitution (S_N2) and the endothermic proton transfer channel. For this system it is predicted that the C-H symmetric stretch (v_1) does not affect the S_N2 pathway but does influence the proton transfer. By setting the collision energy below

the endothermicity of the proton transfer and adding energy via vibrational excitation we can monitor the change of the branching ratio of proton transfer vs S_N2 and thereby observe whether the added energy facilitates the opening of the proton transfer channel. We observe only a minute effect in the S_N2 channel and a significant increase of the proton transfer cross-section.

In the future, we plan to extend this approach to other systems, such as the reaction of F^- with CH_3Cl. For this system Czakó *et al.* published calculated cross-sections for the reaction with ground state and symmetric C-H stretch excited CH_3Cl [5]. They predict the S_N2 channel to be only marginally affected and a significant increase of the proton transfer cross-sections, similar to what we observed in the CH_3I case. Here we would be able to directly compare our results with theory. Furthermore, we aim at controlling the competition between S_N2 vs E2 using infrared excitation.

[1] Vollhardt, K. P. C. & Shore, N. E., Organic Chemistry, Structure and Function (Pallgrave Macmillan, Basingstoke, UK, 2007).
[2] Stei, Martin, *et al.* Influence of the leaving group on the dynamics of a gas-phase SN2 reaction. *Nature Chemistry* 8.2 (2016): 151-156.
[3] Carrascosa, Eduardo *et al.* Imaging Dynamic Fingerprints of Competing E2 and S_N2 Reactions. *Nature Communications* 8 (2017): 25.
[4] Stei, Martin, *et al.* in preparation
[5] Szabó, István, and Gábor Czakó. Revealing a double-inversion mechanism for the $F^- + CH_3Cl$ S_N2 reaction. *Nature Communications* 6 (2015): 5972.

Isomers detection by ion mobility spectrometry- mass spectrometry

Bartosz Michalczuk, Ladislav Moravský, Martin Sabo, Štefan Matejčík
Department of Experimental Physics, Comenius University,
Mlynska dolina F2, 84248 Bratislava, Slovakia

Introduction

Nowadays phthalates are widely used. This group of chemicals can be found in building materials or in packaging materials for food industry and cosmetics and also in toys. They are used as a plasticizers in the manufacturing PCV or plastics based on cellulose. Phthalates undergo photodegradation, biodegradation and anaerobic degradation, nevertheless concentration in environment is still significant especially in indoor environment [1].

In recent years phthalates have been accused of showing negative impact on human health. Breast cancer in females or mental and motor development in children can be caused by long term exposure on phthalates [2,3]. So it is important to have a good tool to detect them rapidly even at very low concentrations. In many laboratories research groups have been studying phthalates using different methods. The most common technique that phthalate esters were investigated is gas chromatography coupled with mass spectrometry (GC-MS), but also high performance liquid chromatography (HPLC) was used [4,5]. Recently Midey et al. present some results where high-performance ion mobility spectrometry with direct electrospray ionization (ESI-HPIMS) was used to detect some phthalates [6].

In our laboratory several phthalates have been investigated using corona discharge ion mobility spectrometry- mass spectrometry technique at atmospheric pressure including isomers of dimethyl phthalate- dimethyl isophthalate (DMIP) and dimethyl phthalate (DMP).

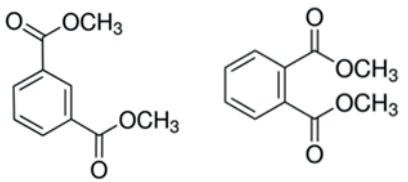

Fig. 1 *Structural formulas of dimethyl isophthalate (left) and dimethyl phthalate (right)*

Results

Chemicals which we have been studied are characterized by low vapour pressures, for example vapour pressure of dimethyl isophthalate is 9,63*10^{-3}Torr [7], which means that these are non-volatile compounds and detection in gas phase can be difficult.

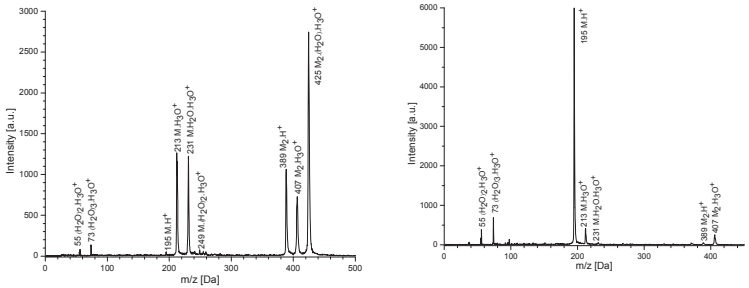

Fig.2 *Mass spectra for dimethyl isophthalate (left) and dimethyl phthalate (right) for 299 K*

As it is demonstrated in Fig.2 DMP and DMIP isomers show different mass spectra. The detected ions are nearly the same but ratio between them is distinctly different. In the case of DMIP we observe strong dimer formation ($M_2 \cdot H^+$; $M_2 \cdot H_3O^+$; $M_2 \cdot H_2O \cdot H_3O^+$) whereas for DMP the dimer is barely visible ($M_2 \cdot H^+$; $M_2 \cdot H_3O^+$). However, DMP possess higher vapour pressure in comparison to DMIP.

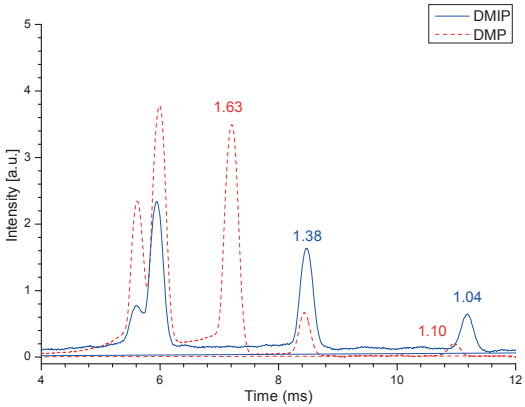

Fig. 3 *Ion Mobility spectra for dimethyl isophthalate (solid line) and dimethyl phthalate (dashed line) for 299 K*

The ions mobility spectra of DMP and DMIP are as well very different. DMP exhibits two peaks first with reduced mobility K_0 = 1,63 $cm^2V^{-1}s^{-1}$ (corresponds with protonated monomer) and second one with K_0 = 1,10 $cm^2V^{-1}s^{-1}$ which can be assigned to dimer. The second peak partially overlaps with peak from DMIP, however the first one is clearly separated and can be considered as a characteristic peak for dimethyl phthalate.
Experiments that we have performed in our laboratory and obtained results show clearly that atmospheric pressure discharges in our case corona discharge applied in ion mobility spectrometers can be used to detect phthalates and even can be useful for detecting isomers.

Acknowledgment
This research has been supported by the European Union's Horizon 2020 project "Ion-Molecule Processes for Analytical Chemical Technologies — IMPACT" action. MARIE SKŁODOWSKA-CURIE ACTIONS Innovative Training Network. Project Number 674911 and research and innovation programme under grant agreement No 692335. The project has been partially supported by Slovak project APVV-0259-12.

References
[1] T. Schettler, Int. J. Androl., 29 (2006) 134-139,
[2] M. Gascon et al., Int J Hyg Environ Health, 218 (2015) 550-558,
[3] Z. Fu et al., Reprod Toxicol., (2017),
[4] A.O. Earls et al., J. Chromatogr. A 983 (2003) 237–246,
[5] J. Fisher et al., Chromatographia 37 (1993) 47-50,
[6] A.J. Midey et al., AnalyticaChimica Acta 804 (2013) 197–206,
[7] T E Daubert; R P Danner., Physical and thermodynamic properties of pure chemicals: data compilation, Taylor & Francis (1989) Washington,

Nickel Cluster Surface Morphologies by Cryo Kinetics and Cryo Spectroscopy

Jennifer Mohrbach*, Sebastian Dillinger* and Gereon Niedner-Schatteburg
Fachbereich Chemie und Forschungszentrum OPTIMAS,
Technische Universität Kaiserslautern, 67663 Kaiserslautern, Germany

1. Motivation

It is short of hundred years ago that surface science reached maturity at the molecular level [1]. Knowledge driven surface science elucidates well defined surfaces, e.g. of single crystals and at high perfection. Application driven research in catalysis aims at high figures of merit, e.g. turn over numbers (TON), product yields and specificity [2]. Both disciplines often ran in parallel with seeming risk to miss each other. Cross fertilization did occur [3], and sometimes it was omitted.

The cluster surface analogy has been recognized long time ago [4]. We have studied the C-H bond activation of various organic molecules by naked transition metal clusters before [5]. It showed, that cluster size dependent variations of reaction rates were in part beyond comprehension, and they withstood quantum chemical interpretation by and large. It became mandatory to invoke (a) temperature control and (b) dedicated means of spectroscopy – and to switch to simpler systems.

2. Methodology

We have taken time to setup a tandem cryo ion trap instrument that allows for the study of adsorption and reaction kinetics of clusters under single collision conditions in conjunction with temperature control to as low as 11 Kelvin. In the present cases it proved advantageous to utilize a doped Helium buffer gas at 26 Kelvin.

Spectroscopy comes into play through application of Infrared Multiple Photon Dissociation (IR-MPD) by optical parametric oscillator/amplifier (OPO/OPA) photon sources. One and two colour investigations of metal organic complexes by such technique were subject of presentation at SASP 2014, and according results are published elsewhere [6].

3. Findings in short

We have started a systematic study of N_2 and H_2 cryo adsorption on Fe, Co, and Ni clusters and alike, very first results being published [7] and presented at SASP 2016. In the meantime, we have extended our investigations systematically[8].

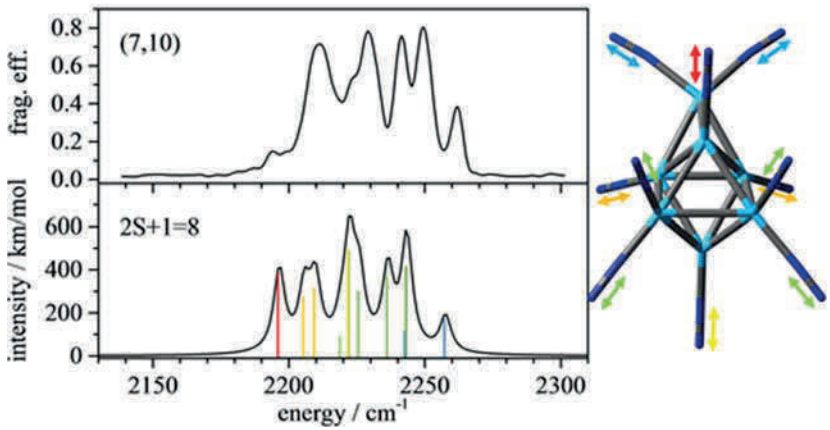

Figure 1: *Infrared Multiple Photon Dissociation (IR-MPD) spectrum of the $[Ni_7(N_2)_{10}]^+$ complex (top), a scaled IR absorption spectrum by according DFT simulations (bottom), and the corresponding structure of the cluster adsorbate complex (right). The calculated stick spectra depict pairwise couplings of N_2 oscillators.*

Here, we present the cryogenic (26 Kelvin) IR spectra of selected cluster adsorbate complexes $[Ni_n(N_2)_m]^+$ ($n = 5 – 20$, $m = 1 – m_{max}$). The spectra reveal strongly n- and m-dependent features in the N_2 stretching region, which we interpret in conjunction with density functional theory (DFT) modelling of some of these findings. The observed spectral features allows to define four classes of structure related surface adsorption behavior: Class (1) of Ni_6^+, Ni_{13}^+, and Ni_{19}^+, are highly symmetrical clusters with smooth surface of equally coordinated Ni atoms, that entertain stepwise N_2 adsorption up to stoichiometric $N_2 : Ni_{surface}$ saturation. Class (2) of Ni_{12}^+, and Ni_{18}^+ encompasses clusters which are short of one Ni atom to the smooth surface class (1) species. Their relaxed smooth surfaces reorganize by enhanced N_2 uptake towards some low coordinated Ni surface atoms with double N_2 occupation. Class (3) of small clusters Ni_5^+, and Ni_7^+ through Ni_{11}^+ possess rough surfaces with low

coordinated Ni surface atoms, some reveal semi internal Ni atoms of high next neighbor coordination. Surface reorganization upon N_2 uptake turns rough into rough surface by Ni atom migration and turns octahedral based structures into pentagonal bipyramidal structures. Class (4) of large clusters of Ni_{14}^+ through Ni_{17}^+, and Ni_{20}^+ possess smooth icosahedral surfaces with some proximate capping atom(s) on one hemisphere of the icosahedron with the other one largely unaffected – thus allowing for N_2 saturation beyond the Ni cluster surface atom count by double N_2 occupation of low coordinated Ni surface atoms.

We have conducted synchrotron X-ray based studies of spin and orbital contributions to the toal magnetic moments of isolated iron, cobalt and nickel clusters, presented at SASP 2012 and published subsequently [9]. The found magnetic magnitudes do not clearly correlate with the findings of our current studies in kinetics and spectroscopy, and we strive to elucidate further why this is so..

4. Summary and outlook

This presentation elucidates cluster surface morphologies and their adsorbate induced reorganization under cryo conditions and in isolation. It aims to put into perspective the findings from adsorption kinetics, IR spectroscopy, DFT modelling and magnetic spectroscopy. It finally provides for an outlook onto further studies of N_2 adsorption to Rhodium clusters [10].

5. Acknowledgements

This work was supported by the Deutsche Forschungsgemeinschaft in the framework of the transregional collaborative research center SFB/TRR 88 **3MET.de**. These co-authors (*) contributed equally.

6. References

[1] I. Langmuir, J. Am. Chem. Soc. **1918**, *40*, 1361-1403.
[2] G. Somorjay and Y. Li: *Introduction to Surface Chemistry and Catalysis*, 2nd edition, Wiley Hoboken **2010**; *Catalysis from A to Z – A concise Encyclopedia* (B. Cornils, W. A. Hermann, R. Schlögl, C.-H. Wong eds.), Wiley-VCH, Weinheim **2000**.
[3] G. Ertl, *Angew. Chem. Int. Ed.*, **2008**, *47*, 3524 – 3535.
[4] E. L. Muetterties, T. N. Rhodin, E. Band, C. F. Brucker, W. R. Pretzer, *Chem. Rev.*, **1979**, *79*, 91-137.
[5] B. Pfeffer, S. Jaberg, and GNS, *J. Chem. Phys.* **2009**, *131*, 194305; L. Barzen, M. Tombers, C. Merkert, J. Hewer, and GNS, *Int. J. Mass Spectrom.* **2012**, *330*–

332, 271–276; M. Tombers, L. Barzen, and GNS, *J. Phys. Chem. A* **2013**, *117*, 1197-1203.

[6] Y. Nosenko, F. Menges, C. Riehn, and GNS, *Phys. Chem. Chem. Phys.* **2013**, *15*, 8171; J. Lang, M. Gaffga, F. Menges, and GNS, *Phys. Chem. Chem. Phys.* **2014**, *16*, 17417 – 17421.

[7] S. Dillinger, J. Mohrbach, J. Hewer, M. Gaffga, and GNS, *Phys. Chem. Chem. Phys.* **2015**, *17*, 10358; J. Mohrbach, S. Dillinger, and GNS, *J. Phys. Chem.C* **2017**, *121*, 10907.

[8] J. Mohrbach, S. Dillinger, and GNS, *J. Chem. Phys.* **2017**, accepted 14.10.2017; S. Dillinger, J. Mohrbach, and GNS, *J. Chem. Phys.* **2017**, accepted 14.10.2017.

[9] S. Peredkov, M. Neeb, W. Eberhardt, J. Meyer, M. Tombers, H. Kampschulte, and GNS, *Phys. Rev. Lett.* **2011**, *107*, 233401; J. Meyer, M. Tombers, C. van Wüllen, GNS, S. Peredkov, W. Eberhardt, M. Neeb, S. Palutke, M. Martins, and W. Wurth, *J. Chem. Phys.* **2015**, *143*, 104302.

[10] M. P. Klein, A. Ehrhard, S. Dillinger, J. Mohrbach, and GNS, *Topics in Catalysis* **2017**, accepted 13.10.2017

Electron induced fluorescence of water relevant for comet coma measurements by Rosetta

Juraj Országh, Michal Ďurian, Štefan Matejčík
Comenius University Bratislava, Slovakia

Dennis Bodewits
University of Maryland in College Park, USA

Analysis of the data from the Rosetta mission to comet 67P/Churyumov-Gerasimenko shown that the emission from the comet coma is induced mostly by electron impact outside the 2 AU pre-perihelion [1]. The emission fades if the comet is within 2 AU of the Sun. The effect can be caused by increased concentration of water in the coma leading to different energy distribution of electrons [2]. To assess such an effect it is necessary to thoroughly study the electron impact fluorescence of water including the cross sections in laboratory conditions.

The experimental study has been performed at electron-molecule crossed beams setup described in detail in [3]. In this study the electron gun with energetic resolution of approximately 1eV has been used as a source of the electron beam. The molecular beam was formed by an effusive capillary and the optical resolution of the monochromator was set to 0.4nm and thermoelectrically cooled photomultiplier unit working in photon counting regime was used as detector. The measurements were performed at the pressure ensuring only binary electron-molecule collisions.

The spectral region between 200nm and 900nm has been studied. In the spectrum measured at electron energy 50eV the emission corresponding to deexcitation of atomic hydrogen (Balmer series), OH ($A^2\Sigma^+$-$X^2\Pi$), OH^+ ($A^3\Pi$-$X^3\Sigma^-$) and H_2O^+ ($\tilde{A}^2A_1$-X^2B_1) has been detected. The spectral bands corresponding to OH, OH^+ and H_2O^+ were identified according to the [4] and [5].
The relative cross sections were measured in the electron energy range from 2eV to 100eV for selected transitions and threshold energies for the corresponding processes were determined.

An example of the measured spectrum corresponding to OH ($A^2\Sigma^+$-$X^2\Pi$) transition is shown in the figure 1.

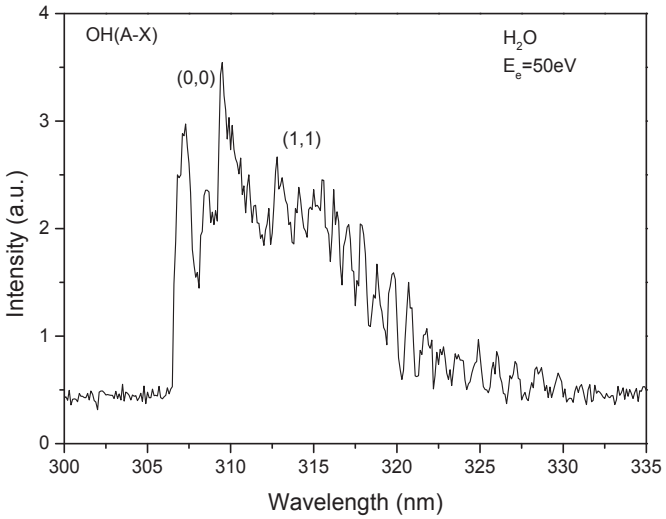

Fig.1. *Spectral band corresponding to the deexcitation of OH ($A^2\Sigma^+$-$X^2\Pi$) at impact electron energy 50eV.*

Acknowledgments

This project received support from the Slovak Research and Development Agency, project Nr. APVV-15-0580, the grant agency VEGA projects Nr. 1/0733/17. This project has received funding from the European Union's Horizon 2020 research and innovation programme under grant agreement number 692335.

References

[1] Feldman, P. D. et al. *Astron. Astroph.* **583**, A8 (2015).
[2] Bodewits, D. et al. *The Astronomical Journal* **152**, 130 (2016).
[3] Országh, J. et al. *The Astrophysical Journal* **841**, 17 (2017).
[4] Müller, U. et al. *Z. Phys. D* **25**, 167 (1993).
[5] Tsuji, M. et al. *Chem. Phys. Lett.* **147**, 6 (1988).

Structure and Photodissociation of Copper Formate Clusters

Tobias Pascher, Milan Ončák, Emanuel Oswald, Jozef Lengyel, Christian van der Linde and Martin K. Beyer
Institut für Ionenphysik und Angewandte Physik, Universität Innsbruck, Technikerstraße 25, 6020 Innsbruck, Austria

The catalytic properties of copper have been studied extensively [1,2]. Here the structure, fragmentation patterns and infrared multiphoton dissociation of small $Cu_n(HCO_2)_m^-$ ($n < 4$; $m < 9$) clusters have been investigated in the gas phase using a 9.4 T FT-ICR mass spectrometer equipped with a tuneable OPO laser system in the region of 2500–4475 nm. The results are compared to quantum chemical calculations.

After pumping the C-H bonds of the formate ligands with the OPO laser system, a fragmentation cascade has been observed. The bigger clusters (n = 2,3,4; m = 5,7,9) dissociate into smaller ones. For the smaller clusters (n = 1,2; m = 2,3,5), more interesting dissociation pathways, as illustrated in Figure 1, with significant secondary fragmentation were observed. The sequence of events was verified by measuring dissociation kinetics under irradiation at several absorption bands.

The measured spectra have been compared to theoretical calculations at the DFT level using multiple isomers (e.g. in Figure 2). Theory was further used to gain insight into the dissociation mechanism and secondary fragmentation. A hydrogen atom can be transferred from one formate ligand to another one, resulting into the release of CO_2 and HCOOH. In this reaction, two formate ligands are neutralized. Their charge is transferred to the copper atoms, which change their oxidation state from +II to +I. Alternatively, the hydrogen atom is transferred directly to the copper atoms, resulting in the dissociation of a CO_2 molecule. Further radiation introduces either another transfer of a hydrogen atom to a copper atom or a dissociation of a hydrogen atom. CID measurements were performed for comparison, which yield analogous fragmentation pathways.

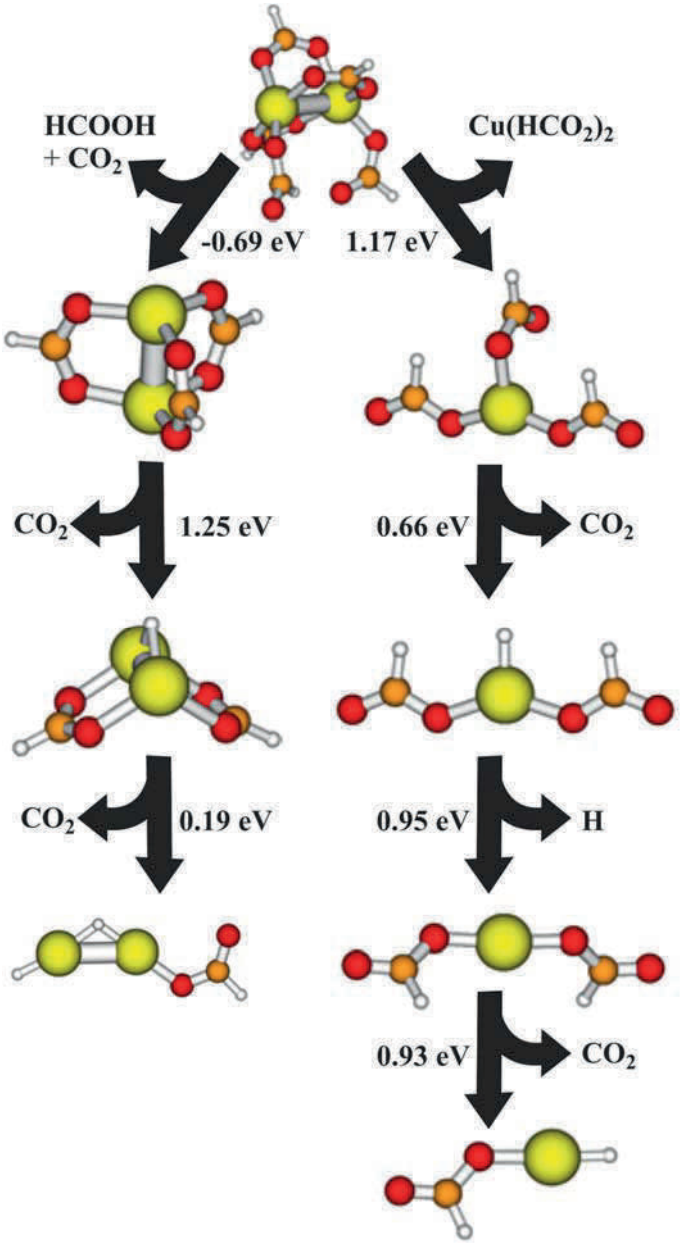

Figure 1: *Fragmentation pathway of a $[Cu^{(II)}_2(HCO_2)_5]^-$ molecule with the calculated reaction energies and structures.*

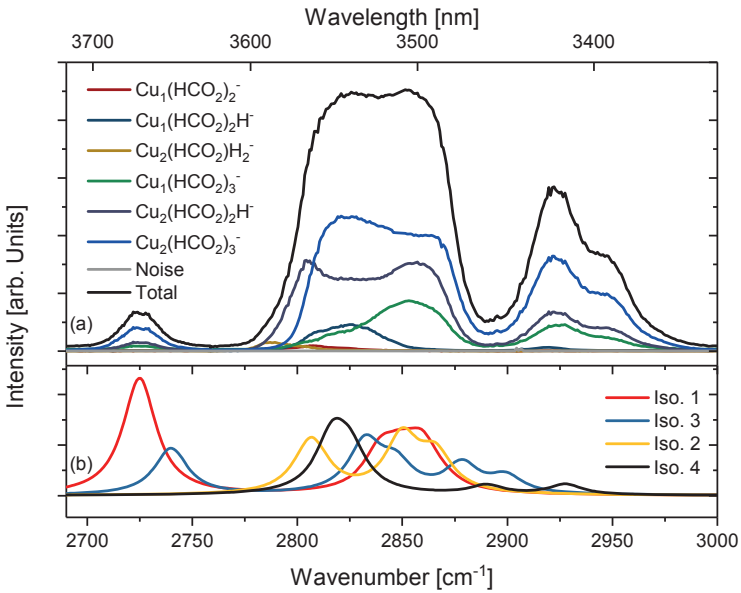

Figure 2: *(a) Experimental infrared multiphoton dissociation yield normalized to laser intensity of a $Cu_2(HCO_2)_5^-$ cluster. (b) Calculated absorption spectra of the four most stable isomeres.*

References

[1] C. E. Elwell et al.; Copper–Oxygen Complexes Revisited: Structures, Spectroscopy, and Reactivity. *Chem. Rev.* 2017, **117**, 2059–2107.

[2] A. Tsybizova, J. Roithová; Copper-catalyzed reactions: Research in the gas phase. *Mass Spectrom. Rev. 2016, **35**, 85-110.*

Investigating conformational effects in chemical reactions under single-collision conditions

L. Ploenes, A. Kilaj, P. Stranak, U. Rivero, H. Gao, S. Willitsch
Department of Chemistry, University of Basel, Klingelbergstrasse 80, 4056 Basel

J. Küpper
Center for Free-Electron Laser Science, DESY, Notkestrasse 85, 22607 Hamburg, Germany
The Hamburg Center for Ultrafast Imaging, University of Hamburg, Luruper Chaussee 149, 22761 Hamburg, Germany,
Department of Physics, University of Hamburg, Luruper Chaussee 149, 22761 Hamburg, Germany

The chemical structure of molecules has a profound impact on their chemical reactivity [1]. Conformers are among the dominant forms of structural isomers of molecules. Despite their great importance, the influence of the molecular conformation on the mechanism of reactions is still poorly understood. This is because the thermal interconversion of conformers imposes high experimental difficulties in performing conformation-selective experimental investigations. So far, the isolation and control of individual conformers was the major experimental obstacle. Consequently, only a very limited number of single-collision studies characterising the impact on conformational effects on chemical reactivity have been reported [2, 3].

In the single-collision and low-temperature environment of a supersonic expansion, thermal interconversion of conformers is effectively suppressed, making the molecular-beam techniques the ideal tool for the investigation of the chemical properties and reactivity of individual conformers. Recently, the successful spatial separation of specific conformers entrained in a molecular beam was demonstrated by exploring the interaction of strong, inhomogeneous electric fields with their different dipole moments [4, 5]. The resulting molecular beams of isolated conformers provide the ideal starting point to perform controlled, conformer-selective reaction experiments.

For an in-depth characterisation of the reaction mechanisms and dynamics of a wide range of conformation-dependent reactions, we here report the development of two experimental setups.

In the first setup, a molecular beam of spatially separated conformers is aimed at a cloud of sympathetically cooled molecular ions in an ion trap, enabling us to study conformationally selected reactions between neutral molecules and charged collision partners. Product analysis is performed by an integrated high-resolution time-of-flight mass spectrometer (TOF-MS). This method has already been successfully applied to the study of reactive collisions of 3-aminophenol with a Coulomb crystal of Ca^+ ions [6, 7]. Recently, this approach has also been adapted to the investigation of the individual reactivities of the two nuclear-spin isomers of water (*ortho*- and *para*-water) with sympathetically cooled N_2H^+ ions (see accompanying poster by Ardita Kilaj).
The second setup is a crossed-molecular beam machine (CBM) in which a beam of spatially separated conformers is crossed with a beam of neutral molecules or free radicals. Product detection is performed by a combination of TOF-MS and velocity-map imaging [8] allowing us to obtain angle-, energy- and mass-resolved distributions of the reaction products. Currently, first proof-of-principle experiments are performed on the CBM to validate the proper functioning of the conformer selector and to characterize and calibrate the product detection setup. In contrast to the setup which combines the conformer selector with the ion trap where only ion-neutral reactions can be investigated, the CBM setup will allow us to investigate neutral-neutral reactions. Additionally, the implementation of imaging methods will provide us with a more comprehensive picture of the dynamics behind the investigated target reaction.

At present, we are applying these setups to unravel conformational effects in two important classes of chemical reactions: reactions involving free radicals and Diels-Alder chemistry. Free radicals are important chemical agents in a variety of contexts such as planetary atmospheres, interstellar spaces and combustion. Understanding conformational effects in these processes is of major importance. Diels-Alder cycloaddition reactions, on the other hand, are one of the most important pathways for the synthesis of cyclic compounds in organic chemistry. Despite their importance, the mechanistic details of Diels-Alder reactions still remain an unsolved and extensively discussed question. [9, 10].
Here, we report progress towards investigating conformational aspects in these types of reactions under single-collision conditions. The combination of both setups will give us the experimental means to unravel their mechanistic details from the perspective of both, neutral-ionic and neutral-neutral reaction partners.

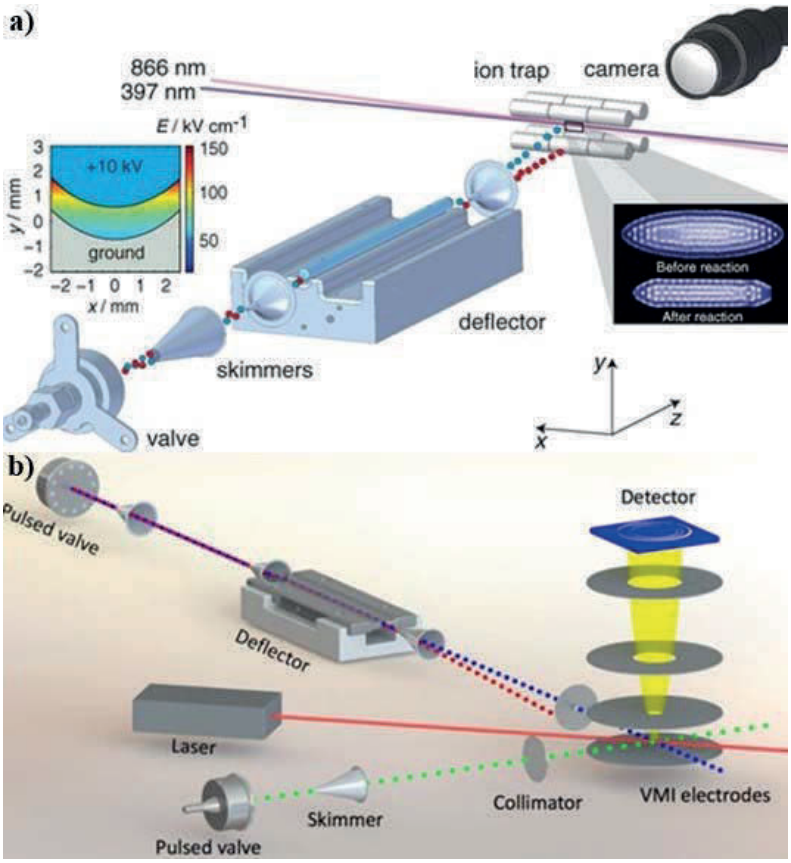

Figure 1: *Schematic setup of the conformer selector coupled to an ion trap (a) and of the conformer-selective crossed-molecular-beam machine (b).*

[1] E. L. Eliel and S. H. Wilen, Stereochemistry of organic compounds, New York, 1994.
[2] C. A. Taatjes et. al., Science 340, 177 (2013).
[3] L. Khriachtchev et. al, J. Phys. Chem. A 113, 8143 (2009).
[4] F. Filsinger, et. al., Phys. Rev. Lett. 100, 133003 (2008).
[5] F. Filsinger, et. al., Angew. Chem. Int. Ed. 48, 6900 (2009).
[6] Y. P. Chang, et. al., Science, 342(6154), 98-101 (2013).
[7] D. Rösch, et. al., J. Chem. Phys. 140, 124202 (2014).
[8] A. T. J. B. Eppink et. al., Rev. Sci. Instrum. 68, 3477 (1997).
[9] M. Eberlin, Int. Journal of Mass Spectrometry. 235, 263 (2004).
[10] U. Rivero et. al., Chem. Phys. Lett. 683, 598-605 (2017).

The structure of coronene cluster ions inferred from H_2 uptake in the gas phase

Marcelo Goulart, Martin Kuhn, Johannes Postler, Michael Gatchell, Paul Scheier
Institute for Ion Physics and Applied Physics, University of Innsbruck, A-6020 Innsbruck, Austria

Bilal Rasul
Department of Physics, University of Sargodha, 40100 Sargodha, Pakistan

Henning Zettergren
Department of Physics, Stockholm University, S-10691 Stockholm, Sweden

Olof Echt
Physics Department, University of New Hampshire, Durham, NH 03824 USA

High resolution mass spectra of helium nanodroplets doped with H_2 and coronene, a polycyclic aromatic hydrocarbon (PAH), feature anomalies in the ion abundance (see figure 1). These anomalies reveal differences in the energetics of possible adsorption sites of H_2 on coronene. The coronene monomer ion strongly binds up to n = 38 H_2 molecules indicating a commensurate solvation shell that preserves the D_{6h} symmetry of the substrate. However, no such feature is seen in the observed abundances of the coronene dimer through tetramer complexed with H_2. The shell closures change for these ions to n = 51, 61 and 71 H_2 ions molecules, respectively. This observation rules out a vertical columnar structure. Instead we see evidence for a columnar structure in which adjacent coronenes are displaced in parallel, forming terraces that offer additional strong adsorption sites, hence explaining the increasing number of H_2 molecules for increasing coronene cluster size.

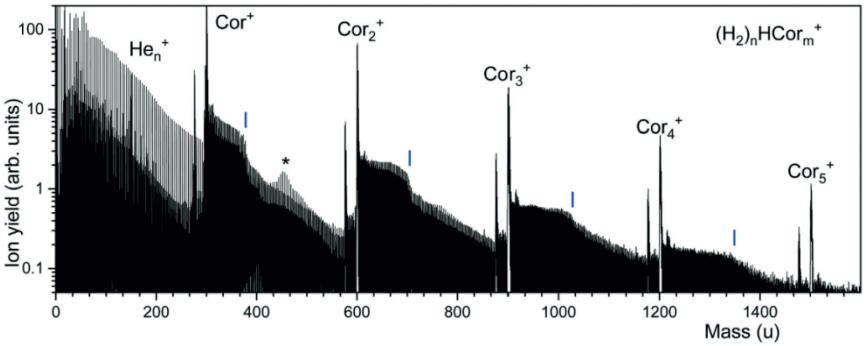

Figure 1 *Electron ionization mass spectrum of helium nanodroplets doped with coronene ($C_{24}H_{12}$, mass 300.09u for the most abundant isotope) and molecular hydrogen. The most prominent mass peaks are due to Cor_m^+ with m= 1, 2, 3, 4, 5. They are followed by a series of $(H_2)_nHCor_m^+$ ions; abrupt drops in their ion yields are marked by vertical lines.*

The experimental value for the number of adsorption sites per terrace, approximately six, barely depends on the number of coronene molecules hinting at a constant displacement for each added coronene molecule. The displacement estimated from this number exceeds the value reported in several theoretical studies of the bare, neutral coronene dimer [1, 2].
In addition, observation of doubly charged coronene clusters will be reported. Surprisingly, Cor_3^{2+} seems to be the smallest observable cation which is in excellent agreement with theoretical predictions. Preliminary, unpublished data will be presented.

References:

[1] H. Ruuska, T. A. Pakkanen, J. Phys. Chem. B, 2001, 105 (39), pp 9541–9547
[2] O. I. Obolensky, V.V. Semenikhina, A.V. Solov'yov and W. Greiner, Int. J. Quantum Chem., 2007, 107, pp 1335–1343

Acknowledgement: This work was supported by the FWF (Project numbers P26635 and M1908-N36), the Swedish Research Council (Contract No. 2016-06625 and 2016-04181), the COST Action CM 1201, XLIC and the European Commission (ELEVATE, Horizon 2020 research and innovation programme under grant agreement No. 692335)

Full-dimensional Quantum Dynamics and Spectroscopy of Ammonia Isotopomers

Csaba Fábri,[1, 2, 3] Roberto Marquardt[1, 4] and Martin Quack[1]
[1)]Physical Chemistry, ETH Zürich, CH-8093 Zürich, Switzerland
[2)]Laboratory of Molecular Structure and Dynamics, Institute of Chemistry, Eötvös University, Pázmány Péter sétány 1/A, H-1117 Budapest, Hungary
[3)]MTA-ELTE Complex Chemical Systems Research Group, P.O. Box 32, H-1518 Budapest 112, Hungary
[4)]Laboratoire de Chimie Quantique, Institut de Chimie UMR 7177 CNRS/Université de Strasbourg, 1 rue Blaise Pascal, BP 296/R8, Strasbourg CEDEX,France

We report full-dimensional quantum-dynamical calculations including all vibrational and rotational degrees of freedom for ammonia isotopomers using selected available potential energy and electric dipole moment hypersurfaces. Both the time-independent Schrödinger equation for the isolated molecules and the time-dependent Schrödinger equation under coherent irradiation are solved numerically. We have extended the general rotational-vibrational GENIUSH program package (utilizing a numerically constructed exact and general rotational-vibrational kinetic energy operator with arbitrarily chosen internal coordinates and body-fixed frame embeddings) by implementation of contracted vibrational bases and the vibrational subspace (VS) method for the solution of the rotational-vibrational Schrödinger equation. In addition GENIUSH has been extended to solve the time-dependent Schrödinger equation with coherent infrared multiphoton excitation.

Ammonia and its isotopomers have been prototypes for spectroscopy and quantum-mechanical tunneling dynamics since the early days of quantum mechanics [1-3]. While early treatments entering textbooks have been usually restricted to one-dimensional models, more recently extended models including several degrees of freedom and full-dimensional potential energy hypersurfaces have become available (see [4-12] and references cited therein).

In particular, comparison with results from stationary-state high-resolution spectroscopy has demonstrated the great progress achieved recently in the formulation of accurate potential energy hypersurfaces and spectroscopic eigenstate calculations (see [4-12] and references cited therein). Much less work is available on the explicitly time-dependent quantum dynamics either of the isolated molecules or molecules under the influence of a coherent radiation

field. The present work is intended to fill this gap, paying particular attention also to the chiral isotopomers NHDT (see Figure 1) and NHDMu, which allows us to study a prototypical stereomutation reaction converting enantiomers by inversion as to be compared to a related stereomutation by internal rotation in molecules such as hydrogen peroxide HOOH [6, 7].
In this paper we report extensions of the GENIUSH program package [13-16] with time-dependent quantum-dynamical features [17]. The new version of GENIUSH is applied to study the quantum dynamics of selected NH_3 isotopomers (see also previous studies on the time-dependent quantum dynamics of NH_3 isotopomers [18-20] and references cited therein).
We report time-dependent level populations and other observables such as probability densities for the positions of the nuclei, which are representative of the time-dependent quantum mechanical molecular “structure”, thus true molecular quantum motion [21].

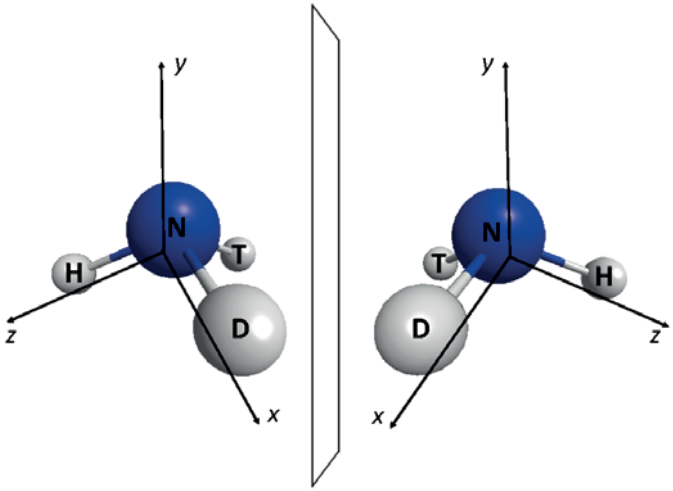

Figure 1. *Structures of the two enantiomers of NHDT.*

These results, being ultimately based on the analysis of highly accurate and precise experimental data from high-resolution spectroscopy, are equivalent to obtaining a time-dependent picture or movie of the true quantum physics of molecules .This includes tunnelling processes, phenomena such as quasiadiabatic above barrier tunnelling [6,19-21] and also the time-dependent absolute configuration of chiral molecules and the possibility of nonclassical

bistructural states, which would be impossible with classical representations of molecules.

Acknowledgments
Our work is supported financially by the Swiss National Science Foundation, ETH Zürich, an ERC Advanced Grant No. 290925, the COST project MOLIM and NKFIH (Grant No. PD124699). We thank Siggi Albert, Irina Bolotova, Ziqiu Chen, Attila G. Császár, Fabien Gatti, Frédéric Merkt, Carine Manca Tanner, Ruth Schüpbach and Georg Seyfang for help and discussion.

[1] F. Hund, *Z. Phys.* **1927**, *43*, 805-826.
[2] G. Herzberg, *Molecular Spectra and Molecular Structure, Vol. II, Infrared and Raman Spectra of Polyatomic Molecules*, 1 ed., van Nostrand Reinhold, New York, **1945**.
[3] F. Merkt, M. Quack, *Molecular Quantum Mechanics and Molecular Spectra, Molecular Symmetry, and Interaction of Matter with Radiation,* in *Handbook of High-Resolution Spectroscopy, Vol. 1*, Chap. 1. (Eds.: M. Quack, F. Merkt), Wiley, Chichester, New York, **2011**, pp. 1-55, (see also preface to this Handbook).
[4] A. G. Császár, C. Fábri, T. Szidarovszky, E. Mátyus, T. Furtenbacher, G. Czakó, *Phys. Chem. Chem. Phys.* **2012**, *14*, 1085-1106.
[5] R. Marquardt, M. Quack, *Global Analytical Potential Energy Surfaces for High Resolution Molecular Spectroscopy and Reaction Dynamics,* in *Handbook of High-Resolution Spectroscopy, Vol. 1*, Chap. 12. (Eds.: M. Quack, F. Merkt), Wiley, Chichester, New York, **2011**, pp. 511-549.
[6] B. Fehrensen, D. Luckhaus, M. Quack, *Chem. Phys.* **2007**, *338*, 90-105.
[7] B. Fehrensen, D. Luckhaus, M. Quack, *Chem. Phys. Lett.* **1999**, *300*, 312-320.
[8] R. Marquardt, K. Sagui, W. Klopper, M. Quack, *J. Phys. Chem. B* **2005**, *109*, 8439-8451.
[9] R. Marquardt, K. Sagui, J. Zheng, W. Thiel, D. Luckhaus, S. Yurchenko, F. Mariotti, M. Quack, *J. Phys. Chem. A* **2013**, *117*, 7502-7522.
[10] R. Marquardt, M. Quack, I. Thanopulos, D. Luckhaus, *J. Chem. Phys.* **2003**, *119*, 10724-10732.
[11] S. N. Yurchenko, R. J. Barber, A. Yachmenev, W. Thiel, P. Jensen, J. Tennyson, *The Journal of Physical Chemistry A* **2009**, *113*, 11845-11855.
[12] S. N. Yurchenko, R. J. Barber, J. Tennyson, W. Thiel, P. Jensen, *J. Mol. Spectrosc.* **2011**, *268*, 123-129.
[13] E. Mátyus, G. Czakó, A. G. Császár, *J. Chem. Phys.* **2009**, *130*, 134112.
[14] C. Fábri, E. Mátyus, A. G. Császár, *J. Chem. Phys.* **2011**, *134*, 074105.
[15] C. Fábri, E. Mátyus, A. G. Császár, *Spectrochim. Acta A* **2014**, *119*, 84-89.
[16] C. Fábri, M. Quack, A. G. Császár, *J. Chem. Phys.* **2017**, *147*, 134101.

[17] M. Quack, *Reaction dynamics and statistical mechanics of the preparation of highly excited states by intense infrared radiation,* in *Adv. Chem. Phys., Vol. 50* (Eds.: K. Lawley, I. Prigogine, S. A. Rice), John Wiley & Sons, Chichester and New York, **1982**, pp. 395-473.
[18] R. Marquardt, M. Quack, I. Thanopulos, D. Luckhaus, *J. Chem. Phys.* **2003**, *118*, 643-658.
[19] R. Marquardt, M. Sanrey, F. Gatti, F. Le Quéré, *J. Chem. Phys.* **2010**, *133*, 174302.
[20] F. Gatti, R. Marquardt, *Comp. Theor. Chem.* **2012**, *990*, 90-93.
[21] M. Quack,Molecules in Motion, *Chimia.* **2001**, *55*, 753-758.

Correlation of target properties and plasma parameters in DC magnetron sputtering

Stefan Raggl and Johannes Postler
Institute for Ion Physics and Applied Physics, University of Innsbruck, Technikerstrasse 25, 6020 Innsbruck, Austria

Jörg Winkler
PLANSEE SE, Metallwerk-Plansee-Straße 71, 6600 Reutte, Austria

Georg Strauss
PhysTech Coating Technology GmbH, Knappenweg 34, 6600 Pflach, Austria

Christian Feist
CENUMERICS, Haspingerstraße 16, 6020 Innsbruck, Austria

Arno Plankensteiner and Michael Eidenberger-Schober
PLANSEE SE, Metallwerk-Plansee-Straße 71, 6600 Reutte, Austria

Paul Scheier
Institute for Ion Physics and Applied Physics, University of Innsbruck, Technikerstrasse 25, 6020 Innsbruck, Austria

1. Introduction

Utilizing different manufacturing methods for producing sputtering targets leads to significant variations in target microstructure with the latter showing a pronounced impact on the performance of the target in direct current magnetron sputtering (DCMS) in terms of varying sputtering yields. This study aims at correlating measured plasma parameters on the one hand with varying microstructure of molybdenum targets on the other hand. To this end, the sputtering performance of targets manufactured by means of selected powder metallurgy as well as melting metallurgy processes in DCMS is experimentally investigated. Ranging over two orders of magnitude, the mean grain size is identified as the major varying microstructural parameter of the investigated targets. Measurements of spatially varying plasma parameters under steady-state sputtering conditions are carried out by means of a Langmuir probe moved over the target at several distances perpendicular to the target top surface. The largest differences in the measured parameters are found in the

vicinity of the target surface. In particular, the electron density is found to decrease with increasing mean grain size.

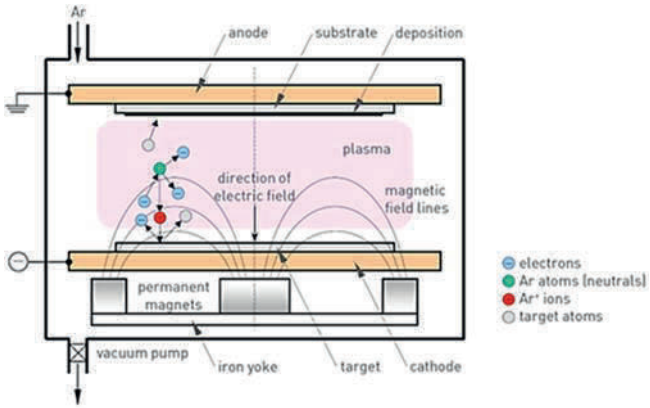

Fig. 1 *Sketch of DC magnetron sputtering process, taken and altered from [1].*

In order to investigate the origin of the differences in electron densities additional measurements of the secondary electron emission coefficient (SEEC) form the target surface are carried out. Utilizing a focused argon ion beam with an energy similar to the ion energies during DCMS, the incoming ion current and the released electron current upon ion impact are measured with high precision pA-meters. Spatial resolution of the SEEC is achieved by means of a linear manipulator, which gives the possibility to move the target under the stationary focused ion beam. Especially for the target with large mean grain size (target C) a spatial variation of the SEEC is visible.

2. Langmuir probe measurements

Measurements with the Langmuir probe are carried out for three targets with a mean grain size ranging from 10 µm (target A) over 150 µm (target B) to 5000 µm (target C), see Fig. 2. The probe is positioned at various heights above the target surface and orientated as shown in Fig. 3.

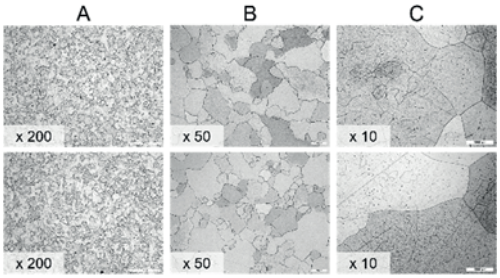

Fig. 2. *Micro sections (light optical micrographs) of the investigated molybdenum targets from the center region (top row) and outer diameter region (bottom row) of targets A, B, and C (from left to right) with a mean grain size of 10, 150, and 5000 µm, respectively.*

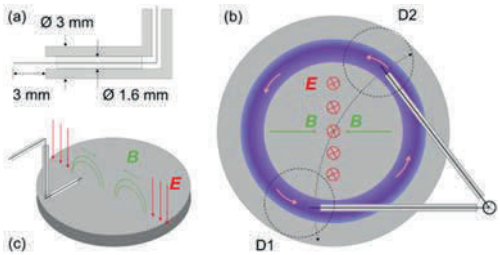

Fig. 3. *Schematic of the Langmuir probe manipulation. Two coaxial ceramic tubes insulate the tungsten probe tip (a). It is moved along a circular path, crossing the center of the target (b) and oriented perpendicular to the dominant axial component of the electric field E and approximately normal to the magnetic field H (c).*

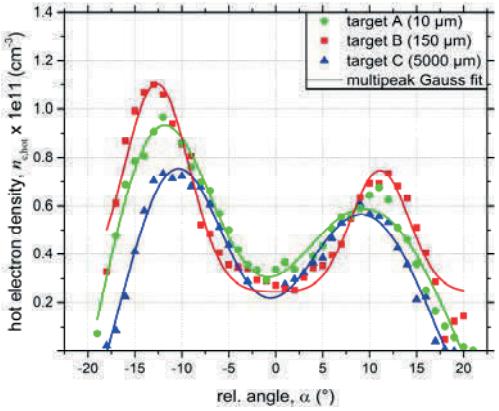

Fig. 4. *Hot electron density distribution $n_{e,hot}$ at 10 mm distance normal to the target surfaces. Target B exhibits about 1.5 times larger electron densities than target C. The data are fitted with multi-peak Gaussian functions.*

3. Secondary electron emission coefficient (SEEC) measurements

The targets are moved via a linear manipulator (stroke of 25 mm) under the stationary focused argon ion beam. Thus, a spatial variation in the SEEC is measurable. Shown in Fig. 5. is the SEEC for target C with the largest mean grain size.

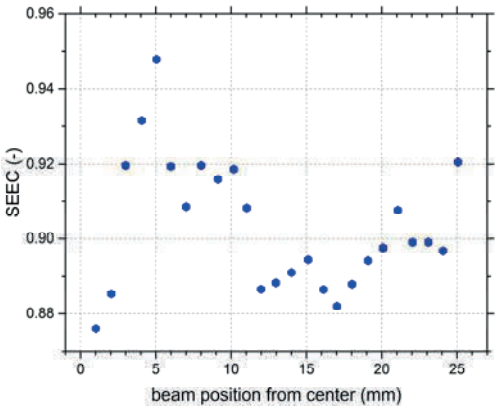

Fig. 5. *Preliminary data of the spatial variation of the SEEC for measuring target C (mean grain size of 5000 µm). A drastic change of the SEEC is visible in the range from 3 to 10 mm apart from the target center. This result suggest the presents of a grain in this area.*

4. References

[1] Studying Target Erosion in Planar Sputtering Magnetrons Using a Discrete Model for Energetic Electrons, C. Feist et al, Proc. 18th Plansee Seminar, pp. RM12/1-RM12/13, Plansee SE, Reutte, 2013

[2] Raggl S., *et al*., J. Vac. Sci. Technol. A **35**, 061308 (2017)

Electron energy distribution of electrons after transition through nanometric Si_3N_4 membranes

Matúš Sámel, Michal Stano, Miroslav Zahoran and Štefan Matejčík
Faculty of Mathematics, Physics and Informatics, Comenius University, Mlynská dolina F1,842 48 Bratislava, Slovakia

Synopsis
We present electron source for atmospheric pressure ionization (API). In present study we have focused on the characterization of the electron source, its electron energy distributions function (EEDF) after transition through Si_3N_4 membrane. EEDFs were measured for different initial kinetic energies and for different membranes modifications.

1. Introduction

Recently, electron guns with nanomembrane vacuum-atmosphere interface (window) of 300 nm thickness were reported, applicable for transport of keV electrons from vacuum to atmosphere [1-3]. Such electron sources are suitable replacements for radioactive ion sources based on β radiation and could be applied for Atmospheric Pressure Ionization (API) in Mass Spectrometry (MS) and Ion Mobility Spectrometry (IMS) or other analytical methods at atmospheric pressure (fluorescence) [4].

2. Results

In this work we present results of recent studies involving measurements of Electron Energy Distribution Function (EEDF) after transition through ceramic Si_3N_4 membrane as a function of initial kinetic energy of electrons. The measurements were carried out for several different membranes modifications of the 100 and 150 nm Si_3N_4 membranes (unplated or plated by gold layer of various thicknesses).

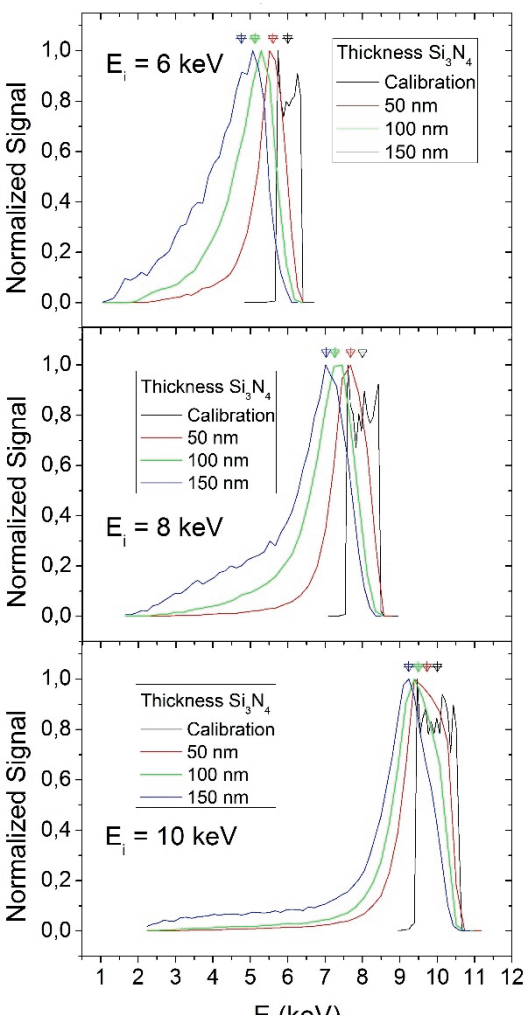

Figure 1 *The EEDFs at three differenct initial electron energies E_i after electron transition through membranes of various thicknesses.*

The Figure 1 shows the normalized EEDFs of the electron source without the membrane (blank window, which we used for calibration measurements (black curves) and with Si_3N_4 membranes of three different thicknesses. The EEDFs were measured for three different initial electron energies E_i. The blank window measurements serve for calibration purposes (no electron energy loss). The markers above the EEDFs represent the mean peak positions of the corresponding EEDFs. The comparison reveals a decrease of absolute energy loss with increasing initial electron energy. We associate this effect with the strong dependence of EEDF on the initial energy of accelerated electrons, rather than on the thickness of the membrane.

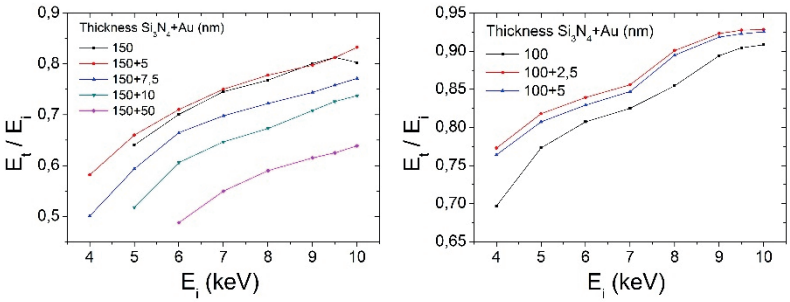

Figure 2 *The ration of mean electron energy after transition through the membrane E_t to the initial electron energy E_i as a function of the initial electron energy E_i for various Si_3N_4 membranes.*

The Figure 2 shows the dependence of ratio of mean electron energy after transition through the membrane E_t to the initial electron energy E_i as a function of the initial electron energy E_i. These functions were measured for unplated and gold-plated Si_3N_4 membranes of 100 nm (left) and 150 nm (right) thicknesses. Gold plating of 100 nm membranes resulted in the increase of the mean energy of transmitted electrons at arbitrary E_i. We attribute this behaviour to the effect of removal of a surface charge in the case of gold plated membranes. In the case of unplated Si_3N_4 membrane the surface charge produced on the ceramic surface decreases the effective potential of the membranes and thus reduces the kinetic energy of the electrons transmitted through the membranes [5]. In the case of 150 nm membrane, we can see similar effect for 5 nm gold plated membrane, whereas thicker gold layers (7.5, 10 and 50 nm) already lead to the reduction of the mean energy of transmitted electrons. We attribute this behaviour to two effects. The first is the increase of the thickness of Si_3N_4 membrane. The second and more significant effect is the increase of Mott scattering in thicker gold layers based on much higher atomic number of gold.

3. Conclusion

The transport of electrons through Si_3N_4 membranes depends on the membrane thickness. Additionally we have shown a positive effect of very thin gold layers deposited on the surface of membranes (below 5 nm), which reduces the electron energy losses during the electron transport. We associate this effect with the phenomenon of surface charge removal by the very thin conductive gold layers.

Acknowledgements
This work was supported by the Slovak Research and Development Agency, project Nr. APVV-15-580 and the grant agency VEGA, project Nr. VEGA-15-089. This project has received funding from the European Union's Horizon 2020 research and innovation programme under grant agreement number 692335.

References
[1] F. Gunzer et al. 2010 Int. J. Ion Mobil. Spec. 13 9-16.
[2] P. Cochems et al. 2012 Int. J. Ion Mobil. Spec. 15 223-229.
[3] P. Cochems et al. 2009 Sens. Actuators A: Phys. 206 165-170.
[4] A. Ulrich et al. 2009 Eur. Phys. J. Appl. Phys. 47 22815.
[5] N. Manivannan et al. 2015 Vacuum 113 19-23.

The Infrared Signature of Mechanically Stressed Polymer Solids

Matthew S. Sammon, Milan Ončák and Martin K. Beyer
Institut für Ionenphysik und Angewandte Physik, Universität Innsbruck, Technikerstraße 25, 6020 Innsbruck, Austria.

Mechanical stress leads to deformation of strands in polymer solids, including the elongation of covalent bonds and widening of bond angles, thus influencing infrared active vibrational modes. Since mechanical stress affects these modes differently depending on their orientation with respect to the direction the stress is applied, it should be possible to detect stress-induced changes by following the behavior of characteristic modes. Previous simulations predicted a strong redshift of infrared bands attributed to vibrations on the polymer backbone as predominant effect of external force on the infrared spectrum [1]. In our work, we simulate the infrared spectrum of solid polymer samples exposed to mechanical stress by density functional theory calculations to determine the feasibility of this method. Mechanical stress is described with the external force explicitly included (EFEI) method [2]. In addition to previous work simulating the infrared spectrum of single polymers, the distribution of the external stress on individual polymer strands is accounted for by a convolution of simulated spectra with a realistic force distribution [3]. The investigation focuses on polymers with strong infrared chromophores, such as polyamide, polyester, polycarbonate and polyethylene glycol.

The effect of a specific force on the backbone of a single polymer strand is a redshift of the infrared bands dependent on the orientation of the respective vibrational mode. The convolution with a realistic force distribution, however, shows that the dominant effect on the strongest infrared lines is not a shift of the peak position, but rather peak broadening and a characteristic change in the relative intensities of the strongest lines. In particular the latter effect may allow the identification and quantification of mechanical stress in polymer solids [4].

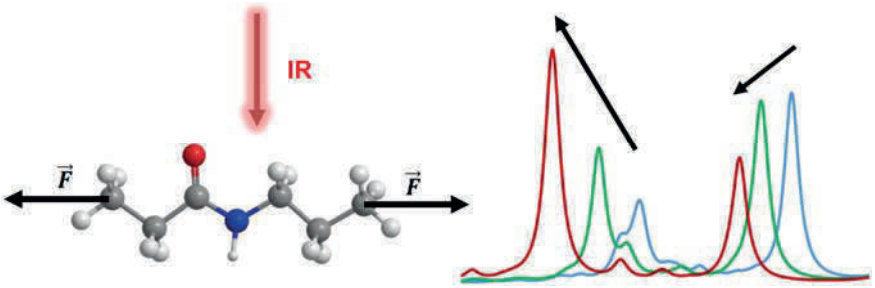

References:

[1] Pill, M. F.; Kersch, A.; Clausen-Schaumann, H.; Beyer, M.K. *Polym. Degrad. Stab.* 2016, *128*, 294-299.
[2] Ribas-Arino, J.; Shiga, M.; Marx, D. *Angew. Chem. Int. Ed.* 2009, *48*, 4190-4193.
[3] Adhikari, R.; Makarov, D. E. *J. Phys. Chem. B* 2017, *121*, 2359-2365.
[4] Sammon, M. S.; Ončák, M.; Beyer, M. K.; *Beilstein J. Org. Chem.* 2017, *13*, 1710-1716.

Single Molecule Force Spectroscopy of the Gold Sulfur Bond

Simone Schirra, Michael Zwölfer, Matthew S. Sammon, Martin K. Beyer
Institut für Ionenphysik und Angewandte Physik, Universität Innsbruck, Technikerstraße 25, 6020 Innsbruck, Austria

The mechanical strength of gold-sulfur bonds is investigated by means of single molecule force spectroscopy. Silicon nitride cantilevers are functionalized using heterobifunctional polyethylene glycol (MW: 10 kDa) with a triethoxysilane and a thiol terminus, termed silane-PEG-thiol (SPT). The silane covalently binds to the cantilever, forming an anchor during silanization. Using an atomic force microscope (AFM), the functionalized cantilever is approached to a gold-coated surface in a PBS buffer solution. The terminal thiol group subsequently is deprotonated to form a gold-sulfur bond.

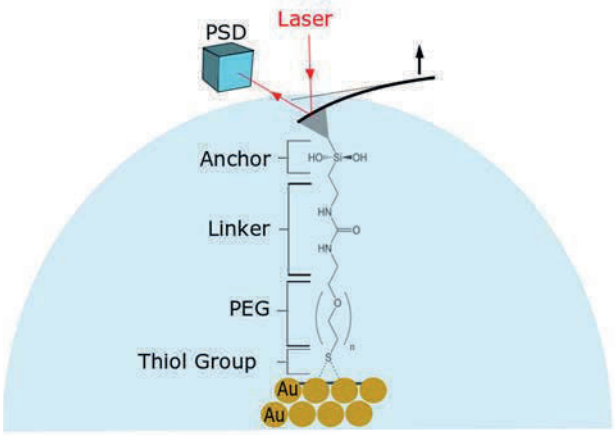

Two types of SMFS modes are used to investigate the gold-sulfur system. First, dynamic force ramp experiments are conducted, during which the cantilever is pulled away from the surface at a constant velocity. This leads to an increasing mechanical force until the weakest bond in the system eventually breaks. The distribution of the rupture forces gives a general understanding of the system. Second, static force clamp experiments are used to determine dissociation kinetics. Here, the cantilever is retracted until a specific force is applied to the system. A feedback mechanism keeps the force constant. Due to thermal activation, over time the weakest bond is cleaved, and the survival

time in this individual experiment is recorded. From repeated measurements of survival times, the dissociation kinetics is retrieved, which is analyzed quantitatively.

Force distributions obtained from preliminary dynamic experiments are in good agreement with previous work on this system [1,2]. From force clamp experiments, multiexponential dissociation kinetics are identified at forces from 400 to 800 pN, indicating chemically different binding motifs. Since, however, we cannot unambiguously distinguish between bond rupture of Au-S, hydrolysis of the anchor and force-induced cleavage of the amide bond, additional experiments are needed. Therefore, temperature and pH are varied in further experiments.

[1] Y. Xue, X. Li, H. Li, W. Zhang, *Nat. Commun.* **2014**, 5, 4348.
[2] M. Grandbois, M. Beyer, M. Rief, H. Clausen-Schaumann, H. E. Gaub, *Science* **1999**, 283, 1727.

Towards inelastic collision rate coefficients of OH^+ with He via photodissociation

Alice Schmidt-May, Malcolm Simpson, Robert Wild, Roland Wester
Institut für Ionenphysik und Angewandte Physik,
Universität Innsbruck, Austria

Cooling internal degrees of freedom by inelastic collisions is a widely applied method in cold molecule physics, especially for species that lack the possibility of laser cooling. [1] Despite this, the state specific rate coefficients are commonly unknown. Experimental data for ions at low temperatures, of the order of a few Kelvin, is particularly sparse. Our group has previously reported rotational state-to-state rate coefficients for the hydroxyl anion, OH^-, in collisions with helium, He. [2] The Langevin capture rate which is commonly used as an estimate in ion-neutral collisions was found to overestimate the rates by an order of magnitude, demonstrating the elasticity of the system.

We now aim to measure the inelastic collision rate coefficients for trapped hydroxyl cations, OH^+, with He buffer gas using photodissociation as a state-specific probe.

OH^+ has been observed in numerous regions in space and is of special astrophysical interest because it could function as a tracer for cosmic and X-ray ionization rates besides serving as an initiator in the oxygen chemistry. [3] The photodissociation of OH^+ also plays an important role in astrochemistry [4] and has interesting dynamics by itself. For excited vibrational levels in the *A* state, dissociation can occur via coupling between bound and dissociative excited electronic states or by tunnelling, and dissociation into both of the quasi degenerate channels O^++H and O+H^+ has been observed. The cross section and the branching ratio were found to be highly state specific. [5, 6]

Our experimental studies, in combination with quantum chemical theory [3, 7] , aim to give a fundamental understanding of collisions including quantum effects which can have a significant contribution when low masses collide at low temperatures. Open shell species like the OH^+, are particularly interesting as collisions can induce changes in the electronic spin as well as the nuclear rotation.

References

[1] A. K. Hansen, O. O. Versolato, S. B. Kristensen, A. Gingell, M. Schwarz, A. Windberger, J. Ullrich, J. R. C. López-Urrutia, M. Drewsen und others, „Efficient rotational cooling of Coulomb-crystallized molecular ions by a helium buffer gas," *Nature,* Bd. 508, pp. 76-79, 2014.

[2] D. Hauser, S. Lee, F. Carelli, S. Spieler, O. Lakhmanskaya, E. S. Endres, S. S. Kumar, F. Gianturco und R. Wester, „Rotational state-changing cold collisions of hydroxyl ions with helium," *Nat. Phys.,* Bd. 11, pp. 467-470, 6 2015.

[3] S. Gómez-Carrasco, B. Godard, F. Lique, N. Bulut, J. Kłos, O. Roncero, A. Aguado, F. J. Aoiz, J. F. Castillo, J. R. Goicoechea, M. Etxaluze und J. Cernicharo, „OH^+ in Astrophysical Media: State-to-state Formation Rates, Einstein Coefficients and Inelastic Collision Rates with He," *ApJ,* Bd. 794, p. 33, 2014.

[4] Heays, A. N., „Photodissociation and photoionisation of atoms and molecules of astrophysical interest," *A&A,* Bd. 602, p. A105, 2017.

[5] J. Levin, U. Hechtfischer, L. Knoll, M. Lange, G. Saathoff, R. Wester, A. Wolf, D. Schwalm und D. Zajfman, „Photodissociation spectroscopy of OH^+ molecular ions at the TSR storage ring," *Hyperfine Interact.,* Bd. 127, pp. 267-270, 01 8 2000.

[6] H. Helm, P. C. Cosby und D. L. Huestis, „Photofragment spectroscopy of shape resonances in OH^+," *Phys. Rev. A,* Bd. 30, Nr. 2, pp. 851-857, 8 1984.

[7] E. Bodo und F. A. Gianturco, „Collisional quenching of molecular ro-vibrational energy by He buffer loading at ultralow energies," *Int. Rev. Phys. Chem.,* Bd. 25, pp. 313-351, 2006.

Cold ion vibrational predissociation spectroscopy of H_2-tagged protonated tryptophan

Steffen Spieler, Felix Duensing, Alexander Kaiser and Roland Wester
Institut für Ionenphysik und Angewandte Physik,
Universität Innsbruck, Österreich

Chinh Duong and Mark Johnson
Sterling Chemistry Laboratory, Yale University, New Haven, USA

The combination of electrospray ionization, mass spectrometry, cryogenic ion trapping and vibrational dissociation spectroscopy many times has proven its power in determining the molecular structure and solvation effects of thermally fragile, weakly bound systems. One such system that has been extensively explored using ion electronic spectroscopy in ion traps is the electron rich aromatic amino acid tryptophan. For example, Rizzo and coworkers found a significantly increased electronic excited state lifetime upon hydration of protonated tryptophan with just one water molecule [1]. The structural deformations induced by the water molecule, however, are not presently clear. Here we explore this issue by applying the technique of $(H_2)_n$ messenger tagging with n=1-5 to obtain the single photon vibrational spectrum of $TrpH^+$ and its partly deuterated isotopomer were investigated in the spectral region of 1000-4400 cm^{-1}. Depending on the number of messenger molecules, the spectra of several conformational isomers associated with multiple H_2 binding locations were found using two photon, IR-IR conformational hole burning. The likely messenger positions were established by comparison with the predictions of DFT (B3LYP) calculations on various candidate structures. In a second step, the $TrpH^+(H_2O)_m$ with m=1 and 2 clusters were investigated along with those of the $TrpH^+(MeOH)(H_2)$ analogues. These spectra reveal broad features in the NH stretching region of the NH_3^+ group, indicating strong hydrogen bonding in acceptor-donor configuration for the first water molecule, while the second appears to attach in to the first as an H-bond acceptor, yielding transitions associated with free OH stretching fundamentals of the OH_2 group. We will discuss the relevance of the microsolvation structures to the motifs thought to be in play in condensed phase, biological processes.

[1] S.R. Mercier et al., J.Am.Chem.Soc. 2006, 128, 16938-16943

Detailed reinvestigation of water nuclear spin conservation/relaxation in supersonic jet expansion

O. Votava, V. Zelenková, and J. Rakovský
J. Heyrovský Institute of Physical Chemistry of the Czech Academy of Sciences, Dolejškova 3, Prague 8, Czech Republic

1. Introduction

Since the discovery of ortho and para hydrogen more than 80 years ago properties of molecules with multiple nuclear spin isomers have been investigated. Processes in which one nuclear spin isomer is converted to other (nuclear spin relaxation) are of prime interest. Indeed it has been discovered that when molecular hydrogen is prepared in the Para isomer, it can be stored for weeks without conversion to the Ortho isomer. Similarly proceses of nuclear spin relaxation have been studied for a wide range of small polyatomic molecules and are generally found to be slow in the gas phase, indicating that inelastic collisions are ineffective in nuclear spin relaxation. Experiments performed with several different molecules in the supersonic expansion showed that the nuclear spin is conserved during the rapid adiabatic cooling. Notable exception from this behavior has been reported by Manca Tanner and Quack [1] in the case of supersonic expansion of water seeded in Ar buffer gas. Efficient nuclear spin relaxation has been deduced from spectroscopic data. The effect has been attributed to formation of clusters that facilitate the relaxation process. However measurements performed later in our laboratory with similar experimental setup did not reproduce those results [2]. In this contribution we report on recent re-investigation of the water nuclear spin relaxation in supersonic jet expansion. We present more comprehensive set of data compared to both previous measurements and use modified approach to data analysis to avoid possible sources of systematic errors present in previous measurements.

2. H_2O nuclear spin and rotational states

Water, in analogy to hydrogen, has two nuclear spin isomers with total nuclear spin I=0 (Para) and I=1 (Ortho). Being an asymmetric top it's rotational levels are labeled by total angular momentum quantum number J and it's projections on the A and C symmetry axes Ka and Kc respectively. Here we use notation $J_{Ka,Kc}$ to label the rotational states. Due to the symmetry, rotational levels with Ka + Kc = even and Ka + Kc = odd belong to the Para and Otrho nuclear spin isomers, respectively. Thus the lowest rotational levels of the Para isomer

are 0_{00}, 1_{11} (37.1 cm^{-1}), and 2_{02} (70.1 cm^{-1}), while they are 1_{01} (23.8 cm^{-1}), 1_{11} (42.4 cm^{-1}), 2_{12} (79.5 cm^{-1}) for Ortho isomer. Values in parenthesis indicate the rotational energies with respect to the ground rotational state (0_{00}).

2. Experiment

The experimental apparatus has been described previously [3]. It combines pulsed (1ms long gas pulses at repetition rate 3Hz) slit supersonic nozzle (dimensions 40×0.1mm^2) as source of cold supersonic molecular beam with high resolution direct-absorption laser spectrometer based on extended cavity semiconductor laser in the near IR spectral range (7100 cm^{-1} to 7300 cm^{-1}). Important to the present study is the modification of the gas inlet system for the supersonic beam: It consists of two arms with gas flow controlled by independent flow controlled. In what is called the “wet arm” the passing Ar gas is saturated with water vapor by passing through a reservoir of liquid water at room temperature. The “dry arm” adds pure Ar to the flow. The gas from both arms is mixed prior to admitting to the slit nozzle assembly. This setup permits independent control of both H_2O molar fraction and the total stagnation pressure.

3. Results

Six ro-vibrational transitions have been selected in the P-branch region of the OH stretch overtone region between 7200 cm^{-1} and 7300 cm^{-1}, such that each of them probes population in one of the six lowest H_2O rotational states. With H_2O molar fraction set to a specified value, the total stagnation pressure has been varied between 50 Torr and 300 Torr and the spectral line profiles have been measured at each expansion conditions. Figure 1 shows typical experimental spectral lines and Gaussian fits to the experimental data. Populations in the lower rotational quantum states were determined from the experimental integrated line intensities using the Einstein A_{21} coefficients from the 2016 edition of the HITRAN spectroscopic database [4]. Expansion temperature is measured by two independent methods: Kinetic temperature is determined from the Doppler broadening of the spectral lines and the internal rotational temperature has been determined independently for the Ortho and Para states by the Boltzmann analysis of the corresponding line intensities. Both techniques give consistent results. Expansion temperature as a function of stagnation pressure is presented in figure 2a.

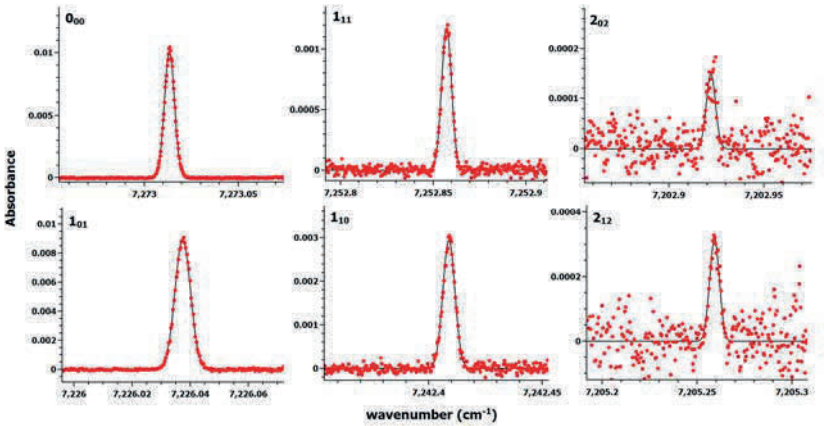

Fig. 1: *Selected absorption lines probing the lowest Para (top) and Ortho (bottom) rotational states*

Total Ortho and Para populations are determined by summing over all the rotational states belonging to given nuclear spin isomer, where the populations in all the higher states not sampled directly by the experiment are estimated by numerical evaluation of the rotational partition function at the experimentally determined temperature. This correction is always below 5% for all the probed experimental conditions. Figure 2b shows the total fraction of H_2O (relative to the high temperature limit), that remains as monomer water vapor at lower temperatures.

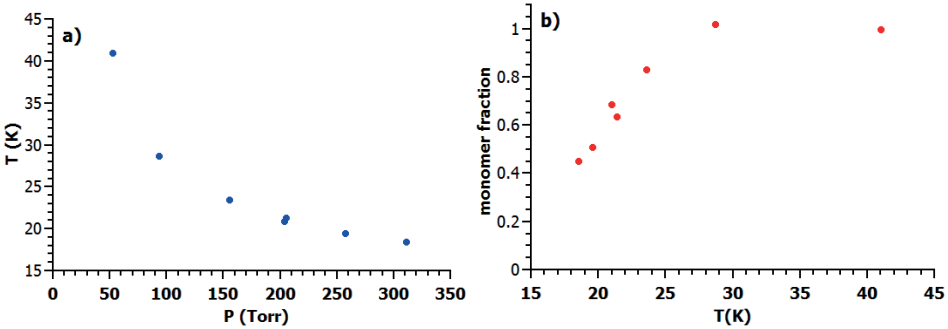

Fig. 2: *Expansion characterization for H_2O for mole fraction 1.3%. in Ar buffer gas. a) Expansion temparature as a function of stagnation pressure P, b) monomer H2O fraction as a function of expansion temperature. Significant clustering is indicated by the of monomer fraction for expansion temperatures below 30K.*

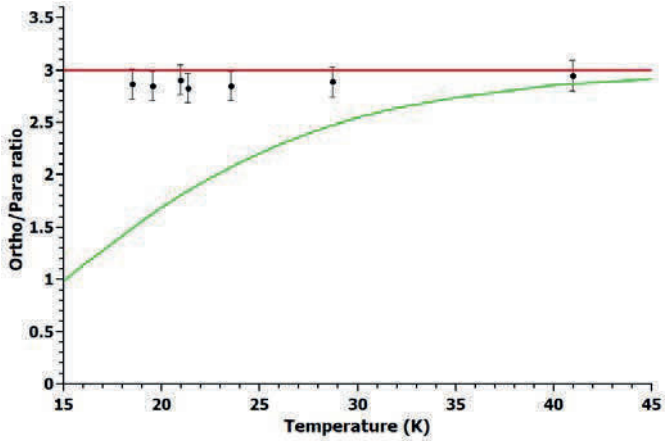

Fig. 3: *Total Ortho/Para population ratio as a function of expansion temperature Solid lines: predicted total Ortho/Para population ratios in the case of nuclear spin conservation (red) and nuclear spin relaxation (green) cases. Black dots are the experimental total nuclear spin population ratios. Error bars are derived from the statistical error of the line intensity measurements*

Significant decrease of monomer population below 30K is indication of onset of clustering.

Figure 3 presents the measured total Ortho/Para population ratio as a function of temperature. Within the experimental uncertainty the data are consistent with the nuclear spin conservation scenario under the probed experimental conditions, despite the fact, that significant clustering is observed at temperatures below 30K.

Acknowledgement: Authors would like to acknowledge financial support from The Czech Science Foundation grant no.: 17-04068S

References:

[1] C. Manca Tanner, M. Quack, and D. Schmidiger. 2013. *J. Phys. Chem. A* 117 **(2013)** 10105

[2] O.Votava, V. Horká-Zelenková, J. Rakovský, and M. Fárník, *The 23-rd International Conference on High Resolution Molecular Spectroscopy, Bologna* **(2014)**, Book of abstract pg. 134

[3] O. Votava, M. Mašát, P. Pracna, S. Kassi and A. Campargue, *Phys. Chem. Chem. Phys.* 12 (**2010)** 3145

[4] Gordon, I. E., L. S. Rothman, C. Hill, R. V. Kochanov, Y. Tan, P. F. Bernath, M. Birk, et al., *J. Quant. Spectrosc. Rad. Trans.* 203, **(2017)** 3

Molecular Frame Young-type Interference in (e, 2e) Reactions on H_2

Enliang Wang[1], Xueguang Ren[1], Khokon Hossen[1], Xingyu Li[2,3], Xiangjun Chen[2,3] and Alexander Dorn[1]
[1]Max-Planck-Institut für Kernphysik, 69117 Heidelberg, Germany
[2]Hefei National Laboratory for Physical Sciences at Microscale and Department of Modern Physics, University of Science and Technology of China, Hefei, Anhui, 230026, China
[3]Hefei Synergetic Innovation Center of Quantum Information and Quantum Physics, University of Science and Technology of China, Hefei, Anhui, 230026, China

The wave-particle duality is one of the fundamental concepts of quantum mechanism where the wave like behaviors of particles were mostly demonstrate through Young's double-slit experiment in which the coherent superposition of different outgoing amplitudes will present interference patterns. In the 1960's, Cohen and Fano [1] discussed the Young's double-slit experiment on the atomic scale by photoionizing a diatomic molecule. The Young-type interference effect was also considered for (e, 2e) reaction, so far, all of the experiments have averaged over the molecular alignment which is one of the essential parameters to determine the interference pattern.

Here we perform a high energy (E_0 = 520 eV) (e, 2e) experiment on H_2 to trace the interference effect using a dedicated reaction microscope [2, 3]. All of the charged state particles are detected with almost 4π solid angle efficiency. The molecular alignment is determined for those ionization events where the residual H_2^+ ground state molecular ion dissociates into a neutral hydrogen atom and a proton. Based on the axial recoil approximation the alignment of the molecular axis can be obtained by the proton momenta. Theoretically the fully differential cross section (FDCS) is described using the standard interference factor [4] multiply with the atomic cross section of Hydrogen atom, $2\sigma_{\mathrm{H}}\left[1+\cos\left(\vec{p}\cdot\vec{R}-\vec{q}\cdot\vec{R}\right)\right]$, where $\vec{R}$ is the internuclear vector, $\vec{p}$ is the momentum of the ejected electron and $\vec{q}$ is the momentum transfer. Alternatively, an *ab inito* claculation is also performed using the multicenter distorted-wave (MCDW) method [5] where the incident and the scattered electrons are described by plane waves while the continuum wave function of the slow ejected electron is solved in the multicenter potential of the residual

ion. The FDCS of MCDW calculation is contributed from two direct terms and a cross term, $\sigma = A_a^2 + A_b^2 + 2A_aA_b\cos(\Delta)$.

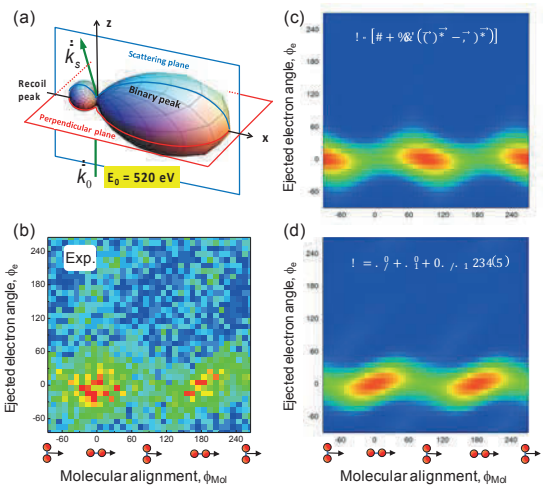

Figure 1. *(a) The collision kinematics used in this study. (b) The experimental FDCS for θ_1 = -20°, E_f=10 eV. (c) Atomic cross section multiplied with interference factor. (d) MCDW calculation.*

The collision kinematics is shown in Fig. 1 (a). In the present study, we analyze electron emission angle ϕ_e and molecular alignment angle ϕ_{Mol} with respect to the *x*-axis in the perpendicular plane. As shown in Fig. 1 (b), a strong dependence to the molecular alignment of the FDCS is observed where two intense areas are observed with molecular alignment at 0 and 180°. The MCDW calculation well reproduce the experimental results while the pure interference description fails completely. This is mainly due to the rather low energy (10 eV) of the ejected electron which does not justify the spherical wave description used in the derivation of the interference factor. Future experiments will consider fast outgoing electrons (up to 80 eV) to trace the interference effect.

References

[1] H. D. Cohen and U. Fano, Phys. Rev. 150, 30 (1966).
[2] Ullrich *et. al.*, Rep. Prog. Phys. 66, 1463 (2003).
[3] Ren *et.al.*, J. Chem. Phys., 141, 134314 (2014).
[4] C R Stia *et. al.*, J. Phys B, 36, L257 (2003).
[5] Zhang, *et. al.*, Phys. Rev. A 89, 052711 (2014).

Towards reaction studies of CN^- with atomic hydrogen in a cryogenic multipole trap

Robert Wild, Malcolm Simpson, Elin Carapovic, Alice Schmidt-May, Markus Nötzold, Roland Wester
Institut für Ionenphysik und Angewandte Physik, Universität Innsbruck

After the radioastronomical discovery of the first interstellar anions, interest has grown in understanding the formation and destruction pathways of negative ions in the interstellar medium. Our group has previously performed photodetachment studies on C_nH^- [1], CN^- and C_3N^- anions [2], but reactions with hydrogen may also play a significant role. Reaction rate studies of C_nH^- with molecular hydrogen show vanishing rates [3]. Here we focus on the role of atomic hydrogen in reactions with interstellar anions. Our 22-pole cryogenic ion trap is a versatile tool to simulate interstellar conditions, and we have incorporated a hydrogen atom source into our system. This allows us to study the reaction rates of CN^- with atomic hydrogen at cold temperatures.

[1] T. Best, R. Otto, S. Trippel, P. Hlavenka, A. von Zastrow, S. Eisenbach, S. Jézouin, R. Wester, E. Vigren, M. Hamberg, Astrophys. J. 742, (2011).
[2] S. S. Kumar, D. Hauser, R. Jindra, T. Best, Š. Roučka, W. D. Geppert, T. J. Millar, and R. Wester, Astrophys. J. 776, (2013).
[3] E. S. Endres, O. Lakhmanskaya, D. Hauser, S. E. Huber, T. Best, S. S. Kumar, M. Probst, and R. Wester, J. Phys. Chem. A, 118, (2014).

Author index


HIDEN
ANALYTICAL


Radiant Dyes Laser

VACUUM SOLUTIONS

A one stop source for the highest standard in vacuums

No two vacuum processes are alike since individual requirements are what matters. Together with our customers, we obtain a vacuum solution based on their specific needs. This process includes all steps in creating a perfect vacuum condition. Besides best-in-class products for vacuum generation, measurement and analysis, we also offer accessories, application training programs and worldwide service.

See for yourself what Pfeiffer Vacuum solutions are about at:

www.pfeiffer-vacuum.com

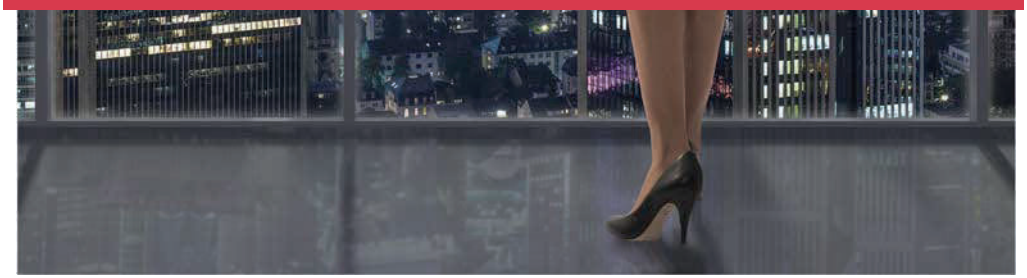

ISBN 978-3-903187-15-3